UiT The Arctic University of Norway

Faculty of Health Sciences

Department of Pharmacy

Drug Transport and Delivery Research Group

Liposomal formulations for membrane active antimicrobials – Assuring safety through an optimised drug delivery system

Ann Kristin Pettersen

Thesis for the degree Master of Pharmacy 2020

MASTER THESIS FOR THE DEGREE MASTER OF PHARMACY

LIPOSOMAL FORMULATIONS FOR MEMBRANE ACTIVE ANTIMICROBIALS – ASSURING SAFETY THROUGH AN OPTIMISED DRUG DELIVERY SYSTEM

BY

ANN KRISTIN PETTERSEN

MAY 2020

SUPERVISORS

Professor Nataša Škalko-Basnet

and

PhD student Lisa Myrseth Hemmingsen

Drug Transport and Delivery Research Group Department of Pharmacy

Faculty of Health Sciences

UiT The Arctic University of Norway

Acknowledgement

The present work in this master thesis was carried out at Drug Transport and Delivery Research Group, Department of Pharmacy, UiT The Arctic University of Norway during the period from September 2019 to May 2020.

First of all, I would like to express gratitude for my supervisors Professor Nataša Škalko-Basnet and Lisa Myrseth Hemmingsen, M Pharm, for excellent support and guidance. This project has made pharmacy even more interesting for me.

I would like to thank Professor Željka Vanić (Department of Pharmaceutical Technology, Faculty of Pharmacy and Biochemistry, University of Zagreb, Croatia) for conducting elasticity experiments.

I would like to thank Dr. Sybil Obuobi for conducting TEM.

I would like to thank Professor II Purusotam Basnet for all the help with cell experiments.

I would also like to thank everyone else in the Drug Transport and Delivery Research Group for helping out whenever needed and making us feel welcome. Hereunder, thanks to Martin Skipperud Skarpeid for technical assistance in the lab. And also thanks to my fellow master students, Luqman Ahsan, Kasi Shorsh and Silje Mork for good conversations in the lab, and a special thanks Julie Olaussen and Sunniva Brurok for support, laugh and many good discussions.

I am grateful for Lipoid GMbH for providing lipids, Chitinor AS for providing chitosan and Lubrizol for providing Carbopol for this project.

Finally, I must express my sincerely gratitude to my family for always encouraging me, believing in me and always supporting me. And last but not least, I am thankful for the person that had to be isolated with me in this stressful and unusual time, and that also has been my biggest supporter for 7 years. Ole Elmer, I am grateful for your patience!

- *Ann Kristin Pettersen, May 2020*

Table of content

List of Tables

List of Figures

Abstract

Skin and soft tissue infections (SSTIs) and chronic wounds are major challenges for the healthcare system worldwide. The additional rapid development of antibacterial resistance and lack of successful treatment strategies increase the chance for infected chronic wounds to be fatal for the patient. Therefore, there is a need for more efficient dermal antimicrobial therapies. A class of promising antimicrobial drug candidates that have captured attention in respect to treating resistant bacterial infections, including skin infections, is membrane active antimicrobial peptides (AMPs). Our particular interest was to develop a novel formulation that is able to deliver membrane active antimicrobials to chronic wounds, and promote wound healing. We developed a liposomes-in-hydrogel formulation and used chlorhexidine (CHX) as our model antimicrobial in this work. CHX was entrapped in liposomes with entrapment efficiency of 96 % and the size analysis indicated a mean vesicle size of 318 ± 8.6 nm. The zeta potential of CHX liposomes was measured to be 45.53 ± 1.33 mV. The vesicle formation of CHX liposomes was confirmed with transmission electron microscopy (TEM). CHX liposomes were incorporated into a 5.0 % (w/w) chitosan hydrogel comprising 10 % (w/w) glycerol and the hydrogel was characterised by a texture analyser (T.A). A novel T.A. method was developed and validated and later applied to characterise our hydrogels. The texture properties to CHX liposomes-in-hydrogels exhibited the cohesiveness of 291.3 ± 9.9 g/sec, hardness of 149.3 ± 4.5 g and adhesiveness of -327.5 ± 3.1 g/sec. The pH of the hydrogels was just below 5 and showed no significant changes upon storage for 4 weeks. *In vitro* evaluation of CHX release from the liposomes-in-hydrogel formulations indicated a sustained release. The investigation of the anti-inflammatory activities of empty liposomes, CHX liposomes, plain hydrogel and CHX liposomes-in-hydrogel, measured as nitric oxide production in murine macrophages, indicated that the novel drug delivery system was safe and exhibited an anti-inflammatory effect.

The results confirmed that the liposomes-in-hydrogel formulation of membrane active antimicrobials has a potential as novel antimicrobial formulation.

Keywords: antimicrobial peptides; chronic wounds; skin and soft tissue infections; antibacterial resistance; drug delivery system; hydrogels; liposomes; chitosan

Sammendrag

Infeksjoner i hud og bløtvev og kroniske sår gir store utfordringer for helsevesen over hele verden. Den raske utviklingen av antibakteriell resistens og mangel på suksessfulle behandlingsstrategier øker sjansen for at infiserte kroniske sår blir dødelige for pasienten. Det er derfor et behov for mer effektive dermal antimikrobielle behandlinger. En lovende klasse av antimikrobielle midler, som har fått oppmerksomhet med tanke på å behandle resistente bakterielle infeksjoner, er membranaktive antimikrobielle peptider (AMP). Vårt mål var å utvikle en ny formulering som kan levere membranaktive forbindelser til kroniske sår og samtidig fremme sårheling. Vi utviklet en liposomer-i-hydrogel formulering og brukte klorheksidin som vår modellsubstans i dette arbeidet. Klorheksidin ble inkorporert i liposomer med en gjennomsnitt vesikkelstørrelse på 318 ± 8.6 nm og en inkorporeringsgrad på rundt 96 %. Zetapotensialet av klorheksidinliposomer ble målt til å være 45.53 ± 1.33 mV. Et transmisjonselektronmikroskop (TEM) bekreftet at klorheksidinliposomene forelå som vesikler. Klorheksidinliposomer ble inkorporert i en 5,0 % (w/w) kitosan hydrogel med 10 % (w/w) glyserol og denne hydrogelen ble karakterisert på en teksturanalysator (T.A.). En metode ble utviklet og validert på T.A for å måle teksturegenskaper og senere brukte vi denne metoden til å karakterisere våre hydrogeler. Teksturegenskapene til klorheksidinliposomer-i-hydrogel ble målt til å ha en kohesjon på 291.3 ± 9.9 g/sec, hardhet på 149.3 ± 4.5 g og adhesjon på -327.5 ± 3.1 g/sec. Den målte pH på hydrogelen var rett under 5 og viste ingen signifikant endring i løpet av en periode på 4 uker. *In vitro* evaluering av klorheksidinfrigjøring fra liposomer-i-hydrogel formuleringen indikerte en forlenget frigjøring. Og evaluering av anti-inflammatoriske aktiviteter av tomme liposomer, klorheksidinliposomer, enkel hydrogel og klorheksidinliposomer-i-hydrogel indikerte at det nye legemiddelleveringssystemet ikke økte inflammasjonen, men heller hadde en anti-inflammatorisk effekt.

Resultatene fra dette prosjektet bekreftet at en liposomer-i-hydrogel formulering for membranaktive antimikrobielle forbindelser har potensial som en ny antimikrobiell formulering.

Nøkkelord: antimikrobielle peptider; kroniske sår; hud- og bløtvevsinfeksjoner; antimikrobiell resistens; legemiddelleveringssystemer; hydrogeler; liposomer; kitosan

List of abbreviations

AMP – Antimicrobial peptide

CHX – Chlorhexidine

ECM - Extracellular matrix

EE – Entrapment efficiency

EGTA- Ethylene glucol tetraacetic acid

FBS – Fetal bovine serum

FDA – Food and drug administration

HEPES – 4-(2-hydroxyethyl)-1-piperazineethanesulfonic acid

HPLC – High performance liquid chromatography

LPS – Lipopolysaccharides

MRSA – Methicillin-resistant *Staphylococcus aureus*

MW – Molecular weight

NO – Nitric oxide

PBS – Phosphate buffered saline

PC – Phosphatidylcholine

PEG – Polyethylene glycol

PG – Propylene glycol

PHEM – PIPES-HEPES-EGTA-Magnesium sulphate

PI – Polydispersity index

PIPES - 1,4 piperazine bis

rhPDGF – Recombinant human platelet-derived growth factor

RPMI – Roswell park memorial institute

RR – Relative recovery

SD – Standard deviation

SEM – Scanning electron microscopy

SSTI – Skin and soft tissue infections

T.A. - Texture analyser

TEM - Transmission electron microscopy

1 General introduction

The antibacterial resistance is a major global threat to all human and animal life, as without the efficient option to threat infections numerous people and animal will die. It is suggested that over 700, 000 people die annually because of antibacterial resistant pathogens (Ragheb et al., 2019). One of the most common types of infections are skin and soft tissue infections (SSTIs); with the rapid development of antibiotic resistance pathogens, there is an urgent need for new dermal antimicrobial treatment (Pfalzgraff et al., 2018).

The skin has many vital functions and one central function is to protect us from environmental exposure, such as pathogens. If the skin was breached over a longer period of time, it would place a patient in significant health risk, which is the case with chronic wounds. Thereupon, chronic wounds are a major burden for health care systems (Saghazadeh et al., 2018). A chronic wound develops when one of the precisely regulated phases in wound healing is disrupted and the non-healing wound persist for a longer period than three months (Drago et al., 2019). A chronic wound creates a hospitable environment for bacterial growth and biofilm formation (Mustoe et al., 2006), further aggravating the healing. Current treatment strategies fail to successfully treat infected chronic wounds and with the emergence of antibiotic resistant pathogens, the patients are put in even a higher health risks.

One promising and upcoming antimicrobial class, in respect to killing antibacterial resistant pathogens, is membrane active antimicrobial peptides (AMPs) (Mahlapuu et al., 2016). Topically administrated AMPs have shown efficacy in several *in vivo* studies (Mookherjee et al., 2020). AMPs are promising due to their broad activity and the fact that they are reported to be less susceptible to antibacterial resistance. They exert antimicrobial effects against both Gram-positive and Gram-negative bacteria, supress biofilm formation and reduce the pro-inflammatory response in wounds (Gomes et al., 2017). However, there are challenges related to delivering AMPs to the desired target in terms of excess proteolytic activity and unwanted toxicity; therefore, it would be beneficial to develop a drug delivery system able to protect and deliver these membrane active compounds (Biswaro et al., 2018).

Chronic wounds require a suitable dressing that ideally promotes wound healing, provides protections against external pathogens and maintains wound moisture (Saghazadeh et al., 2018). Therefore, we proposed to develop a novel formulation that enables delivering membrane active antimicrobials locally assuring prolonged release, to treat infections and promote wound healing. The novel formulation comprises of two delivery systems formulating the liposomes-in-hydrogel formulation.

Liposomes are small spherical vesicles that consist of lipid bilayer membranes surrounding an aqueous core, making them able to incorporate both hydrophilic and hydrophobic compounds (Maherani et al., 2012). Hydrogels are hydrophilic networks that consist of polymers that are insoluble but compatible with aqueous media thus allowing the hydrogel to swell, and the properties of a fully swollen hydrogel resemble the mechanical properties of living tissue (Hua, 2015, Bhattarai et al., 2010). Combining these two drug delivery systems, developing a liposomes-in-hydrogel formulation, could provide sustained release of membrane active antimicrobials to chronic wounds and potentially improved the efficacy of the treatment.

In this project we chose to work with chlorhexidine (CHX) as a model compound in the development of a novel formulation. CHX is selected as model compound because it has similar mechanism of action as AMPs, is cheaper and also commercially available.

2 Introduction

2.1 Antibacterial resistance and skin and soft tissue infections (SSTIs)

The world experienced a turning point when antibiotics were discovered in the 20th century. The British scientist Alexander Fleming isolated penicillin from a fungus called *Penicillium chrysogenom* in 1929 and the antibiotic was in clinical use near the end of World War II in 1945. Since then there have been an ongoing search for new effective antibiotic therapies and development of new antibiotics. The effectiveness of antibiotics has saved many lives, not only due to the antibiotic effect, but also because of their non-antibiotic effects including anticancer and antiviral effects. Extensive use of antibiotics worldwide have unfortunately led to the rise of antibacterial resistance (Theuretzbacher et al., 2019). In the race between discovery of new effective antibiotic treatment and antibacterial-resistant pathogens, we are currently losing against the rapid resistance development. Estimates suggest that around 700, 000 people dies annually because of drug-resistance infections and the numbers are rising (Ragheb et al., 2019). One of the most common types of bacterial infections are skin and soft tissue infections (SSTIs), with increasing resistance against topical antibiotics (Pfalzgraff et al., 2018). SSTIs can be fatal if the patient is infected with a resistance bacteria, therefore there is an urgent need for new treatment options (Barbier and Timsit, 2020). Promising therapeutic compounds for the treatment of resistant bacteria are antimicrobial peptides (AMPs) (Mahlapuu et al., 2016). These compounds are especially promising in the treatment of SSTIs and chronic wounds.

The skin is the barrier that protects us from environmental threats. When the skin is broken, which is the case for a period of time for chronic wounds, the patient is susceptible to skin infections. In the US alone, around 4.5 million people require treatment for chronic wounds and the cost is around US$25 billion (Saghazadeh et al., 2018). It is safe to say that chronic wounds are a major challenge for the healthcare systems worldwide (Frykberg and Banks, 2015). Chronic wounds are wounds that have "failed to progress through a systematized and timely process to get normal anatomic and functional integrity" and that have not healed within three months (Rajendran et al., 2018, Drago et al., 2019). The current strategies for treatment are non-individualised, expensive and do not enhance the patient compliance or therapeutic effectiveness (Saghazadeh et al., 2018). To optimise the treatment, it is important to understand the anatomical and physiological challenges of skin as drug action site.

2.2 Skin and wounds

2.2.1 Skin

The skin is the biggest and outermost organ of the body. The primary function of the skin is to help control the homeostasis of the human body, through temperature control, repair control and protection from exposure to environmental hazards (Sala et al., 2018). Environmental hazards can be a diverse number of pathogens as well as chemical and physical injuries (Pfalzgraff et al., 2018). The skin is on average 0.5 mm thick and is composed of three layers: epidermis, dermis and hypodermis (Figure 1) (Foldvari, 2000). *Stratum corneum* is the outermost layer of epidermis and acts as a physical barrier. The *stratum corneum* maintains the epidermal barrier integrity and it is composed of multiple layers of corneocytes that are embedded in a hydrophobic extracellular matrix (ECM) that provides a watertight seal (Lai-Cheong and McGrath, 2009).

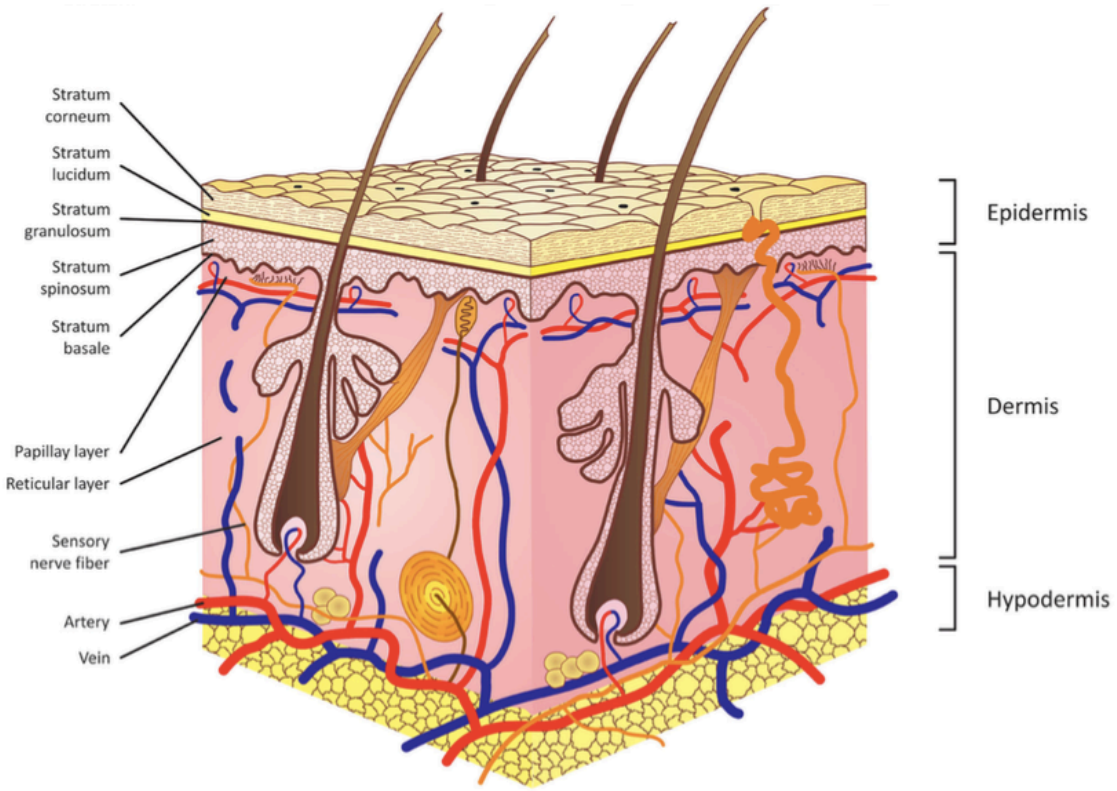

Figure 1: Sketch of the structure of skin. Starting from outside to inside the main layers are; epidermis with *stratum corneum*, dermis and hypodermis (*with permission*) (Ventrelli et al., 2015).

The skin is the first line defence and if the skin barrier breaches, this would place the patient in significant health risk, especially if the skin is impaired for a longer period of time. Therefore skin infections and chronic wounds are major burdens as well as challenges for the health care systems (Saghazadeh et al., 2018).

2.2.2 Normal wound healing

Normally, after a skin injury the body is able to restore skin integrity within a reasonable time (Liu et al., 2018). Normal dermal wound healing is typically divided in four overlapping phases: haemostasis, inflammation, proliferation and remodelling (Figure 2). The haemostasis is the first phase and lasts from seconds to hours and involves vasoconstrictions, platelet aggregation, complement activation and thrombus formation (Rajendran et al., 2018). The immediate response occurs to minimize haemorrhage or stop the bleeding at the injured skin site. Aggregation of platelets reduces blood flow to the wound bed by vasoconstriction (Saghazadeh et al., 2018). Various inflammatory cells, enzymes, cytokines and proteins are present in the inflammation and proliferation. The inflammation phase lasts for about 3 days. The macrophages are activated and remove microbes and dead cells therefore contributing to normal healing processes (Rajendran et al., 2018). The proliferation phase starts around 2-3 days after injury and continues until the wound is closed. Various growth factors stimulate fibroblast proliferation, migration and angiogenesis as the wound start to rebuild. The proliferative phase is followed by the remodelling phase and lasts for over 1 year. In the remodelling phase the ECM are synthesized including the collagen synthesis and the inflammation stops (Saghazadeh et al., 2018).

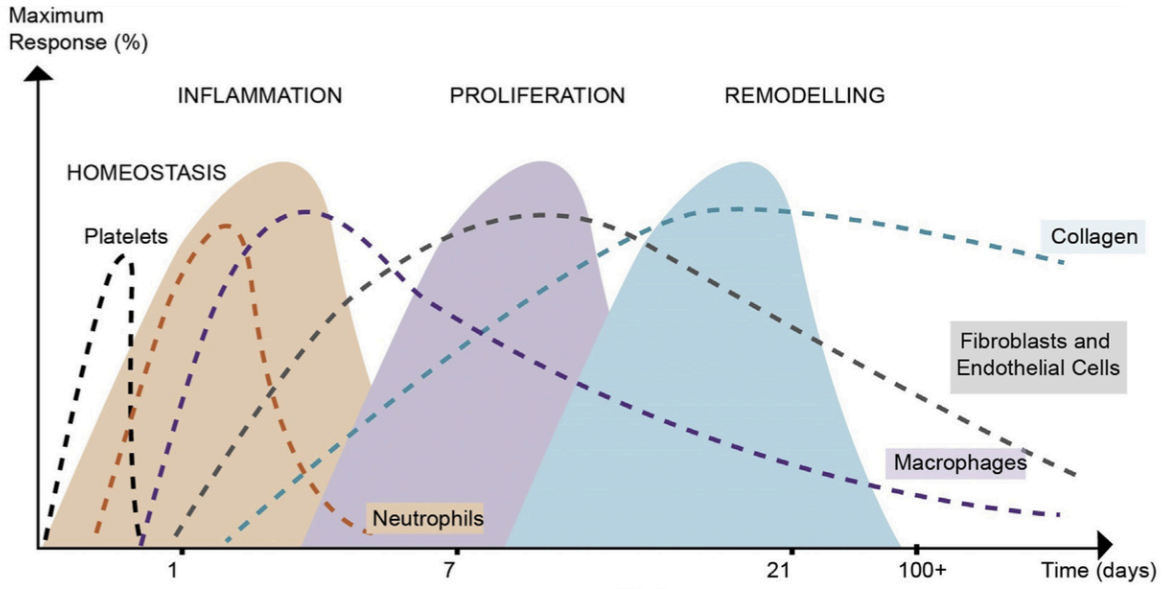

Figure 2: The four phases of tissue repair in skin wound healing: homeostasis, inflammation, proliferation and remodelling showed over time (days) and when they exhibit maximum response (%). The dotted lines show the distinctive contribution of different inflammation cells, the platelets and collagen during the process of wound healing (*with permission*) (Zomer and Trentin, 2018).

A chronic, non-healing wound occurs when one of the phases of precisely regulated set of biological pathways in normal dermal wound healing is impaired (Rajendran et al., 2018).

2.2.3 Pathophysiology of chronic wounds

The pathophysiology of chronic wounds is not yet fully understood but something that is acknowledged is that the healing process remains in the inflammation phase. An extended inflammation phase will lead to overexpression of inflammation cells, which in turn will cause destruction of growth factors and a reduction in cell migration. In addition, fibroses and prolonged wound contraction will occur in a chronic wound, leading to a formation of fibrotic scar tissue. Many factors could potentially increase the chances of the occurrence of a chronic wound, such as scarring, mechanical stress, aging, diabetic condition, vascular disease and infections (Saghazadeh et al., 2018).

2.2.4 Bacterial skin and soft tissue infections

The protective defence mechanisms within intact skin diminish in open skin wounds (Siddiqui and Bernstein, 2010). Regions of non-viable tissue in wounds provide a hospitable environment for bacterial growth. Bacteria will contaminate chronic wounds and critical colonisation can be self-sufficient to lead to a chronic wound (Mustoe et al., 2006). The magnitude of the infection depends on different factors including aging, comorbidities such as for example diabetes mellitus as well as the type of bacteria (Barbier and Timsit, 2020).

2.2.4.1 Gram-positive and Gram-negative bacteria of relevance in skin infections

Commonly, bacteria are divided into two groups: Gram-positive and Gram-negative bacteria. This grouping of bacteria is based on the cell envelope structure (Mahlapuu et al., 2016). The name originates from Gram staining method where crystal violet stain is used; the Gram-positive bacteria takes up the crystal violet stain while the Gram-negative does not (Yazdankhah et al., 2001). The Gram-negative bacteria are enclosed by two membranes, a cytoplasmic and an outer membrane, while the Gram-positive bacteria are only surrounded by a single cytoplasmic membrane (Goldfine, 1984). Both Gram-positive and Gram-negative bacteria's cytoplasmic membranes are rich in phosphatidylserine, cardiolipin and phosphatidylglycerol. The Gram-positive bacteria also have teichoic acids and Gram-negative bacteria have lipopolysaccharides in the outer membrane. This kind of phospholipids have negatively charged head groups in physiological conditions which in turn gives the bacteria an overall electronegative charge on the surface (Mahlapuu et al., 2016).

In contrast to prokaryote cell membrane, the eukaryotic cell membrane main lipids are glycerophospholipids (mainly phosphatidylcholine (PC)) and in addition contain sterols (cholesterol) which prokaryote cells lack (van Meer et al., 2008). The phospholipids in eukaryotic cell membranes are mostly zwitterionic and asymmetrically distributed in the membrane. The distribution of the lipids leads to phospholipids with negatively charged head groups positioned in the inner leaflet and the zwitterionic in the outer leaflet, which provides the eukaryotic membrane a neutral net charge (Mahlapuu et al., 2016).

Examples of Gram-positive bacteria encountered in skin infection are methicillin-resistant *Staphylococcus aureus* (MRSA) and *Enterococcus faecalis,* whereas an example of a Gram-negative bacterium is *Pseudomonas aeruginosa* (Barbier and Timsit, 2020). Considering the Gram-positive and -negative bacteria, it is the multidrug-resistant Gram-negative bacteria that tops the WHO priority list for research and development of new antibiotics (Tacconelli et al., 2018). The antimicrobial class AMPs is a promising antimicrobial approach due to the fact that AMPs exhibit very broad activities and antimicrobial effects against both Gram-positive and Gram-negative bacteria.

2.2.4.2 Bacterial infections of skin

The colonizing flora of chronic wounds is complex and changing over time (Edwards and Harding, 2004). The most recalcitrant pathogens in SSTI are the so called ESKAPE pathogens, namely *Enterococcus faecium, Staphylococcus aureus, Klebsiella pneumonia, Acinetobacter baumannii, Pseudomonas aeruginosa* and *Enterobacter* species. ESKAPE pathogens are resistant to almost all common antibiotics, which in extent is the leading cause for hospital-acquired infections. *S. aureus* is the main pathogen in SSTIs and MRSA is the reason for up to 50 % of all SSTIs (Pfalzgraff et al., 2018). The predominant bacteria in chronic wounds are initially Gram-positive organisms (Edwards and Harding, 2004). But there is observed an increase in chronic wounds infected by the Gram-negative pathogen *P. aeruginosa* and also vancomycin-resistant *Enterococcus* (Pfalzgraff et al., 2018).

An infection of the wound can provoke local and systemic host responses such as purulent discharge, painful spreading erythema or symptomatic cellulitis around the wound. Both the colonisation of bacteria and formation of bacterial biofilm are serious mediators of chronic wounds (Boateng and Catanzano, 2015).

2.2.4.3 Biofilms

A biofilm is an extracellular polysaccharide matrix that have microcolonies of bacteria inside (Drago et al., 2019). Over 70 % of chronic wounds will exhibit microbial biofilm infections (Matica et al., 2019) comprising typical biofilm producers such as MRSA and *Pseudomonas* spp. Biofilms can make the antibiotic treatment difficult and often limited. Compared to a

planktonic cell, a biofilm is less susceptible to antibiotics, in fact bacteria inside a biofilm have been reported to be up to 500 times more resistant (Siddiqui and Bernstein, 2010). The biofilm protects the bacteria from the hosts defence and would act as a physical barrier for antimicrobial compounds (Drago et al., 2019). Biofilm formation will induce even more inflammation in the chronic wound and inhibit tissue repair and ECM deposition (Saghazadeh et al., 2018).

2.2.5 Current wound treatment options

There are several types of treatment options currently available in wound therapy. Choosing a suitable dressing for the wound depends on the amount of exudate, wound type, wound size and risk of infections (Rajendran et al., 2018). Considering a chronic wound, there are different considerations regarding the optimal dressing selection. For an otherwise healthy patient with impaired wound healing, the aim would be to assure the protection from external environment, maintenance of wound moisture to accelerate closure, and minimised scarring. For patients that have comorbidities (diabetes, obesity, advanced age) it would be additionally important to remove biofilm and non-viable tissue, modulate the inflammation as well as oedema, and encourage the reparative phase of healing (Saghazadeh et al., 2018). Available dressings involve the formulations such as hydrogels, films, creams and ointments with or without antimicrobial compounds, often comprising polymers (Rajendran et al., 2018). An example of a promising polymer is chitosan (more in section 2.4.2.2). There are several chitosan-based dressings available in form of hydrogels, films and sponges (Liu et al., 2018).

However, there are only four FDA-approved therapies for chronic cutaneous wounds. These are the human skin equivalents, dermal substitutes and recombinant human platelet derived growth factor (rhPDGF). The human skin equivalent and dermal substitutes are bioengineered and are suggested to be a smart biomaterial. rhPDGF will stimulate chemotaxis of fibroblast, neutrophils and macrophages, all highly beneficial effects during wound healing. There are also recent advances in nanotechnology-based wound therapies that are under clinical investigations. There are several strategies: i) using nanomaterials as intrinsic therapeutic agents (metallic nanoparticles; silver nanoparticles or non-metallic nanoparticles; chitosan nanoparticle), ii) using nanostructure as carrier of therapeutic compounds (gold nanodots

delivering AMP) or iii) using nanoengineered scaffolds (electrospinning nanofiber) (Hamdan et al., 2017).

Another important issue related to the treatment of a chronic wounds is the compliance, therefore the optimal dressing should manage pain, decrease frequency of dressing changes and be affordable and accessible. Antimicrobial therapeutics efficiently used locally instead of systemically will reduce the effective dose required to achieve desired effect as well as limit systemic exposure and adverse effects. It is also an advantage that, in the case of observed unwanted effects or toxicity (itching, pain, redness, inflammation), locally administrated dressing can be easily removed, washed away, whereas systemic administration would lead to serious adverse effects (Saghazadeh et al., 2018). Commonly prescribed systemic antibiotics such as penicillin, gramicidin, tetracyclines, are reportedly suffering from increased development of antibacterial resistance (Friedman et al., 2016)

There is therefore an urgent need for more efficient dermal antimicrobial therapies because of the emerging multidrug-resistant pathogens. A therapeutic class that have captured attention as drug candidates especially in treating resistant bacterial infections, is the membrane active AMPs (Mahlapuu et al., 2016).

2.3 Membrane active antimicrobials

Membrane active antimicrobials are a rather big promising group of antimicrobials; their general actions involve multiple targets on the bacterial membrane which make them less susceptible to resistance. Since they damage the membrane structure they are also promising in treating persisting infections, even biofilms (Hurdle et al., 2011).

2.3.1 Antimicrobial peptides (AMPs)

AMPs were first described in the 1960s and by now the naturally occurring AMPs are listed more than 2,600 times in the AMP database. AMPs are typically small amphipathic peptides consisting of under 50 amino acids. They normally have a positive charge at physiological pH and the composition of amino acid residues are substantially hydrophobic (Mookherjee et al., 2020). AMPs are diverse and distinctive group of molecules. They are produced in all life forms (for example animal, plants, bacteria) and are an essential part of the host innate immune system in eukaryotes. Naturally occurring AMPs are produced either by the nonribosomal peptide synthesis or ribosomal translation. In mammals, they are found in neutrophils and in secretions within skin and mucosal surfaces (Mahlapuu et al., 2016).

The activity of the AMPs is depending on their structure and can range from killing bacteria, modulating immunity, preventing biofilm formation to exhibiting anti-cancer effects. The eukaryotic cationic AMPs mostly kill bacteria or modulate the immune system (Kumar et al., 2018). The antimicrobial activity of some AMPs is exceptionally broad and is covering both Gram-positive and -negative bacteria (Mahlapuu et al., 2016). There are several proposed mechanisms for their antimicrobial activity. The typical antibacterial mechanism of AMPs is proposed to rely on breaking down the bacterial cell membrane, while potentially also exhibiting intracellular activity. AMPs that are positively charged predominantly target the anionic phospholipids in bacterial membranes by electrostatic interactions. There are three different transmembrane pore-forming mechanisms suggested: the toroidal-pore, the carpet and the barrel-stave model (Figure 3) (Brogden, 2005).

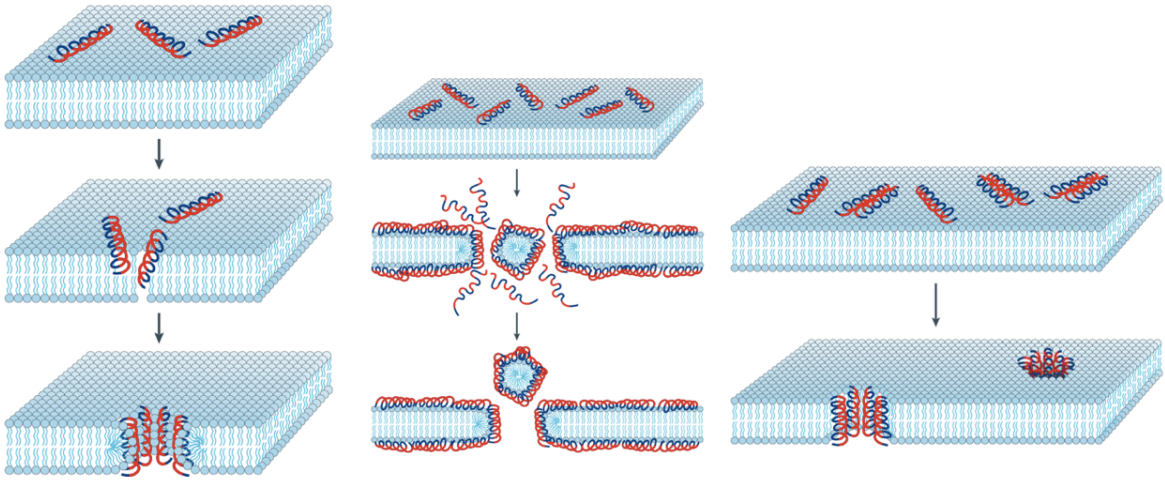

Figure 3: Proposed antibacterial transmembrane pore forming mechanisms of AMP. From left: the toroidal-pore, the carpet and the barrel-stave model. The hydrophilic and hydrophobic regions of peptides are represented in red and blue, respectively (*with permission*) (Brogden, 2005).

In the toroidal-pore model, AMPs hydrophilic residues associate with the hydrophilic heads of phospholipids in the membrane and create a transmembrane pore that have a hydrophilic core. In this pore the phospholipids bend pointing the hydrophilic heads towards the pore. The barrel-stave model is similar to the toroidal-pore model as the hydrophilic residues of AMPs make the core of the pore, with exception that AMPs hydrophobic residues are align with the phospholipids. In the carpet model, AMPs are attached to the membrane by electrostatic forces, then covering the membrane surface like a carpet and disrupting the membrane by causing transient holes (Figure 3) (Brogden, 2005).

Cationic AMPs show certain degree of selectivity because of their initial interaction with membranes. As explained in section 2.2.4.1, there are different components in the bacterial and mammalian cell membrane. The bacterial cell membrane has a higher content of anionic lipids like teichoic acids and phosphatidylglycerol, compared to mammalian cell membranes that have more neutral lipids. This leads to the AMPs exhibiting selective electrostatic interaction and disrupting the bacterial cell membrane structure which in turn leads to lysis of bacteria (Paulsen et al., 2019). It is also suggested that AMPs have several complementary actions inside the cell which increase the efficiency of killing bacteria (Mahlapuu et al., 2016). For example, it is suggested that AMPs have additional antimicrobial effects, as they are able to supress

biofilm formation and stimulate disruption of existing biofilms (Fjell et al., 2012, Hurdle et al., 2011).

Another factor, making AMPs a quite promising antimicrobial therapy, is their lower susceptibility to antimicrobial resistance. Lower susceptibility occurs due to complicated and rapid mechanisms of action often with more than one target in the bacteria, which makes it more difficult for the bacteria to defend themselves by one single resistance mechanism (Mookherjee et al., 2020). This optimism is also reinforced by the fact that AMPs already have been utilised by higher organisms for millions of years and there are only few instances of resistance that are known. However, studies indicate some mechanisms of resistance to AMPs including the cell surface modification and proteolytic degradation (Kuppusamy et al., 2019).

Although AMPs are quite promising in antimicrobial therapy, there are some concern related to their clinical use. AMPs have an unpredictable toxicity profile, are prone to proteolysis and have an inadequately understood pharmacokinetic profile (Biswaro et al., 2018). There are few AMPs tested for systemic administration because of these limitations, most of the clinical trials have so far been for topical applications or as inhalants for treatment of infections. The topically administrated AMPs have shown efficacy in several *in vivo* studies (Mookherjee et al., 2020). However, the wound bed creates some challenges regarding delivery of AMPs to the desired target; there is an ongoing inflammation, hospitable environment for bacterial growth, biofilm formation and excess proteolytic activity (Saghazadeh et al., 2018). To address the challenges, several strategies to improve the efficacy of AMPs have been proposed, such as the chemical modification or incorporation into a drug delivery system (Kumar et al., 2018).

The vast repertoire of natural AMPs provides an excellent platform for development of synthetic peptides (or peptidomimetics). Minor modifications of the peptide structure can significantly influence the characteristics by both improving structural stability and enhancing antimicrobial activity. However, it is important to consider that altering the characteristics of the peptide (or mimicking a natural peptide) could potentially lead to increased cytotoxicity, decreased peptide stability and low solubility (Mookherjee et al., 2020). In this regard, employing nanotechnology and a smart drug delivery system can help to avoid degradation and

enhance AMPs efficacy in treatment of skin. Incorporating peptides into a nanocarrier has shown to reduce toxicity, reduce degradation, provide sustained and predictable release, that can increase the efficiency of AMPs against the desired target (Biswaro et al., 2018, Kumar et al., 2018). Choosing localized treatment by AMPs offers a non-invasive alternative assuring reduced systemic adverse effects. This is especially advantageous considering AMPs toxicity issue as well as providing an opportunity for less frequent administration regimes, which in turn can result in higher patient compliance. Administering AMPs to infected skin have shown not only the ability to prevent infections, but also to reduce pro-inflammatory response, promote both the cell migration and proliferation in wounds (Gomes et al., 2017).

In this project, we have chosen to work with a model compound when developing a novel formulation. There are several reasons for this decision, main related to the cost of AMPs; the production cost of a synthetic peptide alone is estimated between US$300-500 per gram (Biswaro et al., 2018). Moreover, their analytics requires advanced instrumentation and methodologies, therefore, in the process of developing a novel wound dressing we selected to work with chlorhexidine (CHX) as a model compound.

2.3.2 Model compound: chlorhexidine (CHX)

Chlorhexidine (CHX), 1,1´-hexamethylene-bis[5-(4-chlorophenyl)biguanide] is a cationic bisbiguanide with broad antimicrobial activity. The compound occurs as a white crystalline solid (molecular weight 505.45 g/mol) and have a octanol/water partition coefficient of 0.754 (Farkas et al., 2007). CHX is a base (Kudo et al., 2002) and its structure is shown in Figure 4. The compound has commonly been used in global healthcare for several decades. As CHX base is practically insoluble in water, its salt form (digluconate or diacetate) is normally used commercially as it is soluble in water. CHX is used as antiseptic and disinfectant in hospitals, it is widely used as oral antiseptics and also extensively used in topical antimicrobial formulations (Duarte et al., 2019, Ambrogi et al., 2017).

CHX is a membrane active antimicrobial (like AMPs) that targets anionic lipids abundant in the bacterial membrane. The positive charge of CHX interacts with negatively charged phospholipids and teichoic acid in Gram-positive bacterial membrane and with the negatively charged phospholipids and lipopolysaccharides in Gram-negative bacterial membrane. It is also suggested that CHX exhibits a different mode of action, namely acting on an internal target within the cell (Hubbard et al., 2017).

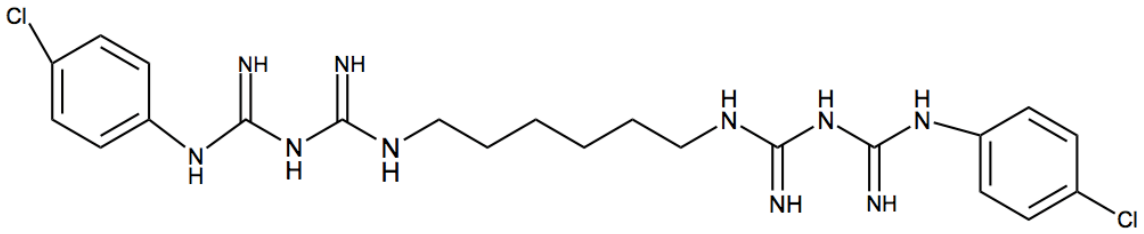

Figure 4: Structure of CHX. Created with chemdrawdirect.perkinelmer.cloud.

In this project, we used CHX as a model compound because it exhibits similar mechanisms of antimicrobial action as AMPs. In addition, CHX creates comparable physicochemical properties to AMPs, considering its incorporation in the delivery system. The targeted AMP we aimed to formulate in wound dressing in the broader project, exhibits similarly limited water solubility as CHX (unpublished data, patent-pending AMP). This master project used CHX base as a mimicked AMP. CHX is significantly cheaper and commercially available.

2.4 Drug delivery systems of choice

There are few nanocarriers with AMPs implemented in clinical trials so far. Developing a suitable drug delivery system for clinical trial is still a challenge (Biswaro et al., 2018). A drug delivery systems that are promising and have received a lot of interest, especially regarding dermal delivery, are liposomes (Sala et al., 2018).

2.4.1 Liposomes

Liposomes are small drug carriers and a promising drug delivery system, due to their versatile characteristics, amphiphilic properties, biocompatibility and biodegradability. Liposomes are spherical vesicles consisting of unilamellar, oligolamellar or multilamellar lipid bilayers surrounding an aqueous chamber (Figure 5). Because of a hydrophobic bilayers surrounding a hydrophilic aqueous core, as drug carrier, liposomes can incorporate or embed both hydrophilic, hydrophobic as well as amphiphilic compounds (Samad et al., 2007, Maherani et al., 2012).

The lipid bilayer of the liposome consists of amphiphilic compounds such as phospholipids, that are biodegradable and biocompatible (Akbarzadeh et al., 2013). A phospholipid that is very often used in the membrane is zwitterionic PC (Olusanya et al., 2018). PC is generally recognised as safe by FDA (Zobel, 1976). PC consist of two fatty acid chains linked to a glycerol bridge and further to the polar head group, choline. Liposomes composed of PC are expected to exhibit near natural zeta potential since PC is zwitterionic (Soema et al., 2015).

When phospholipids are dispersed in aqueous solutions, they are able to self-associate and spontaneously form closed structures (Samad et al., 2007). The formation phospholipids create is thermodynamically favourable due to hydrophobic effect of acyl chains in hydrophilic aqueous medium, in addition the hydrogen bonding, van der Waals forces and other electrostatic interactions will enhance the enclosed structure (Pattni et al., 2015).

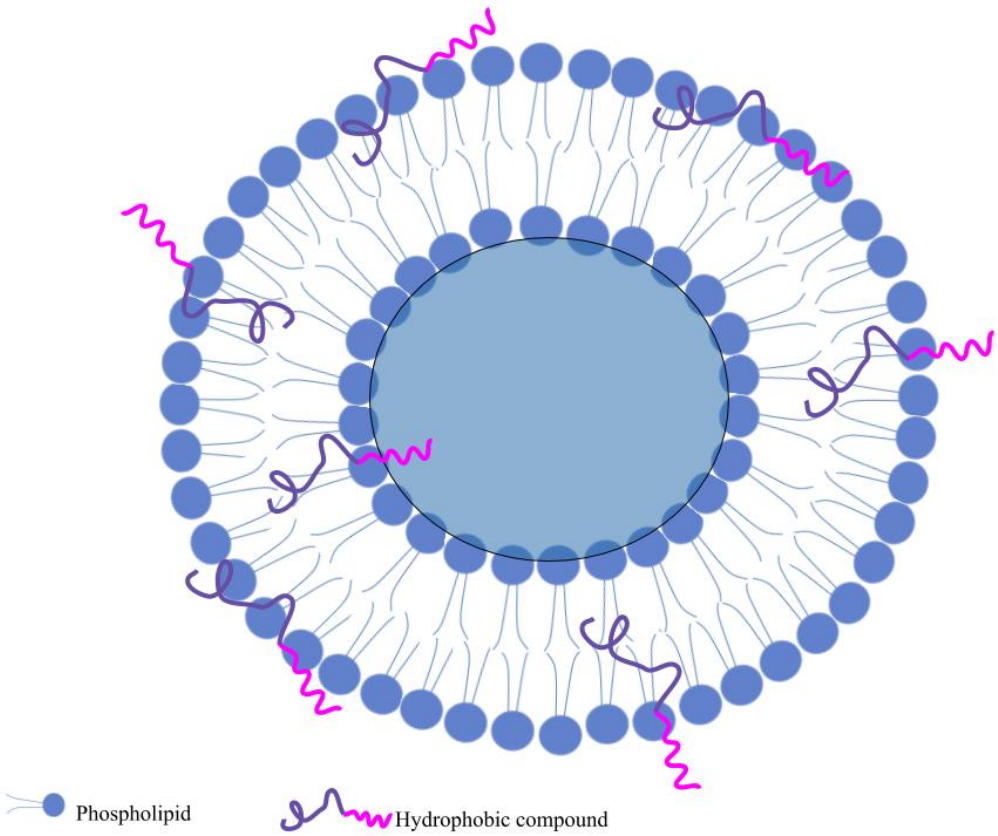

Figure 5: A unilamellar liposome with embedded hydrophobic compound in the phospholipid bilayer. A hydrophobic compound such as AMP can arrange itself in different ways within the phospholipid bilayer as the figure illustrates. Created with Google draw.

The lipid composition, lamellarity, size, size distribution, method of preparation and charge of liposomes are important factors for the drug carrier properties. Liposomal size can vary from 25 nm to 2.5 µm (Akbarzadeh et al., 2013). The liposomal properties will affect the *in vitro* behaviour (drug loading, aggregation and sedimentation) as well as the *in vivo* behaviour (circulation time in the body and biodistribution if administered systemically) (Hupfeld et al., 2006) or skin penetration (Sala et al., 2018). Thus, it is important to optimise the liposomal properties in regard to the desired administration route, which in our project was skin.

2.4.1.1 Liposomes and skin

Although it was thought that conventional liposomes could be used for transdermal delivery, it appears that the conventional liposomes will remain in the upper layer of *stratum corneum* and not penetrate the intact skin (Elsayed et al., 2007). However, liposomal dispersions have potential as a drug delivery system for treating skin disease, especially infections (Ingebrigtsen

et al., 2016). Conventional liposomes are typically used for dermal administration routes. Phospholipids used to build liposomes have structural similarities with the lipids in epidermis, which contributes to them being biocompatible and enables them to promote skin penetration (Hua, 2015). Liposomes can adhere to the skin surface and potentially lead to skin hydration, loose structure, fluidisation and even lipid exchange. However, studies on conventional liposomes penetrating skin and impaired skin are scarce (Sala et al., 2018).

The original technique for preparation of liposomes is the "thin film method" (Bangham et al., 1965). In this method, the lipid is dispersed in organic solvent and the solvent removed under vacuum by evaporation, forming a dry thin lipid film. This dry thin lipid film is rehydrated using an aqueous solution and the lipids are spontaneously forming liposomes as described earlier. However, unless processed, the liposomal size distribution and lamellarity is quite heterogeneous (Samad et al., 2007).

Several factors influence the efficacy of topical delivery via liposomes such as the vesicle size, zeta potential, lipid composition and amount of entrapped drug (Sala et al., 2018). The dermal drug delivery is highly dependent on liposomal size. The liposomal size will regulate the location of the depot effect of a lipophilic compound in the skin. An intermediate vesicle size of 300 nm will provide the highest reservoir deepest in *stratum corneum* and therefore highest drug concentration in the intended tissue (Danaei et al., 2018). Generally large vesicles with a size over 600 nm fail to deliver compounds to the deeper layers of the skin (Hua, 2015). The size distribution of liposomal size is characterized by a dimensionless measurement called polydispersity index (PI) that describes the broadness of the size distribution from cumulative analysis. A PI value is between 0 and 1 (Danaei et al., 2018). A small PI value <0.1 indicates a homogenous size distribution and a PI >0.3 indicates higher heterogeneity (Verma et al., 2003).

Dermal local treatment could provide a higher patient compliance because of decreased adverse effects, faster clinical effect and non-invasive application (Sala et al., 2018). However, a major limitation for liposomal dispersions is their physical and chemical stability. Liposomes are prone to aggregation or fusion which in turn can lead to changes in vesicle sizes and significant loss of the encapsulated compound (Olusanya et al., 2018). Loss of encapsulated drug is

unfortunate as it can lead to therapeutic failure. AMPs should not be absorbed from the wound to systemic circulation because they can cause systemic adverse effects and provoke allergic sensitisation (Pfalzgraff et al., 2018). Wound comprises the impaired skin barrier and, in theory, a very small liposome (< 20 nm) could penetrate wound bed. In addition, when treating a wound a wound dressing should also fulfil the specific properties for successful healing as described earlier (Saghazadeh et al., 2018). The liposomal dispersion would need a secondary vehicle suitable for skin administration due to a short residence time, leakage (sliding) from the skin surface and improvement of physical stability. To expand the contact time between the drug-loaded liposomes and the skin; liposomes can be incorporated into a hydrogel which increase the potential of a successful treatment (Ingebrigtsen et al., 2016). Moreover, the vehicle can provide synergistic properties, especially chitosan-based hydrogels (Hurler et al., 2013, Ternullo et al., 2019, Ternullo et al., 2020).

A wound dressing should support cellular adhesion, prevent growth of bacteria, retain moisture and be oxygen permeable to assure oxygen access to the healing tissue (Saghazadeh et al., 2018). Therefore, by incorporating liposomes into a hydrogel the formulation will comprise two drug delivery systems that are able to provide sustained release of AMPs and promote wound healing.

2.4.2 Hydrogels

Hydrogels can be an excellent drug carrier that can extend a drug residence time on the location applied. Hydrogels are hydrophilic networks that consists of polymers that are insoluble but compatible with aqueous media thus allowing it to swell. The chemical/physical crosslinks between polymers are what makes them insoluble. The polymers have high affinity for water and when the water penetrates the network of the gel, it starts swelling (Peppas et al., 2000, Bhattarai et al., 2010).

The swelling of the hydrogel can be reliant on the external environment, such as pH, temperature and ionic strength (Peppas, 1997). The physical properties of the hydrogels are affected by charge and MW of the polymer and the density of the cross-linking. Polymers with

low MW require a higher concentration to produce adequate gel stiffness, while high MW polymers make more rigid hydrogels at lower concentrations (Bhattarai et al., 2010). In this project, we tested two different polymers; Carbopol and chitosan (see section 2.4.2.1 and 2.4.2.2).

A fully swollen hydrogel is quite similar to living tissue; it is soft, elastic and have low interfacial tension. An advantage with low interfacial tension of the hydrogels is that the absorption of proteins and cell adhesion is decreased which in turn reduce the chance of negative immune response. Hydrogels are able to absorb a large amount of water and are mainly used to draining wounds. Because of the mechanical properties and similarity to natural ECM, hydrogels support cells in the regeneration process and can also deliver a sufficient drug payload (Liu et al., 2018). The network and intrinsic structure of a hydrogel is porous and hydrophilic which will assure gas exchange and fluid balance. Gas exchange ensures access of oxygen for the healing wound and removal of waste, and fluid balance ensures the absorption of excess exudate while maintaining the wound area moistened (Saghazadeh et al., 2018).

In general, a hydrogel system is favourable when it comes to protection from external pathogens to wounds. In the case of wounds exhibiting biofilms, there can be persistent bacterial infections and hydrogels will enable close contact between the wound and antimicrobial. The use of a hydrogel provides a drug depot assuring sustained release of membrane active antimicrobials leading to a higher local drug concentration over a period of time (Pfalzgraff et al., 2018). However, for a hydrogel to achieve successful drug delivery it is important that the gel has desired textural properties (Hurler and Škalko-Basnet, 2012), see section 2.4.3.1.

A hydrogel system must also be biocompatible, non-immunogenic and biodegradable, which is very dependent on the polymer used to make the hydrogel (Pfalzgraff et al., 2018). One of the most widely used polymer is synthetic acrylic acid (Carbopol) (Grip et al., 2017).

2.4.2.1 Carbopol hydrogels

Carbopol is acrylic acid polymer that is cross-linked and insoluble (Figure 6). The polymer becomes a stiff hydrogel when dispersed in water and neutralised with an appropriate amount of base. A typical neutralising agent can be organic amines. At a pH around 7, the gel has desired viscous behaviour and is suited for application on skin. At a lower pH than 6, the gelling process might not be sufficient and at a pH over 10 there can be excess of electrolytes that leads to decreased electrostatic repulsion which results in a reduction of the firmness of the gel (Fresno et al., 2002).

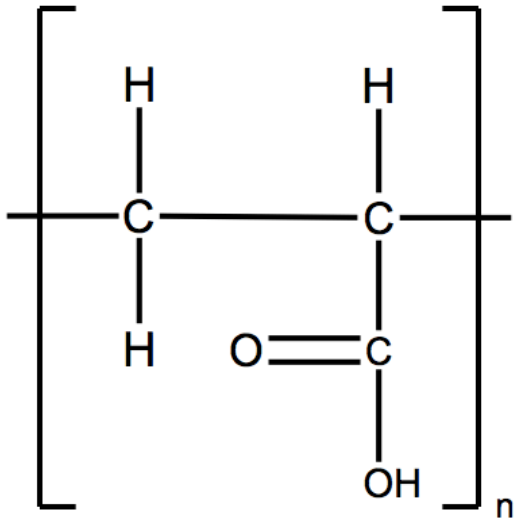

Figure 6: Chemical structure of acrylic acid monomer. Created with chemdrawdirect.perkinelmer.cloud.

The Carbopol hydrogels have unique rheological properties and can absorb large amount of water without much change in the texture properties (Hurler et al., 2013). The gel is very temperature stable (Islam et al., 2004), has high viscosity at low concentration of Carbopol, compatible with many active components and have good bioadhesive properties (Romanko et al., 2009). However, there are some concerns regarding potential toxicity of Carbopol hydrogels as wound dressings (Grip et al., 2017).

Another widely used polymer in the pharmaceutical practice is chitosan. Unlike Carbopol, chitosan offers additional beneficial activities such as enhancing wound healing and antimicrobial activity (Matica et al., 2019).

2.4.2.2 Chitosan hydrogels

Chitosan is made from chitin. Chitin is a polymer quite abundant in nature and can be found in insects, certain fungi, shells and as in this project from shrimps. The polymer chitin is poorly soluble, but by partial deacetylation of chitin the more suitable polymer chitosan is made (Figure 7) (Dash et al., 2011). Chitosan is an excellent excipient as biomaterial because it is well documented biocompatibility, biodegradability and safety, in addition it is also haemostatic, have wound healing properties as well as exhibits intrinsic antimicrobial activity (Bhattarai et al., 2010, Matica et al., 2019).

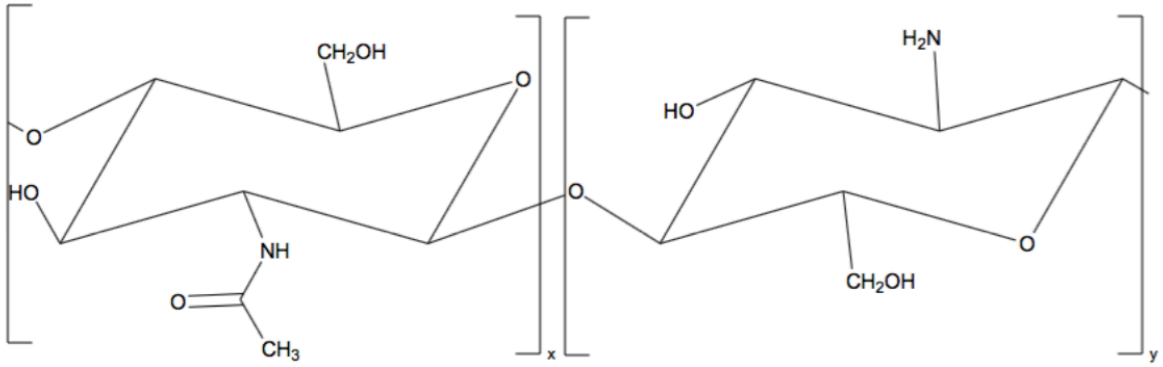

Figure 7: Chemical structure of chitosan. Created with chemdrawdirect.perkinelmer.cloud.

Chitosan has functional amino groups and the amin has pKa at 6.3. It is the nitrogen and the fact that it has cationic charge that make chitosan distinct from others polymers (Bhattarai et al., 2010). The structure of chitosan (seen in Figure 7) is similar to glycosaminoglycan, a component of ECM that is recommended for use in skin tissue engineering (Matica et al., 2019).

Many physicochemical and biomedical properties of chitosan are dependent on the degree of deacetylation and MW. The degree of acetylation refers to the distribution of amino groups in

the polymer chain (Matica et al., 2019). The degree of acetylation and MW affects the antimicrobial effect, because of higher solubility and increasing its positive charge. Chitosan solubility in acidic aqueous medium and its antimicrobial properties are dependent on the acetylation degree. At a pH under 6 chitosan becomes water soluble because of protonating amines and opposite if the pH is above 6, chitosan becomes deprotonated and insoluble (Dash et al., 2011).

Chitosan is soluble in acid medium because of the presence of the amine groups. To make a chitosan hydrogel, the polymer needs to be dispersed in acidic medium and make cross-links that water penetrates, allowing the swelling of the hydrogel to occur. The hydrogels provide a moist environment at the wound site, are water retaining, oxygen permeable, bioadhesive and have high absorption properties (Matica et al., 2019). Chitosan hydrogels also have antimicrobial and anti-inflammatory properties, which are advantageous for wound healing. The positive charge of chitosan is likely to interact with the negatively charged bacterial membrane, which is key for the antimicrobial effect. Chitosan hydrogel will create an appropriate inflammatory microenvironment beneficial for the wound to heal. Since the chitosan hydrogel exhibits antimicrobial and anti-inflammatory effects, the hydrogel formulation can work synergistically with the AMPs. When the chitosan hydrogel is in addition loaded with the antimicrobial compound, the drug delivery system can heal infection and prevent secondary infection which in turn leads to an accelerating wound healing (Liu et al., 2018).

In this project, we chose to further work with chitosan instead of Carbopol because of these additional features of chitosan assuring a strong synergistic effect. We only used Carbopol hydrogel as a control in the development and validation of a texture analysis method, as it is a widely used polymer, particularly by pharmaceutical and cosmetic industries.

2.4.3 Liposomes-in-hydrogel formulation

Liposomes-in-hydrogel formulation is a drug delivery system expected to incorporate and protect active compounds, enable close contact with the wound bed, assure sustained release and be safe to use (Figure 8). The hydrogel is semisolid and viscous; it will adhere to the skin and allow the drug to retain on the skin over desired time for therapeutic effect. If the AMPs or other membrane active antimicrobials are poorly water soluble, liposomes will act as a drug solubiliser. In addition, liposomes are biodegradable and non-toxic and can increase the amount of drug deposited into the upper layers of the skin. Liposomes will also protect substances that can be degraded when formulated in plain hydrogels. All mentioned, makes the liposomes-in-hydrogel formulation a promising and superior drug delivery system for the skin therapy (Hurler et al., 2013).

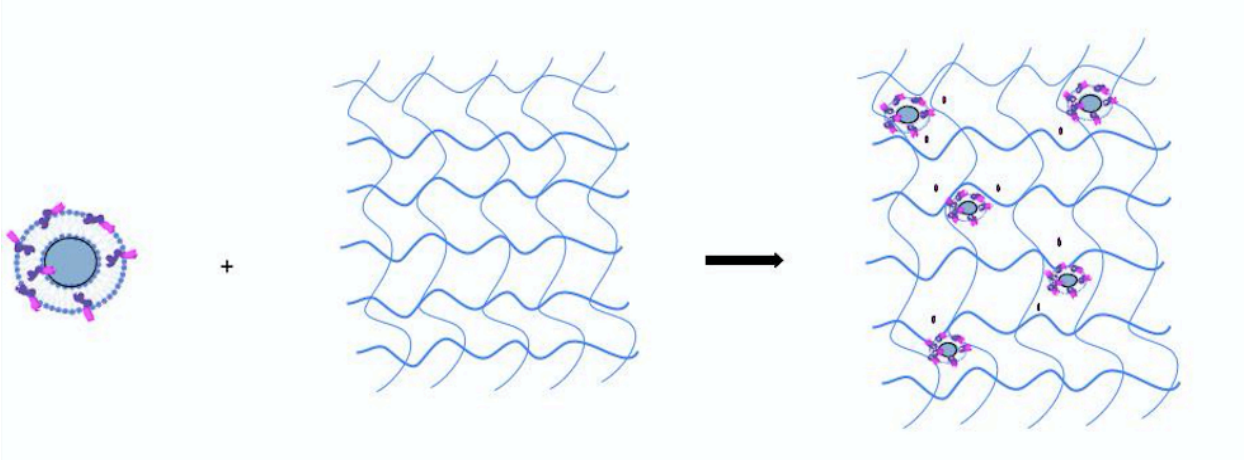

Figure 8: Liposomes-in-hydrogel, from the left: liposome with a hydrophobic compound, cross-linked network of a hydrogel and liposomes loaded with a hydrophobic compound loaded inside a hydrogel network. Created with Google Draw.

For a compound to be released from the liposomes-in-hydrogel formulation, the compound needs to first be released from liposomes into the hydrogel, diffuse through and out of the hydrogel. Hurler *et al.* suggested that liposomes with negative zeta potential had increased release into the hydrogel (chitosan hydrogel), whereas liposomes bearing positive charges had a decreased release into the hydrogel compared to the release measured from neutral liposomes (Hurler et al., 2013). Incorporation of liposomes into a hydrogel will influence rheological properties of hydrogels and the amount of liposomes added to the gels affect the release of

hydrophobic compounds (Mourtas et al., 2008). The liposomes-in-hydrogel formulation should give a stable drug delivery over time and, in wound treatment, mimic ECM structure and functionality; these characteristics are highly dependent on the textural properties of the hydrogel.

2.4.3.1 Textural properties of hydrogels

Textural properties of hydrogel are very important considering the delivery of a topical non-polar compound. To evaluate the textural properties of a hydrogel texture analyser (T.A.) with the backward extrusion rig is often applied. In the setup for the T.A., a beaker is filled with gel and disks of certain sizes are attached to a movable probe. In a T.A.-run the disc is submerged into the gel and when a certain trigger force is attained (the point where the disc's lower surface is in full contact with the gel) the plotting of the graph starts and continuous as the disc proceeds to penetrate the gel down to a specified point. At this point the maximum compressing force is plotted on the graph and the disc starts its return towards the start position (Figure 9). This analysis can provide information about gels parameters such as hardness, adhesiveness and cohesiveness (Jones et al., 1996).

Hardness is the maximum compressing forces applied on the hydrogel and provides the information on the firmness of the gel and the applicability of the gel as skin formulation. Adhesiveness is the work required for the disc on T.A. to redraw from the gel and is displayed as the negative area under the curve. Adhesiveness can indicate the retention time on the application area. Cohesiveness is the work required to deform the hydrogel and is displayed as the positive area under the curve. Cohesiveness indicates the internal stickiness of the hydrogel (Figure 9) (Hurler et al., 2012). More details are provided in the Methods part.

A simplified and reproducible method for the analyser could give information about the texture properties of the hydrogel that could be parameters for stability of the hydrogel and the microgel network. The information about texture properties can also be valuable in the formulation development and in-process control (Hurler et al., 2012) .

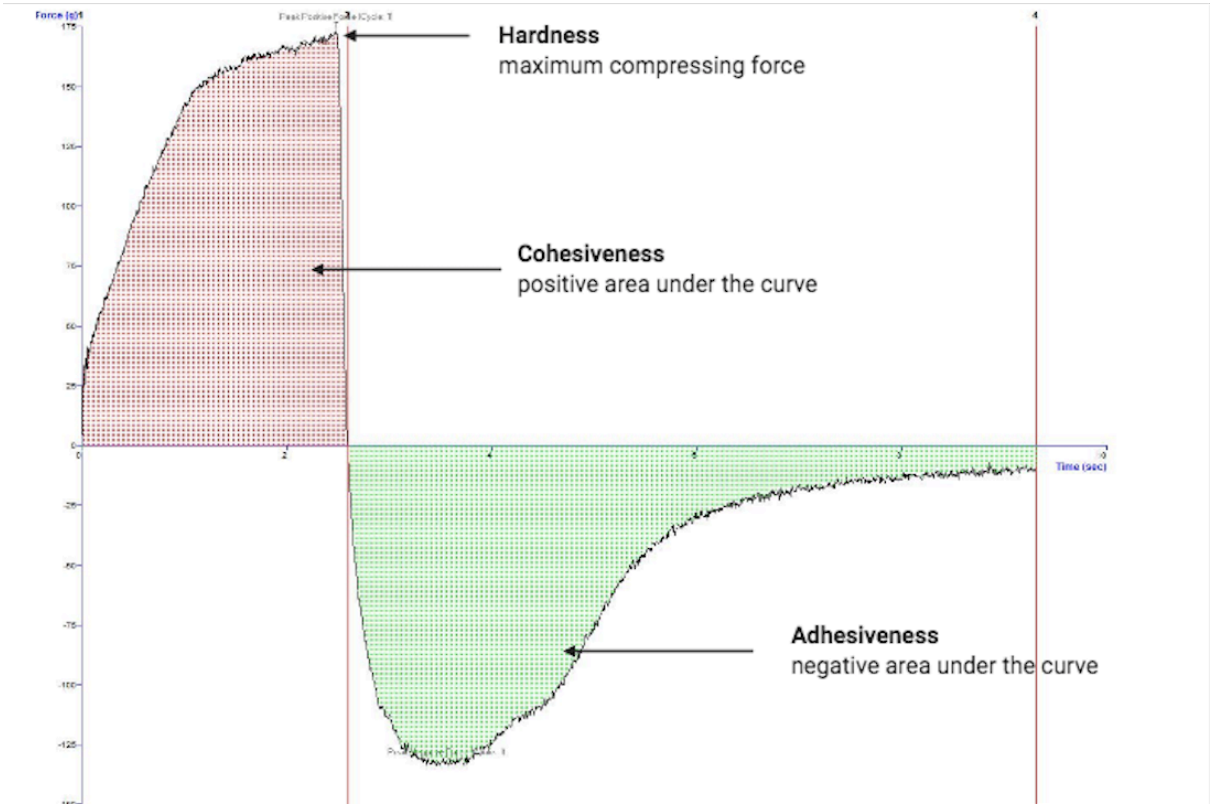

Figure 9: Typical force versus time plot of a backward extrusion measurement of chitosan hydrogels. The y-axis is force and the x-axis is time. The peak of the positive curve is the maximum compressing force, the positive area under the curve represent cohesiveness and the negative area under the curve represent adhesiveness.

The mechanical strength of a hydrogel should comprise a balance between adhesiveness and cohesiveness. The hydrogel should be stable (have high cohesiveness) but not to firm to apply to the skin (not too high hardness that would require strong rubbing of wounded area). Optimal textural properties of the gel should increase the compliance of the patient (Hurler et al., 2012).

Hydrogel as a drug formulation should resist stress that comes from movement of the skin and should retain on the surface long enough for the compound to leave the formulation and provide a desired therapeutic effect. The textural properties must be optimised so that the dressing stays attached and do not slide of therefore interrupting the healing. It is important that the gel is easily applied and removed from the skin to make it less painful for the patient. (Matica et al., 2019).

As mentioned earlier we chose to work further with chitosan hydrogels instead of Carbopol hydrogels in this project. A disadvantage of chitosan hydrogels compared to Carbopol hydrogels, is that chitosan hydrogels have a lower mechanical strength. Therefore, to improve the mechanical strength (and also the retention time to the wound site) a viscosity enhancer can be added to the hydrogel (Carvalho et al., 2013). We choose to use glycerol as viscosity enhancer and stabilising agent. Glycerol is expected to stabilize the network in the chitosan gel and improve the stability (Hurler et al., 2012, Szymańska and Winnicka, 2015).

3 Aim of the study

The aim of this project was to optimise a novel formulation for membrane active antimicrobials for improved wound therapy. A liposomes-in-hydrogel formulation with an antimicrobial has been proposed as a drug delivery system that enable prolonged and controlled release of compound and promote wound healing. We focused on optimisation of liposomes and hydrogels in regards to vesicle characteristics, drug load, drug release, anti-inflammatory effect and hydrogel properties and used chlorhexidine as a model compound.

Specific aims:

- Optimisation of liposomal formulation in respect to drug entrapment efficiency, vesicle size, size distribution, membrane elasticity and morphological observations.
- Evaluation of liposomal stability after storage at 4 °C for up to 12 weeks.
- Development and validation of a reproducible texture analysis method for hydrogel characterisation and evaluating hydrogel texture properties to optimise the formulation.
- Determination of anti-inflammatory effect of the novel formulation in murine macrophages.
- Optimising *in vitro* release study for the novel formulation.

4 Materials, Equipment and Instruments

4.1 Materials

Acetic acid (≥ 99.9 %), VWR International S. A. S., Fontenay-sous-Bois, France.

Albunorm™ 200 g/L, Octapharma AG, Lachen, Sveits.

Bovine serum albumin, Sigma-Aldrich, St. Louis, USA.

Calcium chloride dehydrate, Sigma-Aldrich, St. Louis, USA.

Carbopol ® Ultrez 20 polymer, Lubrizol, Oevel-Westerlo, Belgium.

Chitopharm™ M, 350 - 600 kDa, 87.4 % degree of deacetylation, Chitinor, Tromsoe, Norway.

Chlorhexidine (≥ 99.5 %), Sigma-Aldrich, St. Louis, USA.

Ethanol 96 %, Sigma-Aldrich, St. Louis, USA.

Ethanol absolute, Sigma-Aldrich, St. Louis, USA.

Fetal bovine serum (FBS), Sigma-Aldrich, St. Louis, USA.

Glycerol solution, (86-89 %), Sigma-Aldrich, St. Louis, USA.

Kollisolv ®, polyethylene glycol (PEG) 400, Sigma-Aldrich, St. Louis, USA.

Lipoid S100 (>94 % phosphatidylcholine), Lipoid GMBH, Ludwigshafen, Germany.

Lipopolysaccharides (LPS) from *Escherichia coli* O55:B5, Sigma-Aldrich, St. Louis, USA.

Methanol gradient for HPLC, VWR International S. A. S., Fontenay-sous-Bois, France.

Milli-Q filtered water

Murine macrophage cell line, RAW 264.7, ATCC, Manassas, USA.

N-(-1-Naphthyl)ethylenediamine dihydrochloride, Sigma-Aldrich, St. Louis, USA.

Osmium tetroxide, Sigma-Aldrich, St. Louis, USA.

Phosphoric acid (>85 %), Kebo lab, Oslo, Norway

Potassium chloride (> 99.5 %), Sigma-Aldrich, St. Louis, USA.

Propylene glycol (PG), Sigma-Aldrich, St. Louis, USA.

RPMI-1640 Medium with L-glutamine and sodium bicarbonate, liquid, Sigma-Aldrich, St. Louis, USA.

Sodium hydrogen carbonate, Sigma-Aldrich, St. Louis, USA.

Sodium chloride (NaCl), Sigma-Aldrich, St. Louis, USA.

Sodium nitrite ($NaNO_2$), Sigma-Aldrich, St. Louis, USA.

Sodium phosphate dibasic dihydrate ($Na_2HPO_4 \times 2H_2O$), Sigma-Aldrich, Steinheim, Germany.

Sulfanilamide, Sigma-Aldrich, St. Louis, USA.

Triethanolamine ($\geq$ 99.0 %), Sigma-Aldrich, Steinheim, Germany.

Tween® 80, polysorbate 80, St. Louis, USA.

4.2 Equipment

Cellophane foil, Bringmann folia, Wendelstein, Germany.

Corning UV-plate 96 well transparent, Corning Inc., Kennebunk, USA.

Spectra/Por ® 4, Dialysis membrane tubing, MWCO 6-14 kD, VWR, Wayne, USA.

Hamilton 1725 N, 250 µl Syringe, Hamilton Company, Reno Nevada, USA.

NuclePore ® Track-Etched Membranes (PC) polycarbonate, size 0.8 µm, 0.4 µm, 0.2 µm, Whatman International Ltd., Maidstone, UK.

Nunc™ EasYFlask™ 75 cm^2 Nunclon™ Delta Surface, Thermo Fisher Scientific, Waltham, USA.

Poly-prep slides, Poly-L-lysine coated glass slides, Sigma-Aldrich, Loius, USA.

Sterile Syringe Filter w/ 0.2 µm polyethersulfone membrane, VWR, Wayne, USA.

SuperClear ® Centrifuge Tubes with Plug Style Caps, 15 mL, VWR, Wayne, USA.

Tissue Culture Plate, 24 Well, Flat bottom with low evaporation lid, Corning Incorporated, Durham, USA.

Zetacell DTS1070, Malvern Instrumentals Ltd., Malvern, UK.

4.3 Instruments

Accumet ®, Portable pH meter kit, AP115, Fischer scientific, Massachusetts, USA.

Bransonic ® 5510R-MT Ultrasonic cleaner, Branson Ultrasonics Corporation, Danbury, USA.

Biofuge stratus centrifuge, Heraeus instrument, Kendro laboratory products GmbH, Osterode, Germany.

Büchi Rotoevaporator R-124, with Büchi V-700 Vacuum Pump system, Büci Vacuum Controller V-850 and Büchi WaterBath B-480, Bücho labortecknic, Flawil, Switzerland.

Franz diffusion cell 15 mm, 12 ml chamber, (#4G-01-00-15-12), Permeagear, Hellertown, USA.

Hitachi HT7800 Transmission Electron Microscope (TEM), Hitachi Ltd., Tokyo, Japan.

Mettler Toledo PR5002 Deltarange®, scale, Mettler Toledo AG, Greifensee, Switzerland.

NICOMP Submicron Particle Sizer, model 370, Particle sizing system (PSS), Santa Barbra, USA.

Puranity PU 15+, Water purification system, VWR, Bruchsal, Germany.

Rotavisc hi-vi II Complete, viscometer, IKA-Werke GmbH & CO, Staufen, Germany.

Sartorius LP620S, scale, Sartous AG, Göttingen, Germany.

Sartorius QUINTIX 124-15, scale, Sartourius Lab Instrument GmbH & Co., Göttingen, Germany.

SensION^{TM}+ PH31, GLP laboratory pH meter, Hach, Düsseldorf, Germany.

Tecan Spark M10 multimode plate reader, Tecan trading AG, Männedorf, Switzerland.

TA.XT. Plus Texture Analyser with back extrusion rig (A/BE), Stable Micro Systems Ltd., Surrey, UK.

Vortex Genie 2 ^{TM}, Bender & Hobeinag, Zürich, Switzerland.

Zeiss Sigma Field Emission Scanning Electron Microscope (FE-SEM), Carl Zeiss AG, Oberkochen, Germany.

Zetasizer nanoseries, model Zen 2600, Malvern Instrumentals Ltd, Malvern, UK.

4.4 Computer programs

IKA Rotavisc Hi-Vi II, Labworldsoft 6.2.3.2, IKA-Werke GmbH & CO, Staufen, Germany.

NICOMP particle sizing system, CW388 Application Version 1.68, California, USA.

Texture exponent software, Texture technologies Corporation and stable Micro Systems Ltd., Software version 6.1.16.0, Hamilton. USA.

Tecan sparkcontrol method editor, system version 2.3. Tecan Group Ltd., Männedorf, Switzerland.

Zetasizer software version 7.13, Malvern Instrument Limited, Malvern, UK.

Sigma SmartSEM version 6.03, Carl Zeiss AG, Oberkochen, Germany.

5 Experimental section

5.1 Spectral analysis and standard curve of CHX

To determine the maximum absorbance peak (λ_{max}), a solution of CHX in methanol in a concentration of 1000 µg/mL was made. Tecan Spark M10 multimode plate reader was set at absorbance scan mode to detect λ_{max} for CHX. The λ_{max} was measured to be at 261 nm.

For the standard curve, a stock solution of CHX in methanol in a concentration of 500 µg/mL was prepared. From the stock solution there were made dilutions to prepare the solutions of 40, 20, 10, 5, 2.5 and 1.25 µg/mL with methanol. The measuring wavelength was set at 261 nm. A standard curve was made by plotting each concentration of the standard solutions against their absorbance.

5.2 Preparation of liposomes (thin film method)

5.2.1 Preparation of empty liposomes

Lipoid S100 (200 mg) was directly weighed in a 50 ml round bottom flask, dissolved in 10 ml methanol and hand-shaken until a clear solution was observed. The lipid was dehydrated using a Bütchi Rotovapor. During evaporation, the temperature was set to 45 ºC and rotation at 60 rpm. The pressure was lowered slowly to 60 mBar and the solvent evaporated at the desired pressure for 1 hour. The dry lipid film was rehydrated with 10 ml distilled water and hand shaken a couple of minutes to dislodge all the film. Then the liposomes were stored in refrigerator (4-8 ºC) overnight before any further experiments.

5.2.2 Preparation of CHX liposomes

CHX (10 mg) and Lipoid S100 (200 mg) were weighed directly into the round bottom flaks. The same procedure for preparation of empty liposomes was used for CHX liposomes, with exception that the pressure was lowered even slower down to 60 mBar to avoid boiling of the organic solvent (Figure 10).

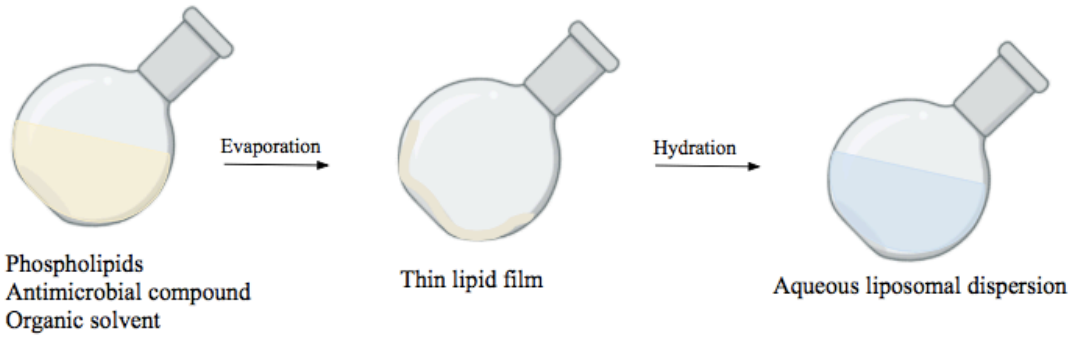

Figure 10: Preparation of liposomes and passive loading of compound. From left: Phospholipid, active ingredient and organic solvent mixed in round bottom flask, a thin lipid film made by evaporation, thin film hydrated forming an aqueous liposomal dispersion. Created with Google Draw.

5.3 Size reduction of liposomes

5.3.1 Membrane extrusion

Empty liposomes were extruded with Nuclepore® polycarbonate membranes at pore sizes 0.8 µm three times, 0.4 µm five times and 0.2 µm two times. CHX liposomes were extruded with a Nuclepore® membrane at sizes 0.8 µm and 0.4 µm five times each. After the extrusion the liposomal dispersions were stored overnight in refrigerator (4-8 ºC) before further investigation.

5.4 Liposomal characterisation

5.4.1 Vesicle size determination

5.4.1.1 Empty liposomes

The size and size distribution of empty liposomes were determined using Zetasizer nano zen 2600. Before the measurement, disposable cells were rinsed with methanol and freshly filtered (0.2 µm filters) deionised water. The liposomal dispersion was diluted 1:100 (v/v) and transferred to the rinsed disposable cells. Each sample was measured in three parallels at room temperature (23-25 ºC).

5.4.1.2 CHX liposomes

The size and size distributions of the CHX liposomal dispersions were determined by photon correlation spectroscopy on a NICOMP Submicron particle sizer. Prior to testing the test tubes were put in distilled water and in an ultrasonic bath for 10-15 minutes. Further preparation of the sample was done in a laminar airflow to avoid contamination of dust particles. Here the test tubes were cleansed three times with distilled water filtered with syringe filter (0.2 µm filters). The sample was diluted with filtered distilled water to achieve an intensity of 250-350 KHz (Hupfeld et al., 2006). The sample was measured in three cycles of 10 minutes at temperature of 24 ± 1 ºC and a scattering angle was of 90º.

5.4.2 Zeta potential determination

Zeta potential was measured on a Zetasizer nano zen 2600. Prior to measurements the liposomal dispersion was diluted with appropriate amount of filtrated deionised water (0.2 µm filters) to a total volume of 1 mL. The dispersion was transferred to a disposable folded capillary cell (DTS1070) that had been cleaned beforehand with methanol and filtered deionised water. The measurements were conducted at room temperature (23-25 ºC) and measured in three parallels.

5.4.3 Liposome elasticity measurements

Before measuring the degree of elasticity of the liposomal bilayer, the liposomal dispersion was extruded through a polycarbonate membrane with a 100 nm pore as size and a constant pressure of 2.5 bar. After 5 minutes of extrusion, the amount of extruded liposomal dispersion was determined. The degree of membrane elasticity (E) of the CHX liposomes was calculated with the following equation:

Equation 1:

$$E = J * (\frac{r_v}{r_p})^2$$

where J is the amount of liposomal dispersion (g) extruded at 5 minutes, r_v is the mean diameter (nm) of liposomes after extrusion and r_p is the pore size of the membrane (nm). Empty liposomes were used as a control (Ternullo et al., 2019).

5.4.4 Entrapment efficiency (EE)

Before determination of the entrapment efficiency (EE), the free CHX had to be separated from the liposomal dispersion. Because of detection limit, the solubility to CHX and CHX interaction with the membrane we used two different methods to separate free CHX from the liposomal dispersion. We used the dialysis and centrifugation as separation methods and compared the findings.

5.4.4.1 Dialysis

Free drug was separated from liposomal entrapped drug by dialysis using dialysis tubing (MW cut-off 12.000-14.000 Da). A ratio of 1:100 mL (liposomal sample: dialysis medium, distilled water) was used and duration of dialysis was 4 hours. After dialysis, the liposomal dispersion in the dialysis bag was diluted 1:40 (v/v) and the dialysis medium was diluted 1:2 (v/v), both with methanol. Both the samples from dialysis and original non-separated liposomal sample

(also diluted 1:40 (v/v) with methanol) were analysed on Tecan Spark M10 multimode plate reader at 261 nm.

The entrapment efficiency and relative recovery was calculated using equations below:

Equation 2:

$$Entrapment\ efficiency\ (EE\ \%) = \frac{B}{A}\ x\ 100\ \%$$

Where A is the amount of CHX in original sample and B is amount of CHX in dialysed sample.

Equation 3:

$$Relative\ recovery\ (RR\ \%) = \frac{A}{C}\ x\ 100\ \%$$

Where A is the amount of CHX in original sample and C is calculated amount CHX based on weighed amount CHX.

5.4.4.2 Centrifugation

CHX was separated from liposomal dispersion by centrifugation. The centrifuge was set to 4872 g for 30 minutes at 4 °C (Maqbool et al., 2018). The incorporated CHX in liposomes (supernatant) was quantified on Tecan Spark M10 multimode plate reader at 261 nm and EE was calculated using equation 2. Prior to the measurement, all samples were diluted 1:40 (v/v) with methanol.

5.4.5 Morphology

5.4.5.1 Transmission electron microscope (TEM)

The morphological characteristics of the CHX liposomes were examined using transmission electron microscope (TEM) at 20-120 kV acceleration voltage. Before TEM measurements, the CHX liposomes were mounted onto glow discharged 400 mesh carbon-coated grids for 5

minutes and stained with uranyless for 20 seconds. The sample air-dried for 30 seconds before measurements (Sybil Obuobi, to be published).

5.4.5.2 Scanning electron microscopy (SEM)

The morphological characteristics of the CHX liposomes were examined using scanning electron microscopy (SEM). Before the image processing, the sample was prepared with a standard method for preparation of cells.

The CHX liposomal dispersion was first prefixed overnight. The following day, a drop of the liposomal sample was transferred to poly-l-lysine-coated glass slides for 5-minute-sedimentation, and rinsed with PHEM (PIPES-HEPES-EGTA-Magnesium sulphate)-buffer for 2 minutes, two times, before the sample was post-fixated with 1 % osmium tetroxide for 30 minutes. Afterwards, the sample was dehydrated with ethanol series: 5 minutes with 30 % ethanol, 5 minutes with 60 % ethanol, 5 minutes with 90 % ethanol, 5 minutes with 96 % ethanol and finally 5 minutes with absolute ethanol four times, before a critical point-based drying was performed. The sample was mounted onto a stub and coated with gold/palladium using a sputter coater before viewing (Hira et al., 2019).

5.5 Preparation of hydrogels

5.5.1 Preparation of plain Carbopol gel

Carbopol Ultrez™ 20 powder was weighed and dispersed in appropriate amount of distilled water (weight of polymer and volume of water concurring to the desired concentration in the hydrogel, which was 0.5 % (w/w)). A couple of drops triethanolamine was added to neutralise the aqueous medium to a desired pH-value and to form the gel. The hydrogel was allowed to equilibrate for 24 hours at room temperature (23-25 ºC).

5.5.2 Preparation of chitosan gel

5.5.2.1 Plain chitosan hydrogel

Chitosan™ M was dispersed in a mixture containing 2.5 % (w/w) acetic acid and distilled water, forming a 5.0 % (w/w) chitosan gel. The hydrogel was stirred manually by hand for approximately 10 minutes. The gel was then bath sonicated for 30 minutes to remove bubbles and allowed to swell for 48 hours at room temperature (23-25 ºC).

5.5.2.2 Chitosan gel with 10 % (w/w) glycerol

Chitopharm™ M and glycerol were dispersed in a mixture containing 2.5 % (w/w) acetic acid and distilled water, forming a 5.0 % (w/w) chitosan gel comprising 10 % (w/w) glycerol. The hydrogel was stirred manually by hand for approximately 10 minutes. The gel was then bath sonicated for 30 minutes to remove bubbles and allowed to swell for 48 hours at room temperature (23-25 ºC).

5.5.3 Preparation of liposomes-in-hydrogel formulation

5.5.3.1 Empty liposomes-in-Carbopol-hydrogel

Empty liposomes were mixed into 0.5 % (w/w) Carbopol hydrogel by a hand stirring until the liposomal dispersion was evenly distributed, and stored at 4-8 ºC in the refrigerator.

5.5.3.2 Empty liposomes-in-chitosan-hydrogel

Empty liposomes were mixed into 5.0 % (w/w) plain chitosan hydrogel (from section 5.5.2.1) by hand stirring until the liposomal dispersion was evenly distributed. The final concentration of empty liposomes was 10 % (w/w) and the normalised concentration of chitosan was 4.5 % (w/w). Empty liposomes-in-hydrogel was stored at 4-8 ºC in the refrigerator.

5.5.3.3 CHX liposomes-in-chitosan-hydrogel

CHX liposomes were mixed into 5.0 % (w/w) chitosan hydrogel comprising glycerol (form section 5.5.2.2) by hand stirring until the liposomal dispersion was evenly distributed. The final concentration of CHX liposomes was 10 % (w/w) and the normalised concentrations of chitosan were 4.5 % (w/w) and glycerol 9.0 % (w/w), respectively. CHX liposomes-in-hydrogel was stored at 4-8 ºC in the refrigerator.

5.6 Determination of pH

The measurement of the pH of samples was done with either or both SensION^{TM}+ PH31 pH meter and Accumet ® portable pH meter kit at room temperature (24 ± 2 °C) for both liposomal dispersions and hydrogels.

5.7 Hydrogel characterisation

5.7.1 Development and validation of reproducible method utilising texture analyser (T.A.)

Characterisation of hydrogels was done on a TA.XT plus Texture analyser with backward extrusion rig set (A/BE). Development of a reproducible method was based on the work of Hurler and co-workers (Hurler et al., 2012). The authors developed a simplified and improved method for the T.A. They also proposed a new definition of gel cohesiveness, where the probe on the T.A. is submerged only once into the gel and they proposed this was the direct measure of the cohesiveness of the gel. When applying the original method developed by Hurler and co-workers, we experienced that the challenging related to reproducibility, related to the amount of gel on top of the disc when the disc was redrawn, retention of the gel on beaker wall, the beaker being lifted with the gel.

In development of a reproducible method, different parameters were evaluated. Such as test and

post-test speed, distance the probe is submerged in to the gel (should avoid being near the bottom), trigger force, start position of the disc and diameter of the disc (35 mm disc versus 40 mm disc) (Table 1). Different T.A. settings were evaluated to optimise a (reproducible) method.

Table 1: Overview of the different T.A. settings evaluated to optimise a (reproducible) method for chitosan hydrogel. All 7 analyses were preformed both applying the 35 and 40 mm discs.

	Test speed (mm/sec)	**Post speed (mm/sec)**	**Distance (mm)**	**Trigger force (g)**	**Probe position (mm)**	**Note**
Analysis 1	1	1	10	10	45	Disc is above gel surface
Analysis 2	1	1	15	10	54	
Analysis 3	1	1	10	10	31	Disc is under gel surface
Analysis 4	1	1	10	10	34	The undersurface of the disc thouches gel
Analysis 5	4	4	10	10	45	
Analysis 6	1	1	10	10	45	Remove gel from disc between each test
Analysis 7	4	4	10	10	45	Remove gel from disc between each test

The 0.5 % (w/w) Carbopol hydrogel described in section 5.5.1 and the plain 5.0 % (w/w) chitosan hydrogel described in section 5.5.2.1 were used to optimise a (reproducible) method. The choice of the most suitable method was based on the experimental set up (Analysis 1-7, Table 1) that provided the lowest standard deviation (SD) obtained for 4 replicates. And chitosan hydrogels exhibited highest level of reproducibility (lowest SD) when the applied settings were as in analysis 7 (Table 1), see section 5.7.2.

5.7.2 Textural analysis

Characterisation of hydrogels were performed with a backward extrusion rig set on TA.XT plus T.A. (Figure 11), with the novel optimised methods.

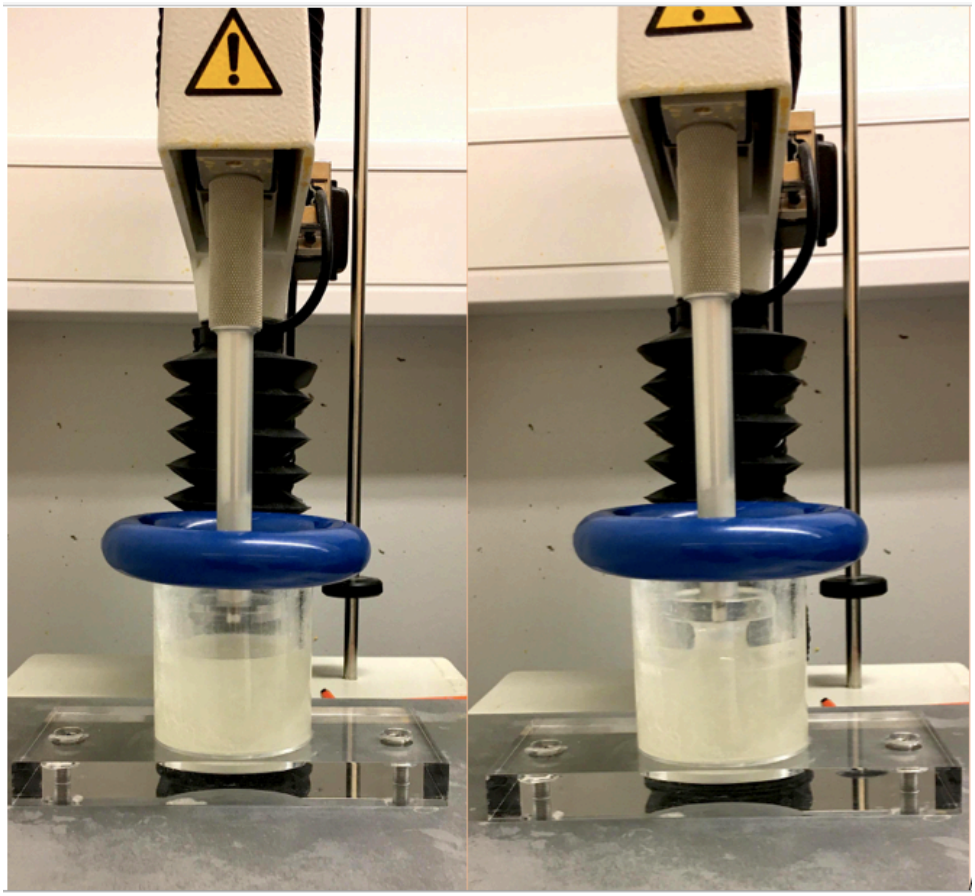

Figure 11: The experimental set up with backward extrusion rig (A/BE) on the T.A. The beaker containing chitosan hydrogel is placed in the centre with weight on top so it will not be lifted during the test. Chitosan gel before (right) and after (left) the probe was submerged into the gel.

The container from the backward extrusion rig set was filled with 65 g hydrogel, assuring that there was no air bubbles and gel exhibited a smooth surface. Five replicates were preformed for each hydrogel, at room temperature (23-25 ºC).

The optimised T.A. settings for chitosan hydrogel were as following:

- Mode: measure force in compression
- Option: return to start
- Use of a 35 mm (diameter) disk
- Start position for probe at 45 mm
- Pre-test speed: 10.0 mm/s
- Test speed: 4.0 mm/s
- Post-test speed: 4.0 mm/s
- Distance: 10 mm
- Trigger force: 10 g

The optimised T.A. settings for Carbopol hydrogel were as following:

- Mode: measure force in compression
- Option: return to start
- Use of a 35 mm (diameter) disk
- Start position for probe at 54 mm
- Pre-test speed: 10.0 mm/s
- Test speed: 1.0 mm/s
- Post-test speed: 1.0 mm/s
- Distance: 15 mm
- Trigger force: 10 g

The textural properties such as the hardness, adhesiveness and cohesiveness were measured. Hardness indicates applicability of the gel to the skin, adhesiveness indicates the retention time on the wound site and cohesiveness indicates the internal stickiness of the hydrogel and its removal from the container (Hurler et al., 2012).

5.8 Stability testing

The liposomes were tested for storage stability in respect to their properties such as size, polydispersity, zeta potential and EE. The liposomes-in-hydrogels stability was tested determining the texture properties (cohesiveness, adhesiveness and hardness) and pH. The samples were stored at 4-8 ºC in the refrigerator and the stability testing preformed at week 2, 4 and 12.

5.9 *In vitro* drug release

5.9.1 Preparation of buffer – Phosphate buffered saline (PBS)

Phosphate buffered saline (PBS) was prepared by dissolving 2.98 g/L disodiumhydrogen phosphate dehydrate, 0.19 g/L monobasic potassium phosphate and 8 g/L sodium chloride in Milli-Q water. Adjusted pH to 7.4 with hydrochloric acid and sodium hydroxide (Ternullo et al., 2019).

5.9.2 Franz cell manual diffusion system

The drug release was explored with Franz cell manual diffusion system with heating circulator for maintaining the temperature at 32 ºC. In the cell, the acceptor chambers had a volume of 12 mL and a diffusion area of 1.77 cm^2. The acceptor chambers were filled with buffer, PBS, with a pH on 7.4. The donor chambers were filled with 600 µl sample. The system was cleaned in advance with methanol, demineralised water and distilled water for half an hour. In this system, there is a donor chamber and an acceptor chamber that are separated with a membrane, which in this case was a cellophane membrane. The compound in the formulation will during the experiment diffuse from the donor chamber, through the membrane and to the acceptor chamber, where a sample (500 µl) was taken out every hour the first 6 hours, then after 10 hours and then after 24 hours. The same amount buffer (500 µl) was added to the acceptor chamber whenever a sample was withdrawn, to assure same condition throughout the experiment (Ternullo et al., 2018).

5.10 CHX solubility testing

To test CHX solubility, CHX was attempted dissolved in different excipients, PBS buffer and wound fluid with albumin. The excipients are listed in materials, PBS buffer described in section 5.9.1. and the wound fluid with albumin was made as followed:

Wound fluid comprising albumin: 5. 84 mg/mL sodium chloride, 3.36 mg/mL sodium hydrogen carbonate, 0.30 mg/mL potassium chloride, 0.35 mg/mL calcium chloride dehydrate and 33 mg/mL bovine albumin dissolved in deionised water (Bradford et al., 2009).

5.11 Evaluation of anti-inflammatory activity

The cell culture used to investigate anti-inflammatory activity was the murine macrophage RAW 264.7 cell line. Cells were maintained in Roswell park memorial institute (RPMI) 1640 medium with 10 % fetal bovine serum (FBS), 100 µg/L streptomycin and 100 IU/mL penicillin at 37 $^{\circ}$C in a 5 % CO_2 atmosphere.

The *in vitro* anti-inflammatory activities of empty liposomes, CHX liposomes, plain hydrogel and CHX liposomes-in-hydrogel formulation were studied measuring the inhibition of nitric oxide (NO) production in lipopolysaccharide (LPS)-induced macrophages. Macrophages were incubated with medium in a 24-wells plate at 37 $^{\circ}$C /5 % CO_2. After approximately 24 hours, the growth of the cells was evaluated before starting the anti-inflammatory test. The old medium was exchanged with new medium containing only 1 µg/mL LPS (to induce inflammation in macrophages), only RPMI medium or filled with 1 µg/mL LPS and the various type of formulation in lipid concentrations of 1, 10 and 50 µg/mL, or in a polymer concentration corresponding to this lipid concentration (Jøraholmen et al., 2019).

After an incubation of 24 hours ± 30 minutes, the nitrite concentration was measured with Griess reagent (5 % phosphoric acid with 0.1 % N-(-a-naphthyl)ethylenediamine and 1 %

sulphanilamide) in 1:1 volume ratio by measuring absorbance at 540 nm using Tecan Spark M10 multimode plate reader. NO produced by the cells is expressed by the measured nitrite (NO_2) and produced NO, in comparison to 100 % NO found in the control (cells treated with only media containing 1 µg/mL LPS). All experiments were conducted in triplicate (Jøraholmen et al., 2019).

5.12 Statistical analyses

Results are expressed as mean and SD, where $n \geq 1$. The Student´s *t*-test was used for statistical significance for the comparison of two means. A *p*-value less than 0.05 was considered statistically significant.

6 Results and Discussion

The focus of this project was to develop a novel formulation, as a drug carrier system for membrane active antimicrobials destined for infected skin and chronic wounds. The rise of antibacterial resistance is a severe problem worldwide and there is an urgent need for new treatment options as current treatment strategies for chronic wounds have an inadequate therapeutic effectiveness (Pfalzgraff et al., 2018). The challenging physiology of chronic wound beds includes an ongoing inflammation, hospitable environment for bacterial growth, biofilm formation and excess proteolytic activity (Saghazadeh et al., 2018). A promising class of membrane active antimicrobials are AMPs as they have broad activity and are less prone to antimicrobial resistance. Treating infected skin/wound locally with AMPs has the potential to prevent and treat infections, reduce pro-inflammatory response and promote cell migration and proliferation in wounds (Gomes et al., 2017). CHX as a model compound was selected in the present work to optimise liposomes and a liposomes-in-hydrogel formulation for the AMPs.

6.1 Spectral analysis and standard curve of CHX

Since CHX is the model compound, it would require a method for quantitative estimation. It was originally planned to use high performance liquid chromatography (HPLC) but we were not able to develop a suitable method on HPLC due to the fact that CHX binds strongly to the column and did not fully elute (data not shown). As a result, Tecan Spark M10 multimode plate reader in absorbance mode was used to detect CHX. A spectral analysis of CHX was performed (Figure 12) to find the maximal absorbance peak (λ_{max}) and the appropriate wavelength to conduct our quantitative analysis.

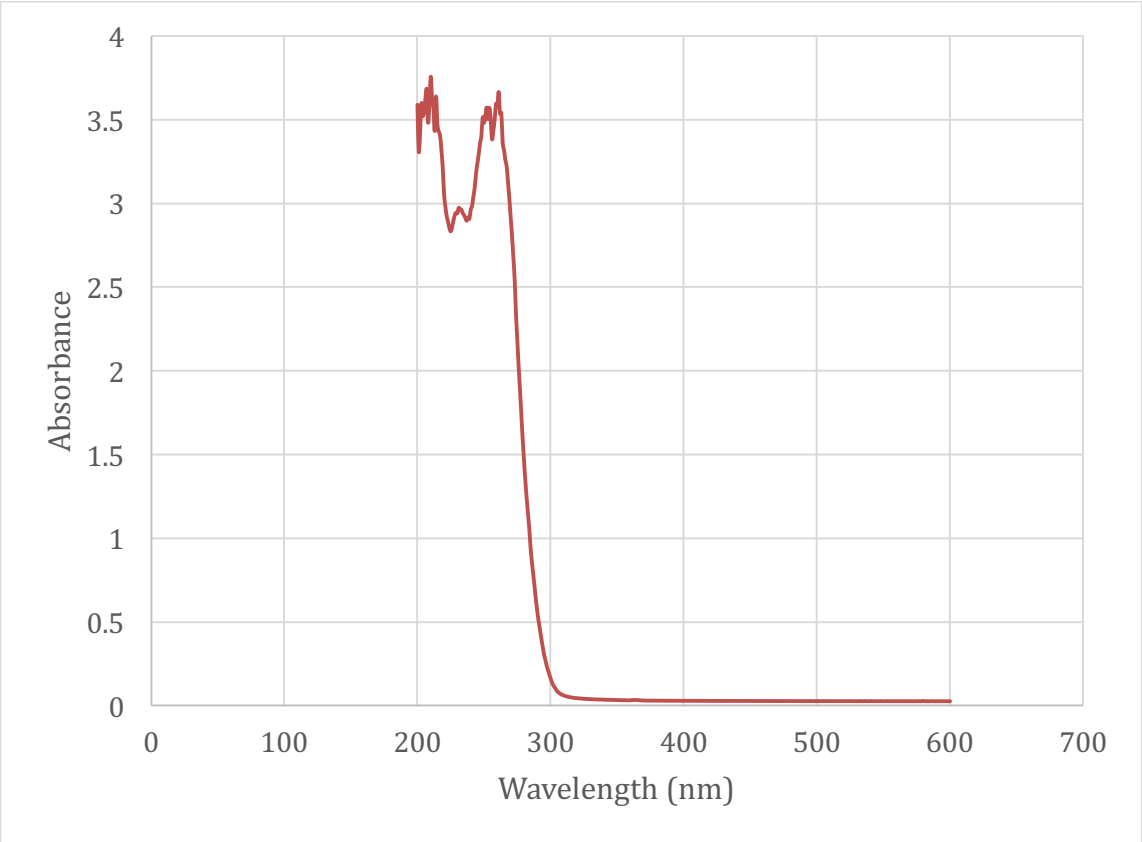

Figure 12: Absorbance scan of CHX in methanol. The λ_{max} was found at 261 nm. The peak at 200-210 was not selected because of the influence of solvent.

From the spectral analysis, we found maximum absorbance in the area 200-210 and 261 nm. Due to influence from the solvent absorbance in the wavelength area 200-210 nm, the λ_{max} was set at wavelength 261 nm.

A standard curve for CHX in methanol (Figure 13) was expressed as absorbance of standard CHX versus corresponding concentrations of the standard CHX.

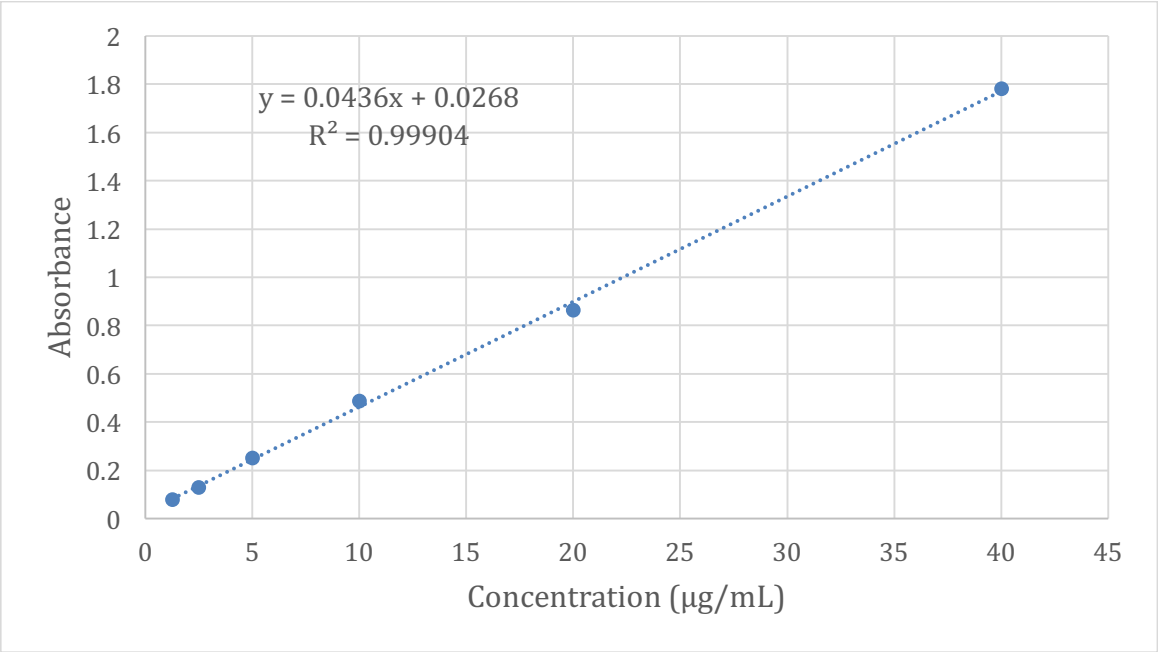

Figure 13: Standard curve for CHX in methanol measured at wavelength 261 nm on plate reader in absorbance mode.

Absorbance of different concentrations of CHX (1.25-40 µg/mL) was measured at wavelength 261 nm and a good correlation ($R^2 = 1.00$) was obtained. From the standard curve, the equation (y=0.0436x + 0.0268) was used to further calculate amount of CHX in liposomes.

6.2 Liposomal formulations

Liposomes are a promising drug delivery system for dermal administration due to their excellent biocompatibility and biodegradability (Sala et al., 2018). By tailoring liposomal surface characteristics, size and polydispersity it is possible to optimise their efficacy as a drug delivery system. Liposomal properties will affect their fate in skin. In this project, liposomes were characterised by zeta potential, vesicle mean diameter and PI that are presented in Table 2. Six independent batches of both empty and CHX liposomes were characterised.

Table 2: Overview of liposomal characteristics for empty and CHX liposomes. The results are presented as mean ± S.D (n=6).

Liposomes	Zeta potential (mV)	Mean diameter (nm)	PI
Empty liposomes	-3.50 ± 1.95	183.6 ± 4.0	0.15 ± 0.01
CHX liposomes	45.53 ± 1.33	318.4 ± 8.6	0.24 ± 0.03

The liposomes were made from the zwitterionic phospholipid PC and empty liposomes were expected to have a zeta potential near neutral (Soema et al., 2015), which can be seen in Table 2. Zeta potential is the electrical potential between the electric double layer of the vesicle and the continuous phase in a colloidal dispersion where the vesicle is moving under electric fields. It is very common to use zeta potential to characterise liposomes as it can be related to the colloid stability and surface charge of vesicles. It is suggest that a zeta potential near zero indicates a highly unstable system, whereas a system with zeta potential over ± 30 mV have shown to be highly stable (Bhattacharjee, 2016). When incorporating CHX into liposomes the zeta potential change towards a more positive potential and indicated a more stable system, compared to empty liposomes. CHX liposomes have an increased zeta potential at + 45.53 mV and a low SD. In comparative literature data, a significant increase in zeta potential was also reported for CHX loaded polymeric nanocapsules (32.4 mV) as compared to unloaded nanocapsules (-20.9 mV) (Lboutounne et al., 2002).

Due to CHX lipophilic character, it is highly probable that the compound is incorporated inside the lipid bilayer in the liposomes. Figure 5 (Introduction) is an attempt to illustrate different ways a hydrophobic compound can arrange itself in the phospholipid bilayer of liposomes. Moreover, depending on how the compound arranges itself, as CHX is cationic, it can thereby affect the total surface charge of the liposomes.

Other important properties of liposomes are their size and size distribution. As the thin film method by Bangham *et al*. provides a quite heterogeneous size distribution and lamellarity, this method will require a size-reducing method for the liposomal dispersion (Samad et al., 2007).

The size-reducing method used in this project was the membrane extrusion method. Size and size distribution obtained through the membrane extrusion method are influenced by the number of cycles the liposomal dispersion is extruded (Ong et al., 2016). In this project, we used different extrusion methods for empty and CHX liposomes. At first, the same extrusion method was used for both empty and CHX liposomes, which resulted in a decreased vesicle size of 163.1 ± 5.8 nm (n=3) and a PI of 0.12 ± 0.0 (n=3) for CHX liposomes; which would make them too small for the intended application.

Comparatively, Nielsen *et al.* reported that incorporation of the AMP indolicidin into liposomes resulted in an increase in overall size and polydispersity, however they used different anionic lipid compositions to mimic membrane of bacteria and sonicated the liposomal dispersion (Nielsen et al., 2018), whereas we used zwitterionic lipids and extruded. On the other hand, similar results were reported in the study conducted of Lboutounne *et al.* where a significant reduction in size from 350 nm to 278 nm was found when incorporating CHX, even though the nanocarrier used in this experiment was nanocapsules not liposomes (Lboutounne et al., 2002).

A liposomal size around 300 nm is considered to be ideal for dermal drug delivery as it enables increased concentration of the drug in desired tissue, but not deliver drug too deep in the skin and risking unwanted systemic absorption. A size around 300 nm can assure depot effect of a sufficient amount of drug over time. There should be a balance between vesicle size and EE, as smaller vesicles lead to lower capacity for drug entrapment. PI is used to describe the distribution of vesicle size where a PI under 0.3 is considered a homogenous size distribution and a PI over 0.3 is considered as a broad size distribution (Verma et al., 2003). For this purpose, the membrane extrusion method was changed for CHX liposomes: extruding through the membrane with the smallest size (0.2 μm) was excluded and the number of extrusion cycles adjusted (section 5.3.1). This resulted in a vesicle size of 318.4 ± 8.6 nm and a PI of 0.24 ± 0.03, which are considered appropriate size and size distribution for dermal delivery. A low PI indicated a homogeneous vesicle size distribution and together with low standard deviations confirmed that extrusion is a suitable downsizing method for liposomal dispersion. In addition, it is advantageous that extrusion is rapid, reproducible and a relatively gentle process (Ong et al., 2016).

The arrangement of CHX in the liposome can also affect the fluidity of the liposomal bilayer. The degree of membrane elasticity (E) was tested as described in section 5.4.3 and the results are presented in Table 3 with the determined parameters used to calculate E.

Table 3: Membrane elasticity of CHX liposomes. The membrane elasticity (E) was calculated from r_v/r_p and J. r_v is the vesicle diameter (nm) after extrusion, r_p is the pore size membrane (nm) and J is the amount (g) of liposomal dispersion extruded. Results are presented mean of triplicates ± SD (n=1).

Liposomes	$\frac{r_v}{r_p}$	J (g)	E
Empty liposomes	1.66 ± 0.01	1.58 ± 1.58	4.35 ± 0.61
CHX liposomes	1.56 ± 0.02	1.35 ± 0.41	3.28 ± 0.93

Empty liposomes exhibited an elasticity of 4.35 ± 0.61 and CHX liposomes had an elasticity of 3.28 ± 0.93, which indicates that the liposomal bilayer of empty liposomes is more elastic than the liposomal bilayer of CHX liposomes. The result might be influenced by the size difference of empty and CHX liposomes. This result is unexpected because it was anticipated that CHX liposomes were more elastic than empty liposomes, due to the fact that the CHX liposomal dispersion was experienced easier to extrude with the "empty liposome extrusion method" (section 5.3.1) and as mentioned earlier a smaller size of the CHX liposomes was obtained with the same method. However, it is possible that CHX liposomes are more "squeezable" but they recover, upon the completion of deformability testing almost instantaneously. This phenomenon needs to be further explored.

A more elastic liposomal membrane qualifies the liposomes to squeeze through skin pores that are smaller than the liposomal size and consequently enhance the transport of incorporated drug into the deeper skin layers (Ternullo et al., 2019). In chronic wounds, the intact skin is broken and the main physical barrier (*stratum corneum*) is missing. When treating chronic wounds with liposomal formulations, it is desired that liposomes deliver the compound with depo-effect

in the deeper layers of skin, however a too elastic membrane can make liposomes diffuse deeper into the skin layers than wanted and risk undesired systemic absorption. Another inconvenience with higher degree of membrane elasticity is lower liposomal stability. Reduced stability can be seen in forms of leakage of drug and reduced EE over time (Olusanya et al., 2018). Consequently, resulting in therapeutic failure.

The results presented above indicate that empty and CHX liposomes differ in terms of zeta potential and membrane elasticity (along with the size, even though we changed the extrusion method). Incorporating CHX affected the liposomal properties and, as mentioned, the properties are proposed to change depending on how CHX arranges itself in the bilayer. CHX is a base (pK_a= 10.3 and pK_a=2.2 and will be protonated between pH 4 and 8, (Lboutounne et al., 2002). Since pH will affect the protonation of CHX, it can also affect the arrangement of CHX in liposomal bilayers. Following this, pH of the aqueous media used to make liposomes could potentially affect how CHX arrange itself in the liposomal bilayer, thereupon the properties of liposomes. Therefore, we tested preparing liposomes from aqueous media with different pH which are shown in Appendix I. In addition, pH of the empty and CHX liposomal dispersions were measured and the results are presented in Table 4.

Table 4: pH of empty and CHX liposomes. Results are presented by mean ± SD (n=3).

Liposomes	pH
Empty liposomes	6.90 ± 0.16
CHX liposomes	8.00 ± 0.10

The empty liposomal dispersion had a pH of 6.90 ± 0.16 and the CHX liposomal dispersion had a more basic pH at 8.00 ± 0.10. CHX is a base and can increase pH of the liposomal dispersion (Kudo et al., 2002), which was observed. However, the pH of the final formulation is of higher importance and will be discussed later.

Another important factor that needs to be considered is the EE. Since liposomes consist of a hydrophilic aqueous core and a hydrophobic lipid bilayer, they can entrap both hydrophilic and lipophilic drugs. CHX is substantially hydrophobic and has a octanol/water partition coefficient of 0.754 (Farkas et al., 2007), therefore as mentioned earlier it is suggested that CHX is embedded inside the phospholipid bilayer, CHX is very poorly soluble in water and will immediately precipitate when not incorporated in lipid bilayers.

Drug encapsulation is expected to increase the stability and local accumulation of drug in desired tissue, and furthermore enhance the efficiency of the drug. The EE (expressed as percentage) of CHX in liposomes was calculated based on a standard curve prepared in methanol (Figure 13). The EE was found to be 96.5 % as shown in Table 5.

Table 5: Entrapment efficiency (EE) and relative recovery (RR) of CHX liposomes found after dialysis (n=3) and centrifugation (n=1).

Method	EE (%)	RR (%)
Dialysis	96.43 ± 9.90	118.62 ± 32.74
Centrifugation	96.50	99.66

Before determining the EE, free CHX had to be removed which was done by dialysis and centrifugation was done to compare the efficacy of separation. The experiment was conducted in this way due to the solubility to CHX (very poorly soluble in water, see Appendix V), detection limit (lowest concentration of the compound that can be reliable detected) and the precision of the Tecan Spark M10 multimode plate reader. In addition, regenerated cellulose membranes (which was the material of dialysis tubing membrane used in this project) have shown to absorb certain compounds (Gago et al., 2020). Likewise, CHX is thought to have some interactions with the dialyses tubing membrane and therefore was dialysis the least preferred separation technique. An EE of 96.5 % is an exceptionally high entrapment, and we used centrifugation to compare and confirm the EE. As seen in Table 5, the EE for both methods were very similar. We planned implementing more parallels of centrifugation to determine the EE and strengthen the result. However, with so high entrapment efficacy one can argue that separation of non-incorporated CHX is unnecessary.

CHX is, as mentioned, poorly soluble in water and substantially hydrophobic and it is most likely that CHX will be incorporated in the bilayer of liposomes. Whereas, free CHX is likely to precipitate. If precipitated CHX was present in the dialyse tube, this would lead to falsely high entrapment values, but with centrifugation the precipitate would be removed. The EE calculated by dialysis was 96.43 ± 9.90 % and the EE calculated by centrifugation was 96.50 %. Compared to similar studies, Lboutounne *et al.* achieved and EE of 60 % by incorporating CHX into polymeric nanoparticles (Lboutounne et al., 2002), however our entrapment was found to be higher, as expected since liposomal bilayers are better environment for hydrophobic molecules than polymeric nanoparticles. A high EE is desirable to assure that a sufficient amount of the compound can be delivered and to guarantee optimal therapeutic effect (Eloy et al., 2014).

The recovery (RR) was originally calculated to be 118 %, but during extrusion some liposomal dispersion was lost. The starting volume of liposomal dispersion was 10 mL, but final volume was approximately 9.65 ± 0.13 mL (n=3) (Table 6).

Table 6: Volume loss of CHX liposomes during extrusion (n=3).

Volume of CHX liposomal dispersion before extrusion	10 mL
Volume of CHX liposomal dispersion after extrusion	9.65 ± 0.13 mL
Volume lost during extrusion	0.35 mL
Percentage lost volume during extrusion	3.5 %
Theoretical amount of lost CHX during extrusion	0.35 mg

The recalculated RR was 113.87 % for the dialysis method and the recalculated RR was 96.17 % for the centrifugation method. Even though there was some loss of sample during extrusion, the extrusion method is still advantageous in comparison to sonication, with respect to preserving structural stability of AMPs. Thermal processing may lead to structural changes of AMPs, thereby potentially changing their activity. And as the RR was high, this is an indication that the methods chosen in preparing liposomes were justified.

However, one needs to keep in mind that exposing AMPs to organic solvent and shear stress caused by extrusion can change the morphology and activity (Biswaro et al., 2018). In addition, since the proposed mechanism of AMPs and CHX is to disrupt the membrane, it was crucial to verify that there still were vesicles even when CHX was embedded in liposomal bilayers and that the liposomes had not been destroyed. Nilsen *et al.* studied the structural interaction between AMPs and liposomes and suggested that the AMP indolicidin has a concentration dependent interaction with the lipid bilayers. Moreover, a high enough concentration of the AMP will lead to disorientation of lipids in the bilayer of the liposomes (Nielsen et al., 2019, Nielsen et al., 2018). Therefore, it was important for us to confirm the vesicle formation of CHX liposomes.

Characterising liposomes by dynamic light scattering and by zeta potential, the data can be prejudiced by the anisometric shape of vesicles. Hence, the information gained from dynamic light scattering can be corroborated with microscopic techniques and confirmed that there are vesicles (Jain and Thareja, 2019).

In Figure 14, a TEM picture of a CHX liposome, a vesicle with a diameter of approximately 400 nm can be observed. This TEM picture provides support to the earlier presented findings in this project, confirming that CHX liposomes were intact.

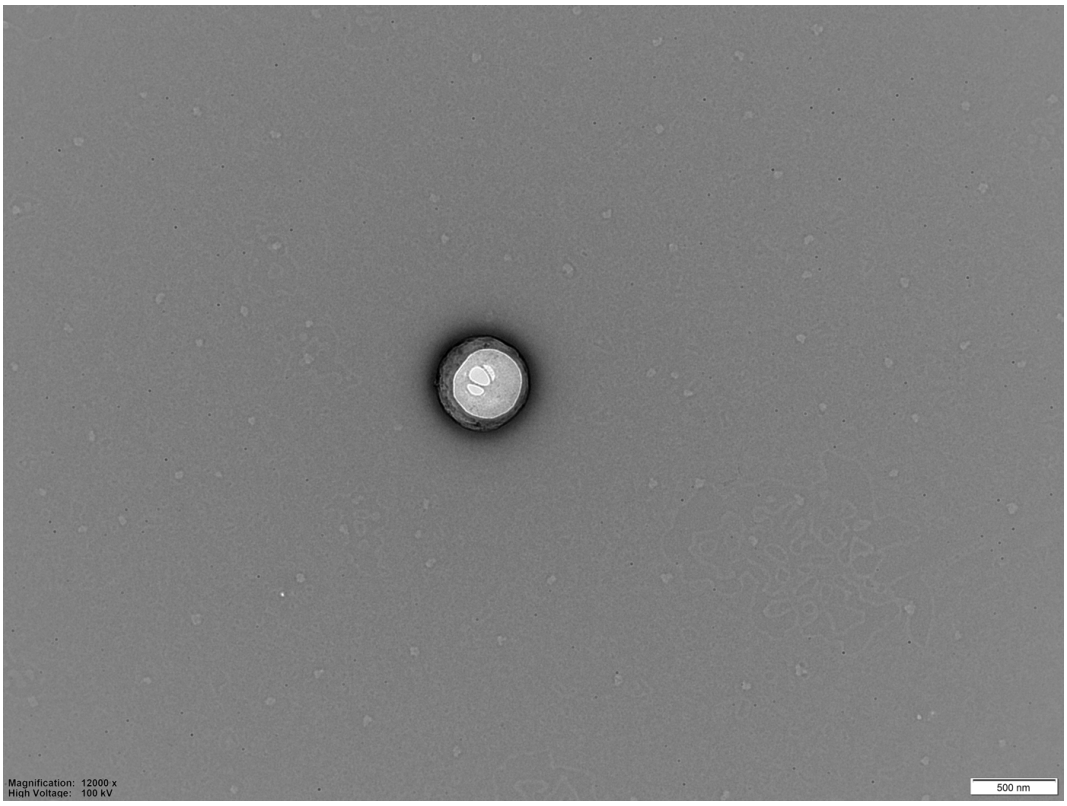

Figure 14: TEM picture of CHX liposome.

Another electron microscopic method frequently used is scanning electron microscopy (SEM). We tried taking a SEM picture of the liposomal dispersion, but the preparation method of the liposomal sample needed to be further optimised to be able to preserve the liposomal characteristics (Appendix II). Nevertheless, a TEM picture is normally used to study morphology and often provides greater resolution than a SEM picture (Jain and Thareja, 2019). Furthermore, it would be interesting to employ cryogenic-TEM where the sample is imaged close to its native state because preparation methods that contains staining and drying of the sample is note required, and this will subsequently lead to disclosure of the structural features more extensively (Gustafsson et al., 1995).

Another important parameter regarding optimisation of liposomes as drug delivery system is their stability.

6.2.1 Stability of liposomes

The stability is important to take into consideration considering the quality of a pharmaceutical formulation. Liposomes exhibit problems with physical stability in terms of aggregation and drug leakage that should be avoided (Olusanya et al., 2018). As mentioned earlier, a zeta potential ± 30 mV is expected to create a more stable system, as an electrical charge on the surface of the vesicle will make vesicles to repel each other by electrostatic forces rather than aggregate, thereby increasing their physical stability (Has and Pan, 2020). The stability of the liposomes was evaluated through particle size, PI and zeta potential for a duration of 12 weeks for empty liposomes and 4 weeks for CHX liposomes after storage in refrigerator (4-8 ºC). For CHX liposomes, the EE was also evaluated after 12 weeks.

The stability measurements of size and PI of empty liposomes are presented in Figure 15.

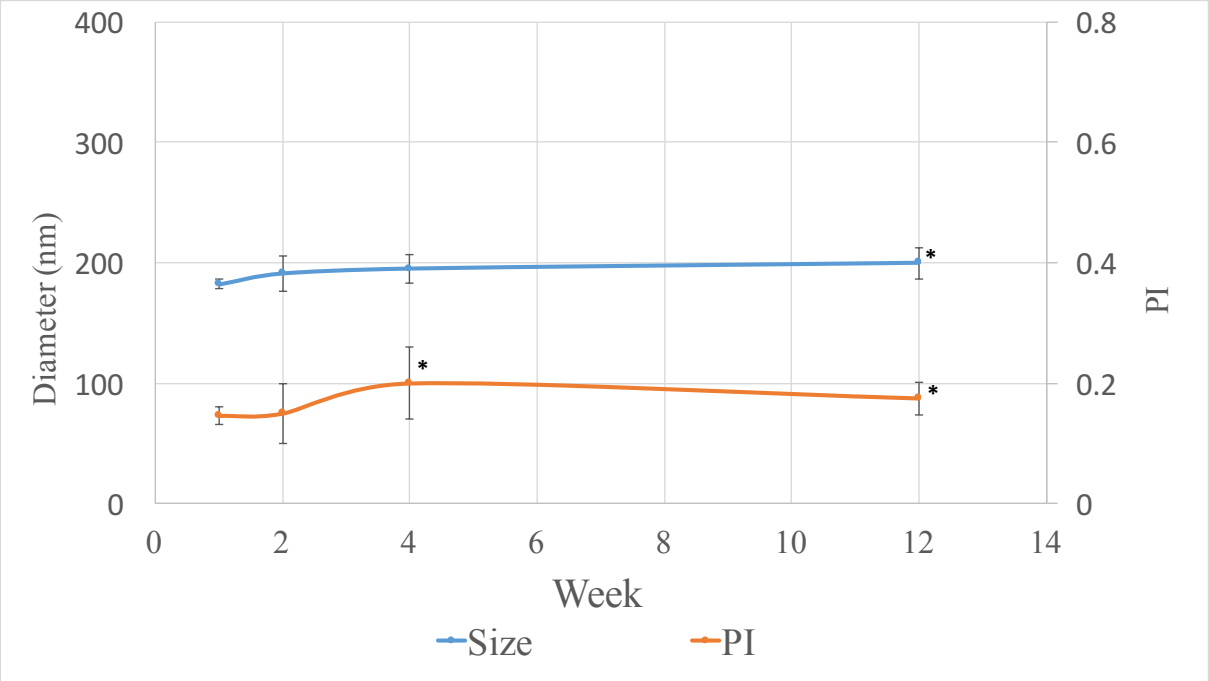

Figure 15: Stability of size and PI for the empty liposomes measured week 1 (n=6), week 2 (n=6), week 4 (n=4) and week 12 (n=3). Results are expressed as mean ± SD. *p< 0.05 as compared to week 1.

In respect to size for empty liposomes there was no significant change over 4 weeks, but a significant change in size (compared to the size in week 1) was observed after 12 weeks. While, the PI was significantly changed after 2 weeks.

Stability measurement of zeta potential for empty and CHX liposomes are presented in Figure 16.

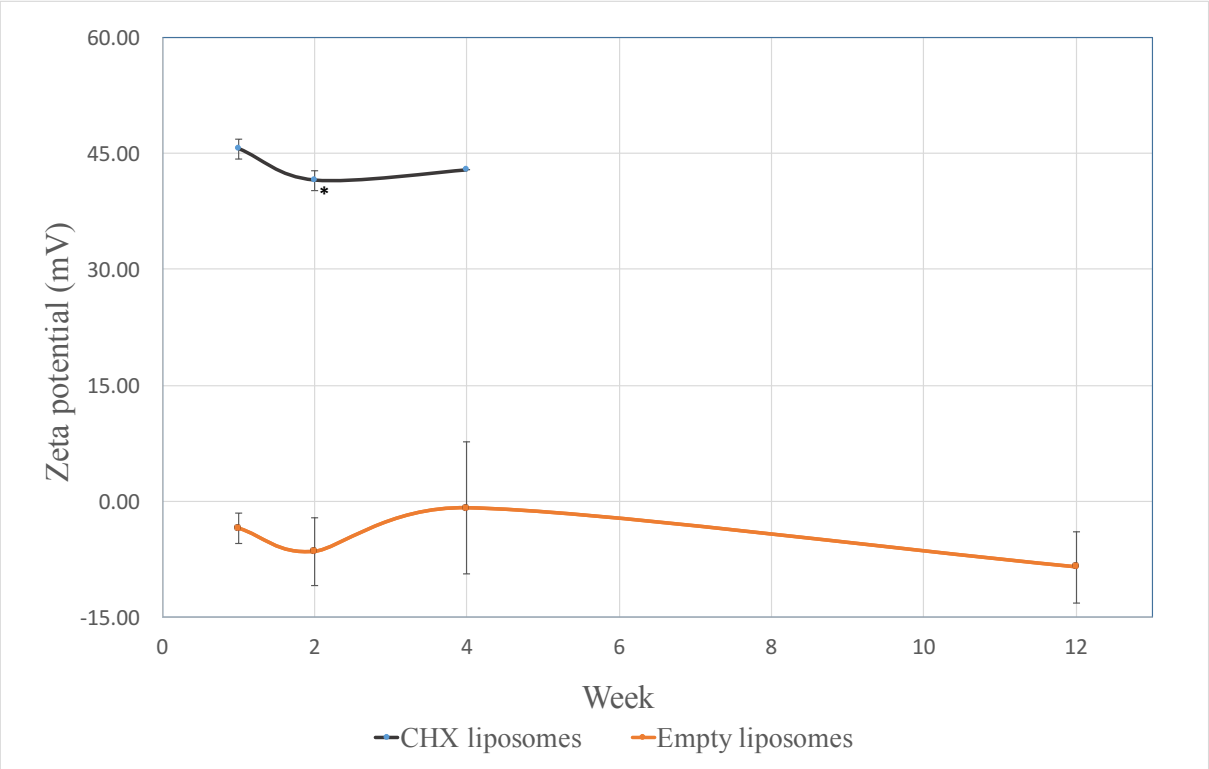

Figure 16: Zeta potential of the empty liposomes week 1 (n=6), week 2 (n=6), week 4 (n=4) and week 12 (n=3) and CHX liposomes week 1 (n=6), week 2 (n=2) and week 4 (n=1). Results are expressed as mean ± SD where n>1. *p< 0.05 as compared to week 1.

The zeta potential for empty liposomes was close to zero and fluctuated over time but with no significant changes compared to week 1. However, the zeta potential became more negative after a 12-week period of time. As mentioned earlier a zeta potential near zero of a vesicle in a colloid system indicates rather unstable dispersion, thus suggestion agglomeration. However, date on size distribution (Figure 15) indicated a more stable system.

Current stability measurement of CHX liposomes showed significant change in zeta potential in week 2. However, in regards to the measured zeta potential of CHX liposomes there is a need for more parallel measurements to support the stability data of week 2 and week 4, as the results are not currently reliable. The same concern applies for stability measurement of size and PI (Figure 17) and EE.

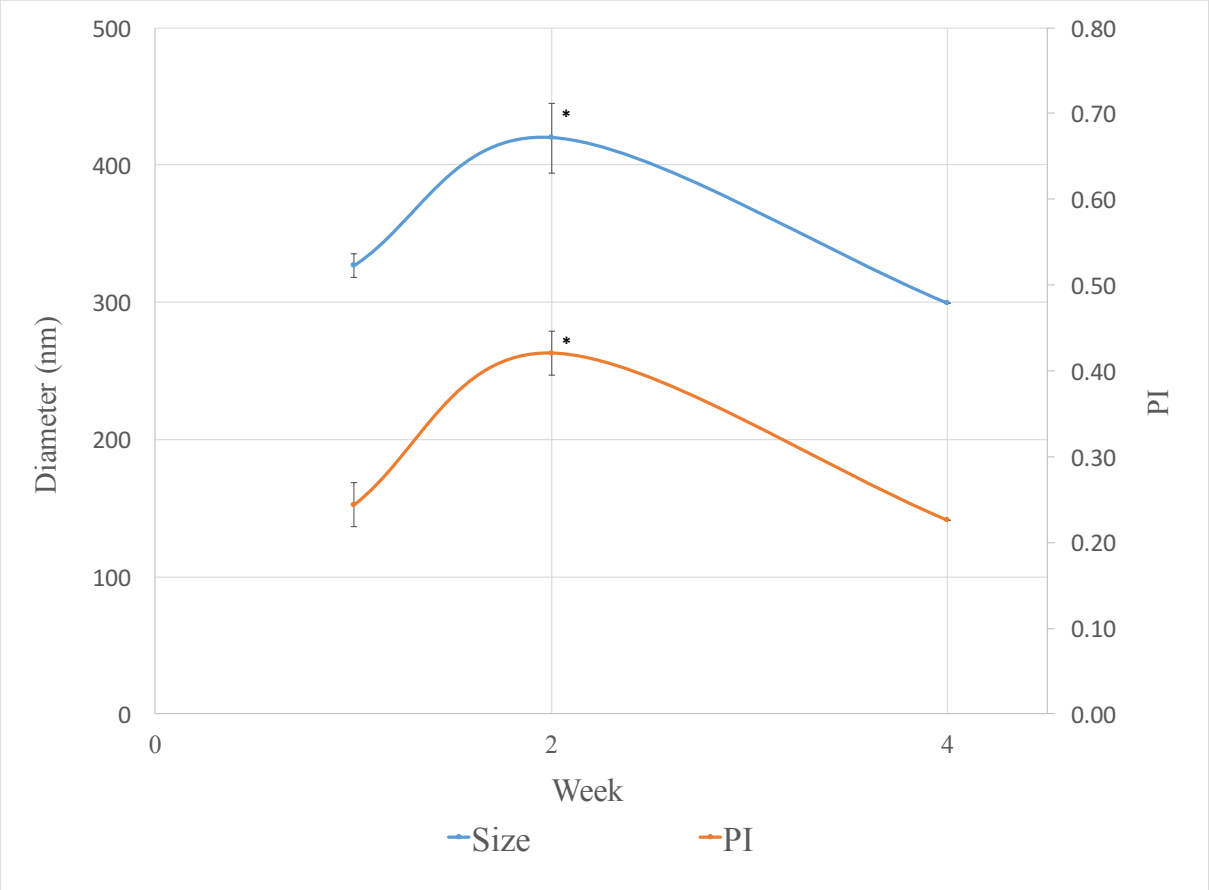

Figure 17: Stability of size and PI for the CHX liposomes measured week 1 (n=6), week 2 (n=2) and week 4 (n=1). Results are expressed as mean ± SD where n>1. *p< 0.05 as compared to week 1.

The size and PI of CHX liposomes were significantly changing after a duration of 2 weeks. The only measurement conducted for EE of CHX liposomes was after 12 weeks (n=1) and EE was determined to be 90.7 %. However, as mentioned the results are not currently fully reliable and can be used as an indication rather than absolute value.

Nevertheless, a liposomal dispersion is liquid and is generally considered an unstable system. To administrate liposomes, the final formulation would require a secondary vehicle, such as a hydrogel. Hydrogels will stabilise the liposomal dispersion and make it more applicable for dermal administration and prolong the residence time on the desired area (Ternullo et al., 2020). For hydrogels to be applicable for skin administration, especially considering the wounds, it is important to characterise textural and pH properties of hydrogels.

6.3 Hydrogels characteristics

Texture analysers are used in both pharmaceutical, cosmetic and food industries to evaluate gel-like structures. This analysis makes it possible to conduct experiments that are reproducible and validated, and provides information about the textural properties of gels. This is highly relevant as a quality control tool as its helps maintain product quality and reducing batch-to-batch variations. Different experimental set ups on the T.A. will affect the obtained results and it is very important that the experimental method provides reproducible results (Hurler et al., 2012).

Carbopol hydrogel was used as a control to develop a reproducible method on the T.A. because it is a quite viscous and stiff hydrogel and tolerate mechanical stress well. Carbopol is one of the most commonly used polymers in hydrogels (Romanko et al., 2009).

Carbopol and chitosan hydrogels have different preparation conditions: chitosan needs an acetic environment to become soluble while Carbopol hydrogels becomes stiff when neutralised with base. As a result, different pH-values of the final hydrogels were obtained (Table 7).

Table 7: pH of different hydrogel formulations (n=3), *(n=2).

Hydrogel	pH
Plain Carbopol hydrogel	5.04 ± 0.02
Empty liposomes in Carbopol hydrogel*	5.65 ± 0.44
Plain chitosan hydrogel	4.68 ± 0.07
Empty liposomes in chitosan hydrogel	4.65 ± 0.05

As mentioned, the experimental set up will affect the results on a T.A. Some of the many factors affecting the result are smoothness of gel, position of beaker, wall-effect between the disc and beaker wall and amount of gel in the beaker (Figure 18). Therefore, the experimental set up needs to allow different modification during a test run.

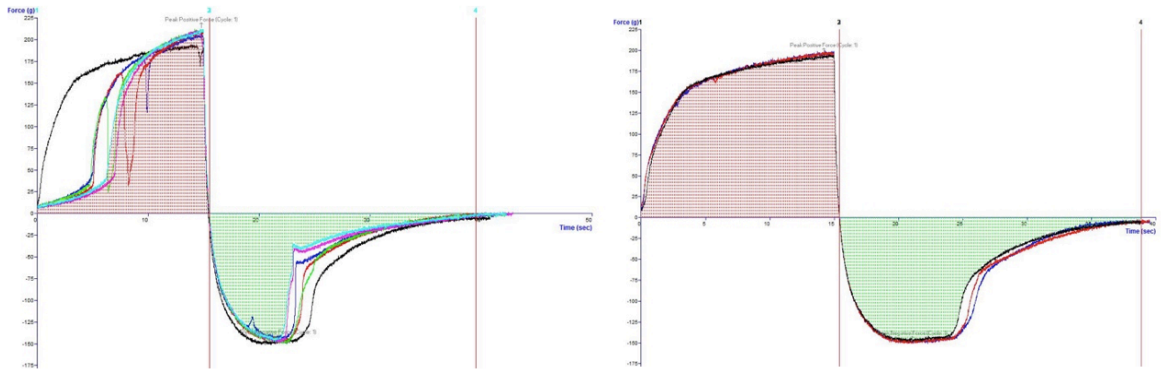

Figure 18: Graph from T.A. measurement of Carbopol 0.5 % (w/w) hydrogel. The graph to the left is Carbopol hydrogel without moving the container with gel, controlling amount hydrogel and smoothing surface between each replicates. The graph to the right is a result after smoothing the surface and controlling the amount of hydrogel in the container between each test.

Different gels also require different settings in the method development. Chitosan hydrogels have different properties compared to Carbopol hydrogels, and appear more fluid and have a

honey-like consistence. Another factor is that the hydrogel becomes more fluid when more kinetic stress that is put into the gel.

With the new individual methods developed on T.A., it was possible to retain information on the textural differences of Carbopol and chitosan hydrogel. Figures 19, 20 and 21 show cohesiveness, hardness and adhesiveness measured on T.A. with the newly developed methods (section 5.7.2), respectively.

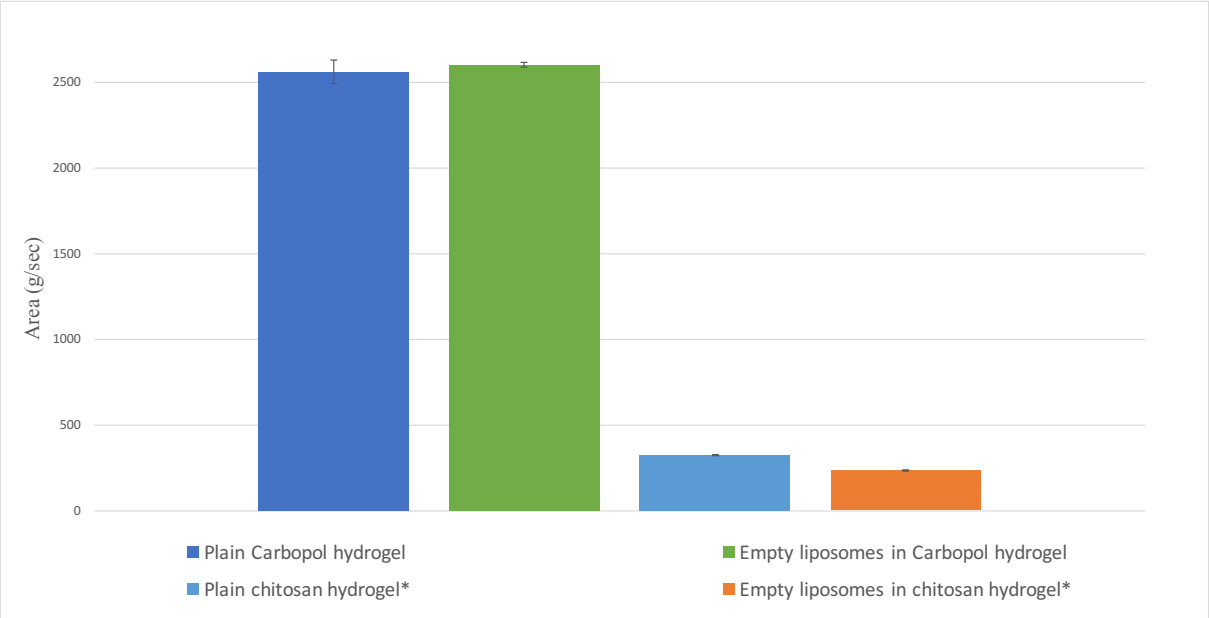

Figure 19: Cohesiveness of plain Carbopol hydrogel, empty liposomes in Carbopol hydrogel, plain chitosan hydrogel and empty liposomes in chitosan hydrogel, (n=3). *chitosan hydrogels without glycerol.

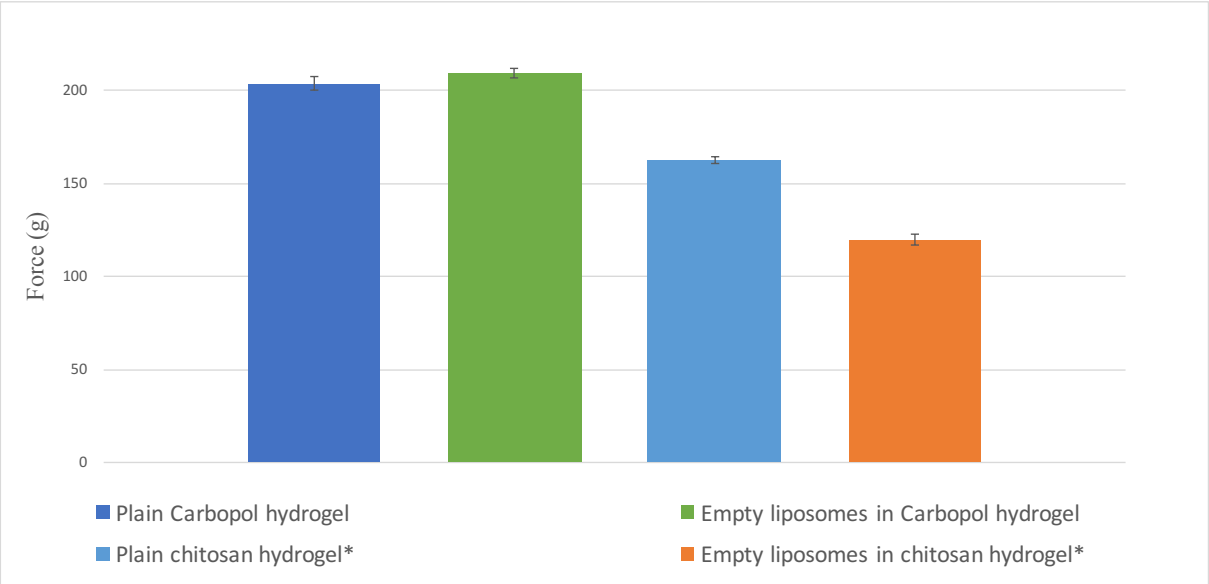

Figure 20: Hardness of plain Carbopol hydrogel, empty liposomes in Carbopol hydrogel, plain chitosan hydrogel and empty liposomes in chitosan hydrogel, (n=3). *chitosan hydrogels without glycerol.

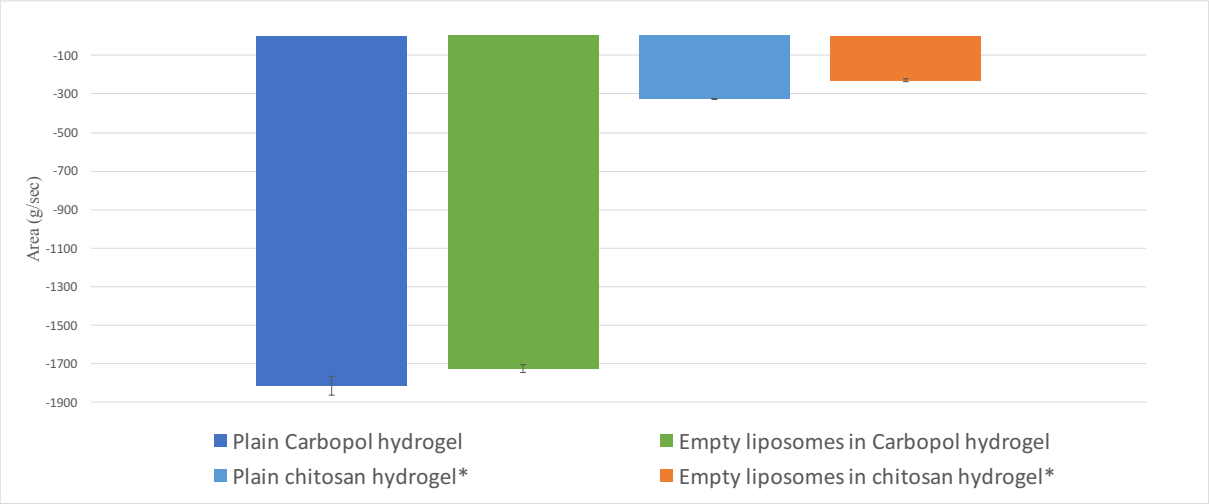

Figure 21: Adhesiveness of plain Carbopol hydrogel, empty liposomes in Carbopol hydrogel, plain chitosan hydrogel and empty liposomes in chitosan hydrogel, (n=3). *chitosan hydrogels without glycerol.

Adhesiveness, that indicates the retention time on the wounds site, was more than 5.5 times higher for plain Carbopol hydrogel compared to plain chitosan hydrogel. Cohesiveness, that indicates the internal stickiness of the hydrogel, was more than 8 times higher for plain

Carbopol hydrogel than plain chitosan hydrogel. The cohesiveness was reduced when incorporating empty liposomes into chitosan hydrogel, whereas it was increased when incorporated in Carbopol hydrogel. Hardness indicates the applicability of the hydrogel to the skin, and it was slightly higher for plain Carbopol hydrogel (force: 203.5 ± 3.7 g) than for plain chitosan hydrogel (force 162.8 ± 1.7 g). Likewise, Hurler *et al*. reported slightly higher hardness for plain Carbopol hydrogel (306.4 ± 9.7 g) than for plain chitosan hydrogel (253.1 ± 1.1 g). However, it was reported that the hardness decreased when incorporating liposomes (Hurler et al., 2012), and in our experiment we observed an increase in both cohesiveness and hardness for Carbopol hydrogel with incorporated empty liposomes.

On the contrary, Jøraholmen *et al.* reported an increase in all textural parameters when incorporating liposomes into chitosan hydrogels (Jøraholmen et al., 2019), while in our study there was only a decrease in textural properties for liposome-in-chitosan-hydrogels, compared to plain chitosan hydrogel. Additionally, in our experiment, hydrogels with empty liposomes contained a lower concentration of polymer than plain hydrogels, which was expected to attribute to the hydrogels lower textural properties. However, it is important to consider that the types of chitosan employed in hydrogel formation, presence and absence of glycerol as well as ratio between liposomes and hydrogel varied among reported data.

Direct comparison of these two hydrogels was not fully reliable because they required different settings on T.A. that are adjusted according to the hydrogels' type. As mention in the introduction, chitosan hydrogel was selected for the further investigations because of its antimicrobial, anti-inflammatory and biocompatible effects and glycerol was added to the hydrogel as a viscosity enhancer and stabilising agent. Since a reproducible method for the T.A. was developed, it was possible to evaluate the cohesiveness, hardness and adhesiveness of the plain chitosan hydrogel and liposomes-in-chitosan hydrogel.

6.4 Chitosan hydrogels characteristic

Chitosan is soluble in acidic aqueous solutions and therefore acetic acid is mixed with water before dispersing chitosan in the acidic aqueous solution. The pH of the final formulation is presented in Table 8.

Table 8: pH of different chitosan hydrogel formulations (n=3).

Type of hydrogel	pH
Plain hydrogel	4.68 ± 0.07
Empty liposomes-in-hydrogel	4.65 ± 0.05
CHX liposomes-in-hydrogel	4.82 ± 0.03

The consequence of incorporating empty liposomes into the chitosan hydrogel was a slightly more acidic pH, while incorporating CHX liposomes into the chitosan hydrogel increases the pH, compared to plain hydrogel. This can be explained considering the original pH of the liposomal dispersion (Table 4) where the arrangement of CHX in the liposomal lipid bilayer leads to higher pH and because CHX is a strong base (Kudo et al., 2002).

Under normal circumstances, the pH of the skin can differ from 4 to 6, depending on anatomical location and age of the person. The normal acidic milieu on skin acts as a barrier and helps counteract bacterial colonisation (Schneider et al., 2007). The environment in wounds can either become more acidic or slightly alkaline depending on the type of bacteria and wound condition (Saghazadeh et al., 2018). Some bacteria need an environment where the pH is above 6, and restoring a natural acidic environment could potentially contribute to inhibition of bacterial growth. However, there is not an established a relationship between measured pH and colonisation of bacteria within the wound so far. As chronic wounds are stuck in the inflammation phase there is a lot of proteolytic activity that contributes to creating a more acidic

environment, but the pH in the chronic wound will fluctuate with time and wound-stage. There is observed a more alkaline environment in wound exudate when the wound is in its healing phase (Schneider et al., 2007). The pH of our CHX liposomes-in-hydrogel formulation was appropriate considering contribution to restore a natural acidic environment and preventing bacterial growth, however the pH of the formulation might not be beneficial when the wound reaches the healing phase. Although this is only speculations and would have to be confirmed by appropriate investigations.

In Figure 22, the pH for empty liposomes-in-hydrogel and CHX liposomes-in-hydrogel formulations over a period of 12 and 4 weeks, respectively, are presented.

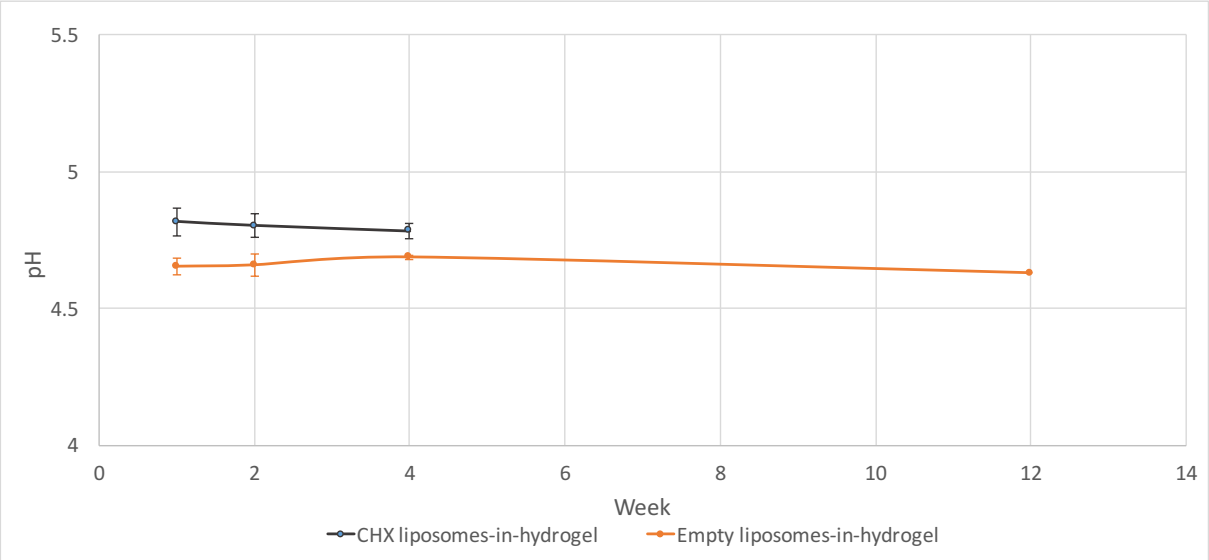

Figure 22: pH changes upon storage for 1, 2, 4 and 12 weeks for empty liposomes-in-hydrogel (n=3) and pH changes from week 1, 2 (n=3) and 4 weeks (n=2) for CHX liposomes-in-hydrogel.

For empty liposomes-in-hydrogel and CHX liposomes-in-hydrogel formulations the pH did not significantly change during a 12-week and 4-week period, respectively. In respect to the stability, in pH measurement of CHX liposomes-in-hydrogel there remains a need for more measurements to strengthen the results.

6.4.1 Chitosan hydrogels textural properties

Textural properties are important for the liposomes-in-hydrogel formulations. By using a T.A. to investigate cohesiveness, hardness and adhesiveness, it is possible to assure that the hydrogel properties correspond to the desired properties, or at least provide an indication of the hydrogels' potential in wound treatment. Hydrogels with desired textural properties are stable, stay on the surface of the skin over a longer period of time and are painlessly removed from the wound (Hurler and Škalko-Basnet, 2012).

The mechanical strength of the hydrogel should have a balance between its adhesiveness and cohesiveness. The hydrogel should be stable in terms of retaining high cohesiveness, but should not be to firm to apply to the skin in terms of having a too high hardness and limited spreadability. Applicability of the gel to the skin should contribute to patient compliance (Hurler et al., 2012).

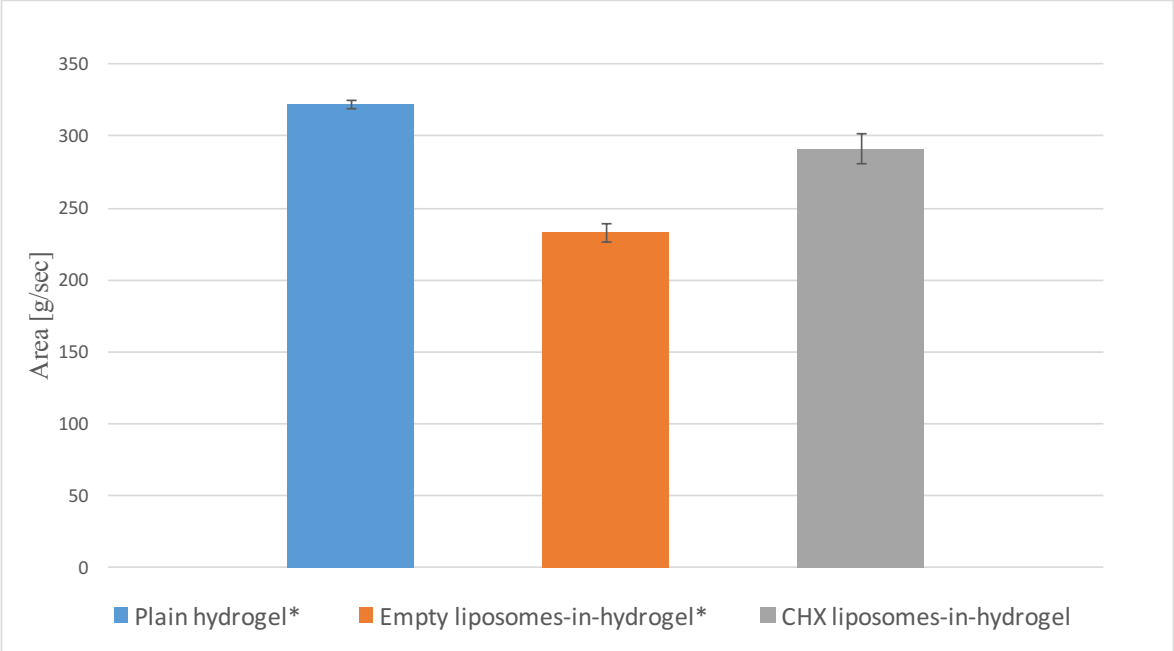

Figure 23: Cohesiveness of plain hydrogel, empty liposomes-in-hydrogel and CHX liposomes-in-hydrogel (n=3). *do not contain glycerol.

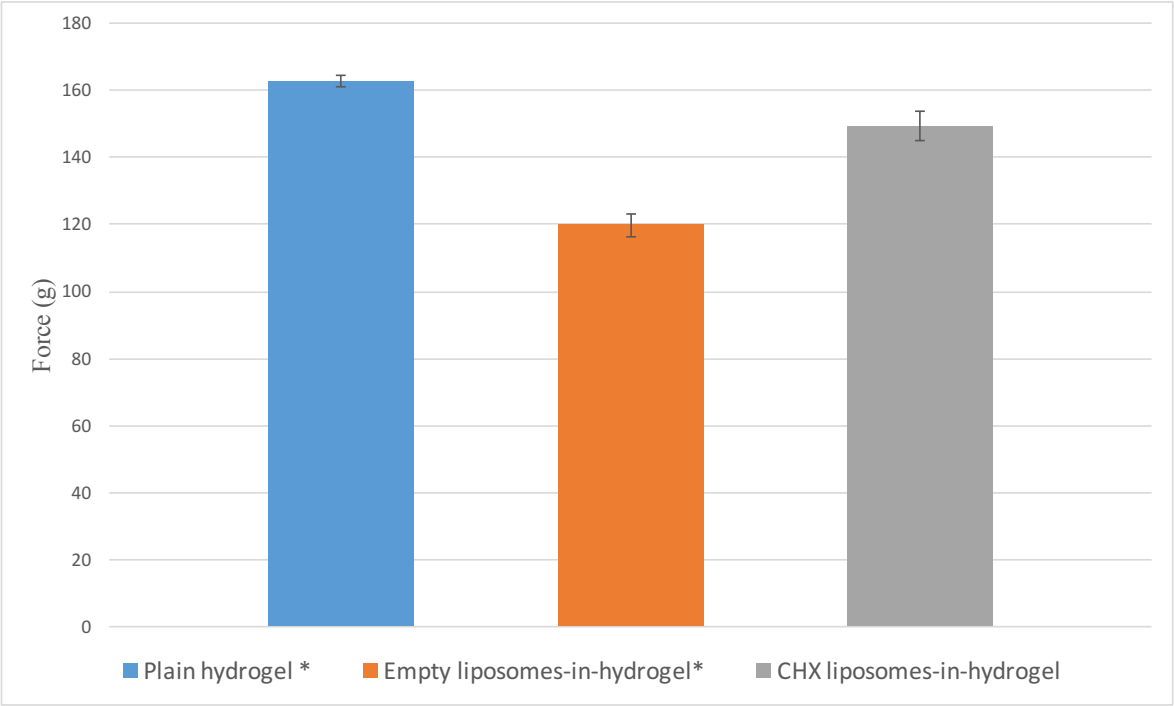

Figure 24: Hardness of plain hydrogel, empty liposomes-in-hydrogel and CHX liposomes-in-hydrogel (n=3). *do not contain glycerol.

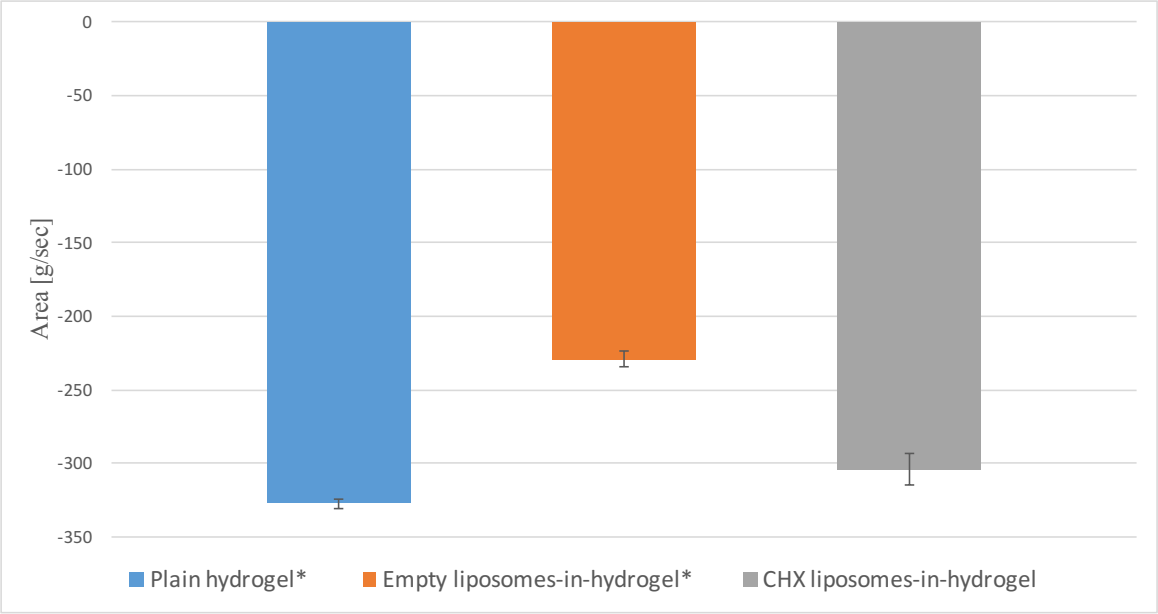

Figure 25: Adhesiveness of plain hydrogel, empty liposomes-in-hydrogel and CHX liposomes-in-hydrogel (n=3). *do not contain glycerol.

In Figures 23, 24 and 25, the cohesiveness, hardness and adhesiveness are presented, respectively. A common trend for texture properties can be observed. The texture properties for chitosan hydrogel decreased when incorporating empty liposomes into the hydrogel and increased for CHX liposomes-in-hydrogel comprising glycerol.

Comparatively, our group have earlier reported increased textural properties of chitosan hydrogel incorporating liposomes as compared to plain hydrogel (Jøraholmen et al., 2019). However, the textural properties of liposomes-in-hydrogel formulations can be affected by both liposomal size, charge and the method used on the T.A. Even though the empty liposomes had similar charge in both reported work and our findings, the polymer concentration, liposome content and liposomal size were different and the comparison is not ideal as different settings were used on the T.A. to characterise the hydrogels.

A proper comparison between plain hydrogel and empty liposomes-in-hydrogel with CHX liposomes-in-hydrogel is difficult, because the CHX liposomes-in-hydrogel contained also glycerol. It has been showed in studies that glycerol is a viscosity enhancer and stabilising agent (Szymańska and Winnicka, 2015), therefore the glycerol can improve the textural properties. Even though CHX liposomes-in-hydrogel exhibited improved texture properties compared to empty liposomes-in-hydrogel, it is difficult to attribute the findings to the addition of 10 % (w/w) glycerol to the hydrogel, incorporation of CHX liposomes, or a combination of both. We planned to characterise textural properties of plain chitosan with glycerol to improve the comparison. The reason we included glycerol at later stage of our study were the rather decreased textural properties of chitosan hydrogels upon incorporation of empty liposomes (Figures 23, 24 and 25).

Summarised, the T.A. results show improved texture properties of CHX liposomes-in-hydrogel comprising glycerol compared to empty liposomes-in-hydrogel, but not improved textural properties compared to plain hydrogel without glycerol. However, as mentioned, the plain hydrogels contain higher concentration of polymer than hydrogels incorporated with liposomes (5.0 % (w/w) versus 4.5 % (w/w) chitosan, respectively), therefore it is expected that lower concentration polymer would lead to lower textural properties.

In addition to textural properties, the viscosity and rheological characterisation are very important for indication of the rigidity and elasticity of the polymer network of the gel. The textural characterisation, viscosity and rheological characterisation will complement each other (Carvalho et al., 2013). We started developing a method to test viscosity of the hydrogel (Appendix VI.IV) and that could additionally be used to evaluate the method developed on the T.A. The plan was to test viscosity over time with different temperatures and different application of shear stress.

The stability is, as mentioned, important to take into consideration to predict the quality of a pharmaceutical formulation and textural properties of hydrogels can correlate with the hydrogels stability. In this project, stability testing of the textural properties was not optimally conducted and the results are not fully reliable (Appendix III). The method developed for texture analysers require 65 g hydrogel, thus it was not made enough hydrogel in the beginning of the project to maintain the amount hydrogel needed for the stability testing. With the transferring of the hydrogel back and forth from container and beaker, the amount of hydrogel decreased. Thereupon, we were not able to conduct the experiment under the same conditions. This makes the results less reliable but it indicates the trend. The stability testing was also given less priority, as it is possible to evaluate stability of the gel in the accelerated conditions later.

Nevertheless, the liposomes in this project (empty liposomes and CHX liposomes) bear different properties in respect to size and surface charge and this is known to affect the hydrogel properties and the release of the drug (Hurler et al., 2013, Ternullo et al., 2019). In the case of release of CHX from liposomes-in-hydrogel formulations, it still remains to be tested in a fully developed method in an *in vitro* experiment.

6.5 *In vitro* CHX release from liposomes-in-hydrogel

In vitro drug release testing is very important when developing a novel formulation and is an important quality control as an indication of the therapeutic potential of the formulation. There are different test methods available, but the Franz cell diffusion system is considered to be the most relevant *in vitro* method for evaluating drug release from topical formulations (Balzus et al., 2016). The receptor medium selected for the experiment was PBS with a pH of 7.4. The release of CHX from CHX liposomes-in-hydrogel formulations can be seen in Figure 26.

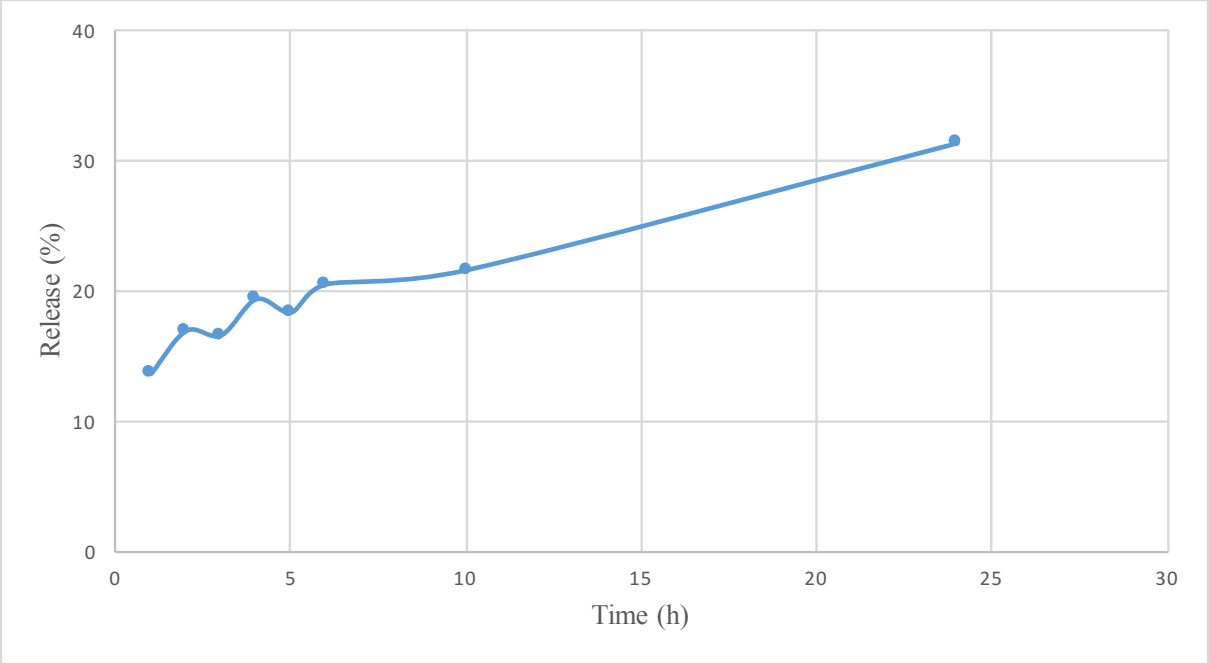

Figure 26: *In vitro* CHX release (presented in percentage) of CHX liposomes in chitosan hydrogel over time (hours) (n=1). Franz diffusion medium: PBS.

The release of CHX was slow in the first 5 hours exhibiting a persistent increased release after 5 hours. After 24 hours, 31 % of the compound was released from the formulation and diffused to the acceptor compartment. The release clearly indicated the sustained release potential of novel formulation. It is important to consider that hydrogel will be exposed to wound exudate which would affect the sustained release as well as that CHX is poorly soluble.

The experiment could have been conducted for a longer period of time. CHX is poorly soluble and can, as mentioned, interact with this membrane, an *in vitro* experiment could be conducted in the medium more adapted for CHX solubility (this is something we tested and planed; see Appendix IV and V). Considering the wound dressing exchange, once a day seems a rather optimal regime and 24 hours in vitro release experiment was found adequate.

Moreover, CHX is only a model compound for this drug delivery system and membrane active antimicrobials such as AMPs are more soluble than CHX (unpublished data). This slow release can be adequate for compounds like AMPs as this group of antimicrobial is highly potent. Since AMPs are very potent, a high concentration is not required to achieve therapeutic effect. Therefore, the observed slow release from the liposomes-in-hydrogel formulation might be sufficient for the desired antimicrobial compound to give desired therapeutic effect. It could also mean that if the concentration of the released compound is sufficient, the dosing regimen could potentially be even reduced to once in two days or similar.

In summary, treating chronic wounds and SSTIs with a membrane active antimicrobial is promising, especially when incorporated into liposomes-in-hydrogel formulations. In a situation with developed infection, one of the first responses are inflammation where a lot of inflammation cells and cytokines are present, subsequently leading to production of NO. Therefore, the anti-inflammatory activity of the established formulation was assessed in terms of their effect on the inhibition of NO production in LPS-induced macrophages.

6.6 Evaluation of anti-inflammatory activity

Macrophages play an important role in both immune response and tissue repair and development. Macrophages can be divided into two different groups: M1 that are classically activated macrophages and M2 that are alternatively activated macrophages. M1 macrophages are stimulated by various cytokines and endotoxin (for example LPS), while M2 macrophages

help with tissue remodelling. M1 macrophages produce reactive oxygen species, like for example NO (Oishi and Manabe, 2018). In this project we used murine macrophages that are stimulated by LPS, to produce high concentration of NO. NO is highly unstable and thus reacts with oxygen instantly to form nitrites (NO_2^-) and nitrates (NO_3^-) (Seminara et al., 2007).

In this project, NO_2^- was measured as it is directly proportional with NO produced by cells. A standard curve was prepared by measuring different concentrations of NO_2^-(0.5 – 10 µM) at wavelength 540 nm. The standard curve can be seen in Figure 27 and the equation y = 0.0212x – 0.0035 was used to calculate NO_2^- in cell culture media.

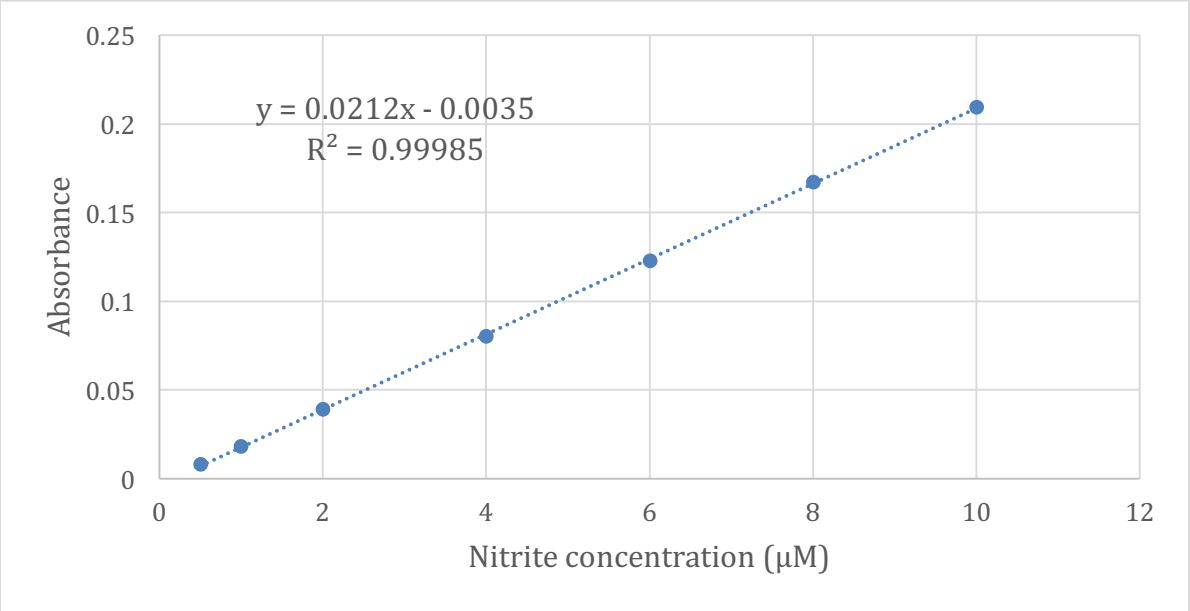

Figure 27: Standard curve of NO_2^-. Standard samples of sodium nitrite ($NaNO_2$) was prepared and mixed with Griess reagent. Absorbance of different standard samples was measured and the standard curve was obtained.

NO is a signalling molecule that plays an important role in the pathogenesis of inflammations and infections. In our project, we evaluated the inhibitory effect of empty liposomes, CHX liposomes (Figure 28), plain hydrogel and CHX liposomes-in-hydrogel formulation (Figure 29) on the production of NO. LPS-induced macrophages were treated for 24 hours ± 30 minutes with empty liposomes, CHX liposomes, plain hydrogel and CHX-liposomes-in-hydrogel

formulation in lipid concentrations or chitosan concentration corresponding to lipid concentration of 1, 10 and 50 µg/mL.

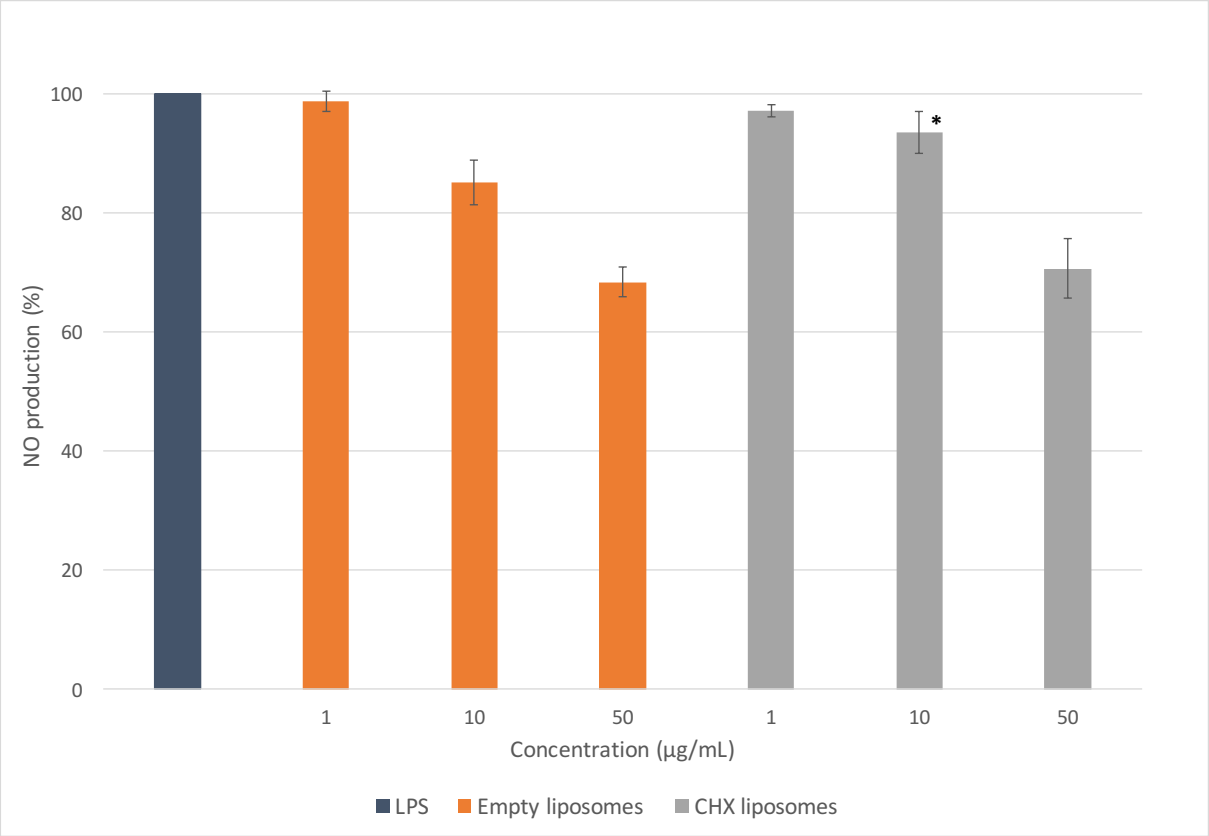

Figure 28: Effect of empty liposomes and CHX liposomes in lipid concentrations of 1, 10 and 50 µg/mL on NO production (represented in percentage) of murine macrophages compared to only LPS activated macrophages. Results are expressed as mean ± SD (n=3). * $p < 0.05$ as compared to empty liposomes in same concentration.

We can see a concentration dependent reduction of NO production trend for both empty liposomes and CHX liposomes compared to non-treated LPS-induced macrophages. Earlier in our group it has been similarly shown that conventional neutral liposomes do not enhance the NO production rather acting as anti-inflammatory agents (Jøraholmen et al., 2019). In our group, cationic deformable liposomes made of the same lipids as our liposomes but with additions of Polysorbate 20 to make them deformable and stearylamine to provide a positive charge of 33.7 mV (Ternullo et al., 2019) were also tested. Those liposomes also did not increas

the NO production, they rather exhibited a concentration depended inhibition of NO production similar to the trend showed for our positively charged liposomes.

Empty and CHX liposomes both exhibited the same concentration dependent inhibition trend of NO production; the CHX liposomes in concentration of 10 µg/mL exhibited significantly lower inhibition effect compared to empty liposomes in the same concentration.

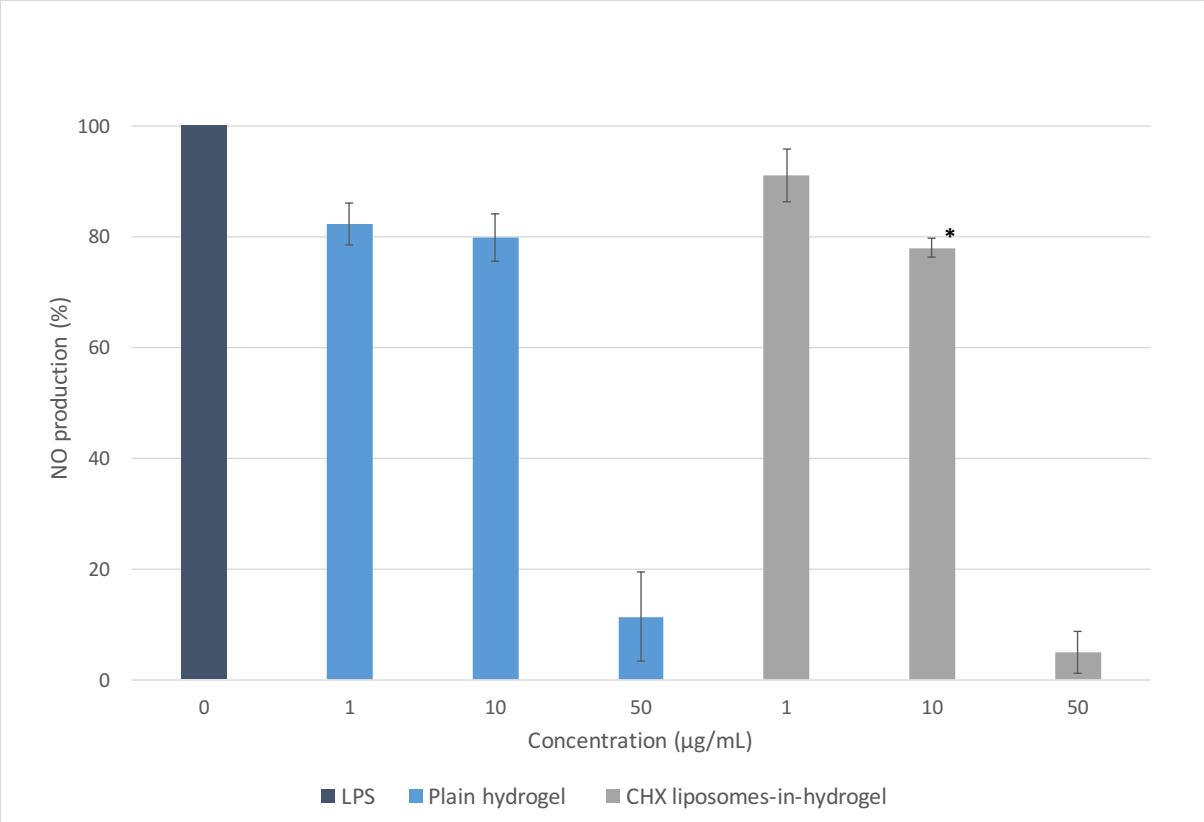

Figure 29: Effect of plain hydrogel (4.5 % (w/w) chitosan) and CHX liposomes-in-hydrogel formulation corresponding in lipid corresponding of 1, 10 and 50 µg/mL on NO production (represented in percentage) of murine macrophages compared to only LPS activated murine macrophages. Results are expressed as mean ± SD (n=3). * $p < 0.05$ as compared to plain hydrogel in same concentration.

Chitosan is well documented to have anti-inflammatory effect (Matica et al., 2019). Thereupon, there was also a concentration dependent reduction of NO production compared to non-treated LPS-induced macrophages. Plain hydrogel and CHX liposomes-in-hydrogel formulation both

showed the same concentration dependent trend with exception of CHX liposomes- in-hydrogel formulation in concentration 1 µg/mL that exhibited significantly lower inhibition effect compared to plain hydrogel in the same concentration.

However, the method for testing anti-inflammatory activity of hydrogels needs to be revaluated or further developed. This is due to the difficulty of evaluating if it is the high concentration of chitosan hydrogel that is the reason for high reduction of NO production or if it is a result of the cells not surviving incubation with high concentration of hydrogel. Although, it has been earlier in our group shown that empty liposomes-in-hydrogel formulations with a lower chitosan concentration (original concentration of 2.5 % (w/w)) have exhibited a concentration dependent inhibitory effect on NO production (Jøraholmen et al., 2019).

These preliminary results can indicate that a novel drug delivery system as liposomes-in-hydrogel formulation do not increase inflammation, but rather have anti-inflammatory effect as none of the components in different concentrations induced NO production. However, it is important that *in vitro* studies are verified through *in vivo* experiments, such as animal testing (Fadeel and Garcia-Bennett, 2010).

7 Conclusions

In this project, we developed a liposomes-in-hydrogel formulation for membrane active antimicrobials with the intent to improve wound therapy. Based on the results presented in this thesis, there is potential in developing a liposomes-in hydrogel formulation as a novel drug delivery system for AMPs administrated locally to the skin. We used CHX as a model compound to optimise the liposomal and liposomes-in-hydrogel formulation.

The developed liposome dispersion had a suitable mean vesicle size of 318.4 ± 8.6 nm appropriate for topical administration, and incorporated sufficient amount of drug in terms of having a high EE around 96 %. A texture analysis method was established and validated to evaluate texture properties of hydrogels and therefore we could compare variation between batches of hydrogels, and stability. The CHX liposomes-in-hydrogel were found to have acceptable textural properties for topical application. Results from the anti-inflammatory experiment indicate an anti-inflammatory effect of the liposomes-in-hydrogel formulation. Current *in vitro* release studies indicated sustained release of CHX from the liposomes-in-hydrogel formulation.

However, several additional steps need to be explored and the optimisation process needs to continue. It is crucial to complete the planned experiments (Appendix VI) that we were not able to conduct and complete more stability studies. It is important to explore the release of the compound from the formulation with a fully developed *in vitro* method and evaluate the antimicrobial activity. Moreover, it remains to be performed the translational research from model compound to the desired AMP.

Based on the findings presented in this thesis, we believe that incorporating a membrane active compound into liposomes and their subsequent incorporated in hydrogels provides potential for development of a novel wound dressing. These results serve as a strong base for further development of the formulation.

8 Perspective

Short-term perspective:

- Complete the planned experiments (Appendix VI) and further optimisation of formulation.

    - Confirm entrapment efficacy of CHX in liposomes by centrifugation method.
    - Measure textural properties of plain chitosan hydrogel with glycerol.
    - Measure phospholipid content of liposomes.
    - Investigate viscosity of hydrogel formulation and rheological properties.
    - *In vitro* release studies on Franz diffusion system.
    - Stability testing of hydrogels and liposomes-in-hydrogel formulation.
    - Improve the method for anti-inflammatory testing of hydrogels.

- Toxicity studies with keratinocytes and fibroblasts.
- Antibacterial testing including both planktonic bacteria and biofilms.
- Incorporating desired AMP into liposomes-in-hydrogel formulation and optimise formulation further.
- Investigate location of the AMP within liposomes by more advanced characterisations such as small-angle X-ray scattering.
- Bioadhesion studies of the formulation on *ex vivo* skin tissue.

Long-term perspective:

- *In vivo* studies of effect and safety of the developed formulation in an appropriate animal model.

9 References

Akbarzadeh, A., Rezaei-Sadabady, R., Davaran, S., Joo, S. W., Zarghami, N., Hanifehpour, Y., et al. 2013. Liposome: classification, preparation, and applications. *Nanoscale Research Letters,* 8**,** 102.

Ambrogi, V., Pietrella, D., Nocchetti, M., Casagrande, S., Moretti, V., De Marco, S., et al. 2017. Montmorillonite–chitosan–chlorhexidine composite films with antibiofilm activity and improved cytotoxicity for wound dressing. *Journal of Colloid and Interface Science,* 491**,** 265-272.

Balzus, B., Colombo, M., Sahle, F. F., Zoubari, G., Staufenbiel, S. & Bodmeier, R. 2016. Comparison of different in vitro release methods used to investigate nanocarriers intended for dermal application. *International Journal of Pharmaceutics,* 513**,** 247-254.

Bangham, A. D., Standish, M. M. & Watkins, J. C. 1965. Diffusion of univalent ions across the lamellae of swollen phospholipids. *Journal of Molecular Biology,* 13**,** 238-252.

Barbier, F. & Timsit, J. F. 2020. Risk stratification for multidrug-resistant bacteria in patients with skin and soft tissue infection. *Current Opinion in Infectious Diseases,* 33**,** 137-145.

Bhattacharjee, S. 2016. DLS and zeta potential - What they are and what they are not? *Journal of Controlled Release,* 235**,** 337-351.

Bhattarai, N., Gunn, J. & Zhang, M. 2010. Chitosan-based hydrogels for controlled, localized drug delivery. *Advanced Drug Delivery Reviews,* 62**,** 83-99.

Biswaro, L. S., Da Costa Sousa, M. G., Rezende, T. M. B., Dias, S. C. & Franco, O. L. 2018. Antimicrobial peptides and nanotechnology, recent advances and challenges. *Frontiers in Microbiology,* 9**,** 855.

Boateng, J. & Catanzano, O. 2015. Advanced therapeutic dressings for effective wound healing - A review. *Journal of Pharmaceutical Sciences,* 104**,** 3653-3680.

Bradford, C., Freeman, R. & Percival, S. L. 2009. In vitro study of sustained antimicrobial activity of a new silver alginate dressing. *The Journal of the American College of Certified Wound Specialists,* 1**,** 117-120.

Brogden, K. A. 2005. Antimicrobial peptides: pore formers or metabolic inhibitors in bacteria? *Nature Reviews Microbiology,* 3**,** 238-250.

Carvalho, F. C., Calixto, G., Hatakeyama, I. N., Luz, G. M., Gremião, M. P. D. & Chorilli, M. 2013. Rheological, mechanical, and bioadhesive behavior of hydrogels to optimize skin delivery systems. *Drug Development and Industrial Pharmacy,* 39**,** 1750-1757.

Danaei, M., Dehghankhold, M., Ataei, S., Hasanzadeh Davarani, F., Javanmard, R., Dokhani, A., et al. 2018. Impact of particle size and polydispersity index on the clinical applications of lipidic nanocarrier systems. *Pharmaceutics,* 10**,** 57.

Dash, M., Chiellini, F., Ottenbrite, R. M. & Chiellini, E. 2011. Chitosan—A versatile semi-synthetic polymer in biomedical applications. *Progress in Polymer Science,* 36**,** 981-1014.

Drago, F., Gariazzo, L., Cioni, M., Trave, I. & Parodi, A. 2019. The microbiome and its relevance in complex wounds. *European Journal of Dermatology,* 29**,** 6-13.

Duarte, B., Pereira, A. P., Freitas, A. R., Coque, T. M., Hammerum, A. M., Hasman, H., et al. 2019. 2CS-CHX(T) Operon signature of chlorhexidine tolerance among Enterococcus faecium isolates. *Applied and Environmental Microbiology,* 85**,** e1519-e1589.

Edwards, R. & Harding, K. G. 2004. Bacteria and wound healing. *Current Opinion in Infectious Diseases,* 17**,** 91-96.

Eloy, J. O., Claro De Souza, M., Petrilli, R., Barcellos, J. P. A., Lee, R. J. & Marchetti, J. M. 2014. Liposomes as carriers of hydrophilic small molecule drugs: Strategies to enhance encapsulation and delivery. *Colloids and Surfaces B: Biointerfaces,* 123**,** 345-363.

Elsayed, M. M. A., Abdallah, O. Y., Naggar, V. F. & Khalafallah, N. M. 2007. Lipid vesicles for skin delivery of drugs: Reviewing three decades of research. *International Journal of Pharmaceutics,* 332**,** 1-16.

Fadeel, B. & Garcia-Bennett, A. E. 2010. Better safe than sorry: Understanding the toxicological properties of inorganic nanoparticles manufactured for biomedical applications. *Advanced Drug Delivery Reviews,* 62**,** 362-374.

Farkas, E., Kiss, D. & Zelkó, R. 2007. Study on the release of chlorhexidine base and salts from different liquid crystalline structures. *International Journal of Pharmaceutics,* 340**,** 71-75.

Fjell, C. D., Hiss, J. A., Hancock, R. E. W. & Schneider, G. 2012. Designing antimicrobial peptides: form follows function. *Nature Reviews Drug Discovery,* 11**,** 37-51.

Foldvari, M. 2000. Non-invasive administration of drugs through the skin: challenges in delivery system design. *Pharmaceutical Science & Technology Today,* 3**,** 417-425.

Fresno, M. J. C., RamíRez, A. D. & Jiménez, M. M. 2002. Systematic study of the flow behaviour and mechanical properties of Carbopol® Ultrez™ 10 hydroalcoholic gels. *European Journal of Pharmaceutics and Biopharmaceutics,* 54**,** 329-335.

Friedman, N. D., Temkin, E. & Carmeli, Y. 2016. The negative impact of antibiotic resistance. *Clinical Microbiology and Infection,* 22**,** 416-422.

Frykberg, R. G. & Banks, J. 2015. Challenges in the treatment of chronic wounds. *Advances in Wound Care,* 4**,** 560-582.

Gago, D., Chagas, R., Ferreira, L. M., Velizarov, S. & Coelhoso, I. 2020. A novel cellulose-based polymer for efficient removal of methylene blue. *Membranes,* 10**,** 13.

Ghica, M. V., Hirjau, M., Lupuleasa, D. & Dinu-Pirvu, C. E. 2016. Flow and thixotropic parameters for rheological characterization of hydrogels. *Molecules,* 21**,** 786.

Goldfine, H. 1984. Bacterial membranes and lipid packing theory. *Journal of Lipid Research,* 25**,** 1501-1507.

Gomes, A., Teixeira, C., Ferraz, R., Prudêncio, C. & Gomes, P. 2017. Wound-healing peptides for treatment of chronic diabetic foot ulcers and other infected skin injuries. *Molecules,* 22**,** 1743.

Grip, J., Engstad, R. E., Skjæveland, I., Škalko-Basnet, N. & Holsæter, A. M. 2017. Sprayable Carbopol hydrogel with soluble beta-1,3/1,6-glucan as an active ingredient for wound healing – Development and in-vivo evaluation. *European Journal of Pharmaceutical Sciences,* 107**,** 24-31.

Gustafsson, J., Arvidson, G., Karlsson, G. & Almgren, M. 1995. Complexes between cationic liposomes and DNA visualized by cryo-TEM. *Biochimica et Biophysica Acta (BBA) - Biomembranes,* 1235**,** 305-312.

Hamdan, S., Pastar, I., Drakulich, S., Dikici, E., Tomic-Canic, M., Deo, S., et al. 2017. Nanotechnology-driven therapeutic interventions in wound healing: potential uses and applications. *ACS Central Science,* 3**,** 163-175.

Has, C. & Pan, S. 2020. Vesicle formation mechanisms: an overview. *Journal of Liposome Research,* 3**,** 1-22.

Hira, J., Bentdal, S., Devold, H., Stensvåg, K. & Landfald, B. 2019. Vibrio echinoideorum sp. nov., isolated from an epidermal lesion on the test of a green sea urchin (Strongylocentrotus droebachiensis). *International Journal of Systematic and Evolutionary Microbiology,* 69**,** 2277-2282.

Hua, S. 2015. Lipid-based nano-delivery systems for skin delivery of drugs and bioactives. *Frontiers in Pharmacology,* 6**,** 219.
Hubbard, A. T. M., Coates, A. R. M. & Harvey, R. D. 2017. Comparing the action of HT61 and chlorhexidine on natural and model Staphylococcus aureus membranes. *The Journal of Antibiotics,* 70**,** 1020-1025.
Hupfeld, S., Holsæter, A. M., Skar, M., Frantzen, C. B. & Brandl, M. 2006. Liposome size analysis by dynamic/static light scattering upon size exclusion-/field flow-fractionation. *Journal of Nanoscience and Nanotechnology,* 6**,** 3025-3031.
Hurdle, J. G., O'neill, A. J., Chopra, I. & Lee, R. E. 2011. Targeting bacterial membrane function: an underexploited mechanism for treating persistent infections. *Nature Reviews Microbiology,* 9**,** 62-75.
Hurler, J., Engesland, A., Poorahmary Kermany, B. & Škalko-Basnet, N. 2012. Improved texture analysis for hydrogel characterization: Gel cohesiveness, adhesiveness, and hardness. *Journal of Applied Polymer Science,* 125**,** 180-188.
Hurler, J. & Škalko-Basnet, N. 2012. Potentials of chitosan-based delivery systems in wound therapy: bioadhesion study. *Journal of Functional Biomaterials,* 3**,** 37-48.
Hurler, J., Žakelj, S., Mravljak, J., Pajk, S., Kristl, A., Schubert, R., et al. 2013. The effect of lipid composition and liposome size on the release properties of liposomes-in-hydrogel. *International Journal of Pharmaceutics,* 456**,** 49-57.
Ingebrigtsen, S. G., Škalko-Basnet, N. & Holsæter, A. M. 2016. Development and optimization of a new processing approach for manufacturing topical liposomes-in-hydrogel drug formulations by dual asymmetric centrifugation. *Drug Development and Industrial Pharmacy,* 42**,** 1375-1383.
Islam, M. T., Rodríguez-Hornedo, N., Ciotti, S. & Ackermann, C. 2004. Rheological characterization of topical carbomer gels neutralized to different pH. *Pharmaceutical Research,* 21**,** 1192-1199.
Jain, A. K. & Thareja, S. 2019. In vitro and in vivo characterization of pharmaceutical nanocarriers used for drug delivery. *Artificial Cells, Nanomedicine, and Biotechnology,* 47**,** 524-539.
Jones, D. S., Woolfson, A. D. & Djokic, J. 1996. Texture profile analysis of bioadhesive polymeric semisolids: Mechanical characterization and investigation of interactions between formulation components. *Journal of Applied Polymer Science,* 61**,** 2229-2234.
Jøraholmen, M. W., Basnet, P., Tostrup, M. J., Moueffaq, S. & Škalko-Basnet, N. 2019. Localized therapy of vaginal infections and inflammation: Liposomes-in-hydrogel delivery system for polyphenols. *Pharmaceutics,* 11**,** 53.
Kawakami, K., Oda, N., Miyoshi, K., Funaki, T. & Ida, Y. 2006. Solubilization behavior of a poorly soluble drug under combined use of surfactants and cosolvents. *European Journal of Pharmaceutical Sciences,* 28**,** 7-14.
Kudo, K., Ikeda, N., Kiyoshima, A., Hino, Y., Nishida, N. & Inoue, N. 2002. Toxicological analysis of chlorhexidine in human serum using HPLC on a polymer-coated ODS column. *Journal of Analytical Toxicology,* 26**,** 119-122.
Kumar, P., Kizhakkedathu, J. N. & Straus, S. K. 2018. Antimicrobial Peptides: Diversity, mechanism of action and strategies to improve the activity and biocompatibility in vivo. *Biomolecules,* 8**,** 4.
Kuppusamy, R., Willcox, M., Black, D. S. & Kumar, N. 2019. Short cationic peptidomimetic antimicrobials. *Antibiotics* 8**,** 44.
Lai-Cheong, J. E. & Mcgrath, J. A. 2009. Structure and function of skin, hair and nails. *Medicine,* 37**,** 223-226.

Lboutounne, H., Chaulet, J.-F., Ploton, C., Falson, F. & Pirot, F. 2002. Sustained ex vivo skin antiseptic activity of chlorhexidine in poly(ϵ-caprolactone) nanocapsule encapsulated form and as a digluconate. *Journal of Controlled Release,* 82**,** 319-334.

Liu, H., Wang, C., Li, C., Qin, Y., Wang, Z., Yang, F., et al. 2018. A functional chitosan-based hydrogel as a wound dressing and drug delivery system in the treatment of wound healing. *RCS,* 8**,** 7533-7549.

Maherani, B., Arab-Tehrany, E., Kheirolomoom, A., Reshetov, V., Stebe, M. J. & Linder, M. 2012. Optimization and characterization of liposome formulation by mixture design. *Analyst,* 137**,** 773-786.

Mahlapuu, M., Håkansson, J., Ringstad, L. & Björn, C. 2016. Antimicrobial peptides: An emerging category of therapeutic agents. *Frontiers in Cellular and Infection Microbiology,* 6**,** 194.

Maqbool, F., Moyle, P. M., Tan, M. S. A., Thurecht, K. J. & Falconer, J. R. 2018. Preparation of albendazole-loaded liposomes by supercritical carbon dioxide processing. *Artificial Cells, Nanomedicine, and Biotechnology,* 46**,** 1186-1192.

Matica, M. A., Aachmann, F. L., Tøndervik, A., Sletta, H. & Ostafe, V. 2019. Chitosan as a wound dressing starting material: Antimicrobial properties and mode of action. *International Jounal of Molecular Sciences,* 20**,** 5889.

Mookherjee, N., Anderson, M. A., Haagsman, H. P. & Davidson, D. J. 2020. Antimicrobial host defence peptides: functions and clinical potential. *Nature Reviews Drug Discovery*.

Mourtas, S., Duraj, S., Fotopoulou, S. & Antimisiaris, S. G. 2008. Integrity of liposomes in presence of various formulation excipients, when dispersed in aqueous media and in hydrogels. *Colloids and Surfaces B: Biointerfaces,* 61**,** 270-276.

Mustoe, T. A., O'shaughnessy, K. & Kloeters, O. 2006. Chronic wound pathogenesis and current treatment strategies: a unifying hypothesis. *Plastic and Reconstructive Surgery,* 117 (supplment 1)**,** 35s-41s.

Nielsen, J. E., Bjørnestad, V. A. & Lund, R. 2018. Resolving the structural interactions between antimicrobial peptides and lipid membranes using small-angle scattering methods: the case of indolicidin. *Soft Matter,* 14**,** 8750-8763.

Nielsen, J. E., Lind, T. K., Lone, A., Gerelli, Y., Hansen, P. R., Jenssen, H., et al. 2019. A biophysical study of the interactions between the antimicrobial peptide indolicidin and lipid model systems. *Biochimica et Biophysica Acta - Biomembranes,* 1861**,** 1355-1364.

Oishi, Y. & Manabe, I. 2018. Macrophages in inflammation, repair and regeneration. *International Immunology* 30**,** 511-528.

Olusanya, T. O. B., Haj Ahmad, R. R., Ibegbu, D. M., Smith, J. R. & Elkordy, A. A. 2018. Liposomal drug delivery systems and anticancer drugs. *Molecules* 23**,** 907.

Ong, S. G. M., Chitneni, M., Lee, K. S., Ming, L. C. & Yuen, K. H. 2016. Evaluation of extrusion technique for nanosizing liposomes. *Pharmaceutics,* 8**,** 36.

Pattni, B. S., Chupin, V. V. & Torchilin, V. P. 2015. New developments in liposomal drug delivery. *Chemical Reviews,* 115**,** 10938-10966.

Paulsen, M. H., Ausbacher, D., Bayer, A., Engqvist, M., Hansen, T., Haug, T., et al. 2019. Antimicrobial activity of amphipathic α,α-disubstituted β-amino amide derivatives against ESBL – CARBA producing multi-resistant bacteria; effect of halogenation, lipophilicity and cationic character. *European Journal of Medicinal Chemistry,* 183**,** 111671.

Peppas, N. A. 1997. Hydrogels and drug delivery. *Current Opinion in Colloid & Interface Science,* 2**,** 531-537.

Peppas, N. A., Bures, P., Leobandung, W. & Ichikawa, H. 2000. Hydrogels in pharmaceutical formulations. *European Journal of Pharmaceutics and Biopharmaceutics,* 50**,** 27-46.
Pfalzgraff, A., Brandenburg, K. & Weindl, G. 2018. Antimicrobial peptides and their therapeutic potential for bacterial skin infections and wounds. *Frontiers in Pharmacology,* 9**,** 281.
Ragheb, M. N., Thomason, M. K., Hsu, C., Nugent, P., Gage, J., Samadpour, A. N., et al. 2019. Inhibiting the evolution of antibiotic resistance. *Molecular Cell,* 73**,** 157-165.e5.
Rajendran, N. K., Kumar, S. S. D., Houreld, N. N. & Abrahamse, H. 2018. A review on nanoparticle based treatment for wound healing. *Journal of Drug Delivery Science and Technology,* 44**,** 421-430.
Romanko, T. V., Murinov, Y. I. & Romanko, V. G. 2009. Optimization of rheological properties of an adsorption vaginal gel based on Carbopol. *Russian Journal of Applied Chemistry,* 82**,** 1488-1493.
Saghazadeh, S., Rinoldi, C., Schot, M., Kashaf, S. S., Sharifi, F., Jalilian, E., et al. 2018. Drug delivery systems and materials for wound healing applications. *Advanced Drug Delivery Reviews,* 127**,** 138-166.
Sala, M., Diab, R., Elaissari, A. & Fessi, H. 2018. Lipid nanocarriers as skin drug delivery systems: Properties, mechanisms of skin interactions and medical applications. *International Journal of Pharmaceutics,* 535**,** 1-17.
Samad, A., Sultana, Y. & Aqil, M. 2007. Liposomal drug delivery systems: an update review. *Current Drug Delivery,* 4**,** 297-305.
Schneider, L. A., Korber, A., Grabbe, S. & Dissemond, J. 2007. Influence of pH on wound-healing: a new perspective for wound-therapy? *Archives of Dermatological Research,* 298**,** 413-420.
Seminara, A. R., Ruvolo, P. P. & Murad, F. 2007. LPS/IFNgamma-induced RAW 264.7 apoptosis is regulated by both nitric oxide-dependent and -independent pathways involving JNK and the Bcl-2 family. *Cell Cycle,* 6**,** 1772-1778.
Siddiqui, A. R. & Bernstein, J. M. 2010. Chronic wound infection: facts and controversies. *Clinics in Dermatology,* 28**,** 519-526.
Soema, P. C., Willems, G.-J., Jiskoot, W., Amorij, J.-P. & Kersten, G. F. 2015. Predicting the influence of liposomal lipid composition on liposome size, zeta potential and liposome-induced dendritic cell maturation using a design of experiments approach. *European Journal of Pharmaceutics and Biopharmaceutics,* 94**,** 427-435.
Szymańska, E. & Winnicka, K. 2015. Stability of chitosan—A challenge for pharmaceutical and biomedical applications. *Marine Drugs,* 13**,** 1819-1846.
Tacconelli, E., Carrara, E., Savoldi, A., Harbarth, S., Mendelson, M., Monnet, D. L., et al. 2018. Discovery, research, and development of new antibiotics: the WHO priority list of antibiotic-resistant bacteria and tuberculosis. *The Lancet Infectious Diseases,* 18**,** 318-327.
Ternullo, S., Basnet, P., Holsæter, A. M., Flaten, G. E., De Weerd, L. & Škalko-Basnet, N. 2018. Deformable liposomes for skin therapy with human epidermal growth factor: The effect of liposomal surface charge. *European Journal of Pharmaceutical Sciences,* 125**,** 163-171.
Ternullo, S., Gagnat, E., Julin, K., Johannessen, M., Basnet, P., Vanić, Ž., et al. 2019. Liposomes augment biological benefits of curcumin for multitargeted skin therapy. *European Journal of Pharmaceutics and Biopharmaceutics,* 144**,** 154-164.
Ternullo, S., Schulte Werning, L. V., Holsæter, A. M. & Škalko-Basnet, N. 2020. Curcumin-in-deformable liposomes-in-chitosan-hydrogel as a novel wound dressing. *Pharmaceutics,* 12**,** 8.

Theuretzbacher, U., Outterson, K., Engel, A. & Karlén, A. 2019. The global preclinical antibacterial pipeline. *Nature Reviews Microbiology,* 18**,** 275-285.
Van Meer, G., Voelker, D. R. & Feigenson, G. W. 2008. Membrane lipids: where they are and how they behave. *Nature Reviews Molecular Cell Biology,* 9**,** 112-124.
Ventrelli, L., Marsilio Strambini, L. & Barillaro, G. 2015. Microneedles for transdermal biosensing: Current picture and future direction. *Advanced Healthcare Mater,* 4**,** 2606-2640.
Verma, D. D., Verma, S., Blume, G. & Fahr, A. 2003. Particle size of liposomes influences dermal delivery of substances into skin. *International Journal of Pharmaceutics,* 258**,** 141-151.
Yazdankhah, S. P., Sørum, H., Larsen, H. J. S. & Gogstad, G. 2001. Rapid method for detection of Gram-positive and -negative bacteria in milk from cows with doderate or severe clinical mastitis. *Journal of Clinical Microbiology,* 39**,** 2228-2233.
Zobel, M. 1976. Toxicological Evaluation of Some Food Additives Including Anticaking Agents, Antimicrobials, Antioxidants, Emulsifiers and Thickening Agents. Who Food Additives Series, No. 5. 520 Seiten. Geneva 1974. Preis: Sw. fr. 23,—. Preis: Sw. fr. 23. *Molecular Nutrition & Food Research,* 20**,** 681-682.
Zomer, H. D. & Trentin, A. G. 2018. Skin wound healing in humans and mice: Challenges in translational research. *Journal of Dermatological Science,* 90**,** 3-12.

Appendices

Appendix I pH and arrangement of CHX in liposomes

As mentioned above, pH might affect the arrangement of CHX in the lipid bilayer in liposomes and thereby affect the liposomal properties. As shown in Appendix Table 1 aqueous medium with different pH were used to hydrate thin lipid film with CHX.

Appendix Table 1: Zeta potential, size, PI and pH for different CHX liposome dispersion made from distilled water with different pH (n=1).

pH aqueous medium	Zeta potential (mV)	Size (d.nm)	PI	pH
Acidic (3.58)	33.7	278.5	0.25	9.64
Neutral	44.3	308.0	0.26	8.01
Basic (8.66)	19.2	266.8	0.23	9.65

Acidic aqueous medium resulted in a lower size and zeta potential, whereas basic aqueous medium resulted in an even lower size and zeta potential. This result tells us that pH somehow affect the arrangement of CHX in liposomal bilayer thereupon its properties. In Appendix Figure 1, there is a picture of the liposome dispersion made from aqueous medium with different pH and here it is possible to notice difference with the bare eye.

When considering the zeta potential and size, we would have expected the appearance of the liposomal dispersion different. We would have expected the liposomal dispersion with the lowest vesicle mean size to be the most transparent dispersion and *vice versa*. Whereas, we can observe that the liposomal dispersion with the highest vesicle mean size to be the most transparent dispersion.

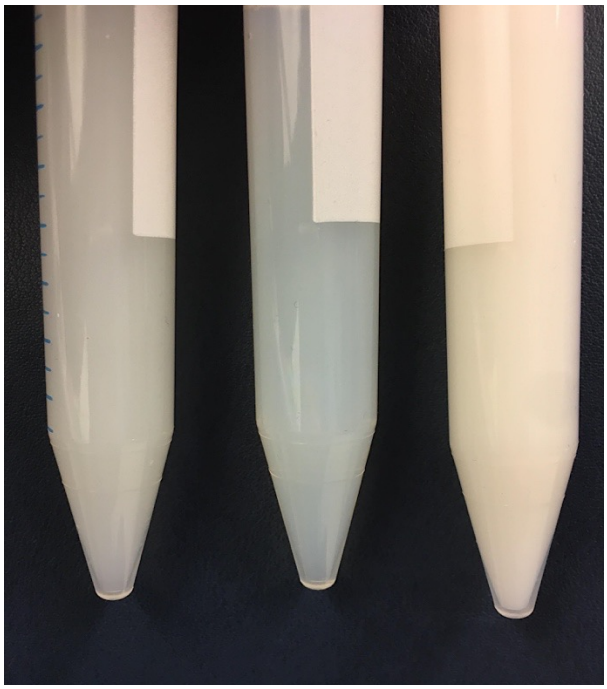

Appendix Figure 1: From left: picture of CHX liposomes made with basic water, neutral water and acidic water.

Additionally, this should further be investigated with respect to EE and conducting more parallels. As CHX is a strong base, the pH in the liposomal dispersion is basic. CHX is an amphiphilic molecule and the hydrophobic part of the structure can be incorporated in the liposomal bilayer in different ways and resulting in different bend of the molecule. This in turn can result in different interactions because distinctive parts of CHX is bending outside the bilayer.

Appendix II SEM

The SEM picture of CHX liposomes is shown in Appendix Figure 2. Here the actual size of the liposomes seems to be better displayed, compared to the TEM picture.

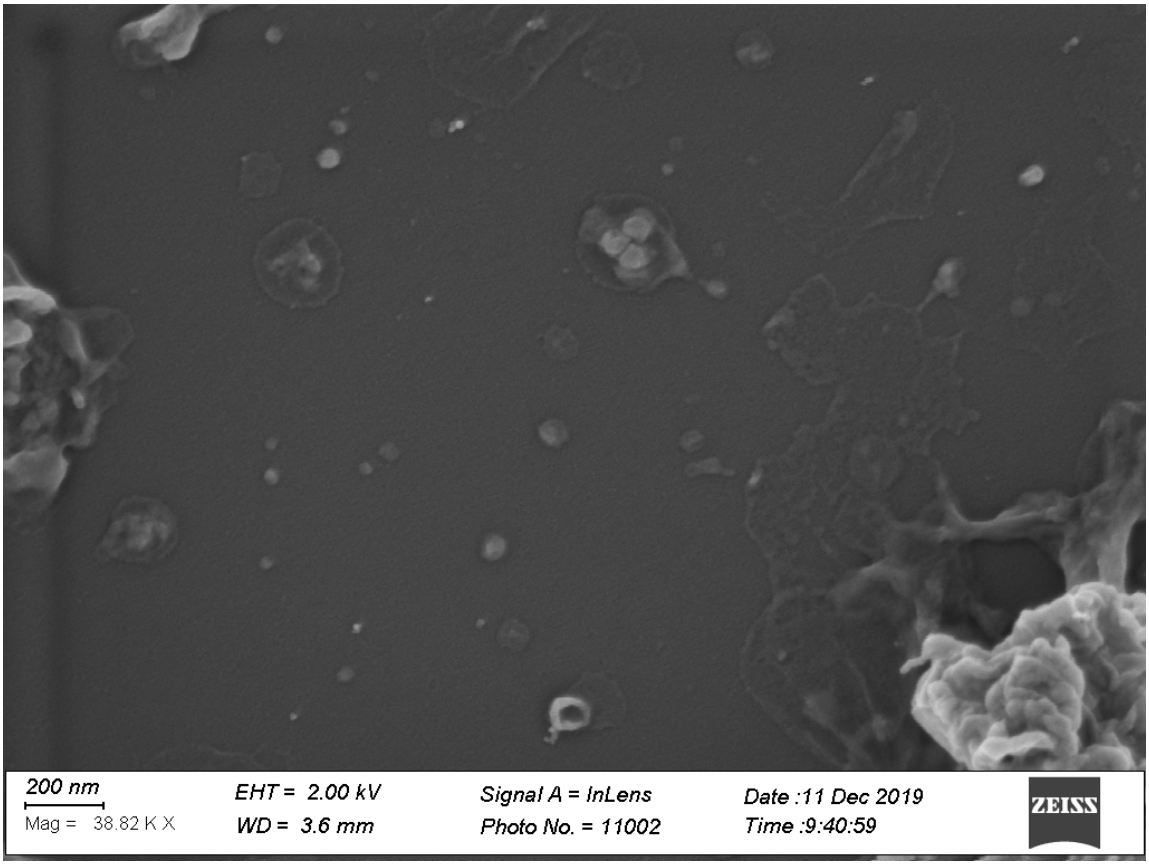

Appendix Figure 2: Scanning electron microscope picture of CHX liposome.

We used a standard method for preparing cells for SEM for our liposomes for SEM. In brief, this preparation includes cleansing with buffer, chemical fixation with osmium tetroxide and dehydrating with ethanol in concentration 30 %, 60 %, 90 %, 96 % and absolute ethanol 5 minutes each and finally coating with the conductive metal gold palladium.

We believe the preparation and especially the drying with ethanol can significantly change the morphology of the liposomes therefore not obtaining a picture of the liposomes in near native state.

Appendix III Stability textural properties for chitosan hydrogels

In Appendix Figure 3-5 the stability of textural properties for chitosan hydrogel with empty liposomes over 12 weeks are shown. As mentioned, it was not possible to maintain 65 g hydrogel for each test run, therefore the test on T.A. were conducted with different weight of hydrogel. This makes it difficult to say if the changes in textural properties comes from different set up (different weight hydrogel) or time.

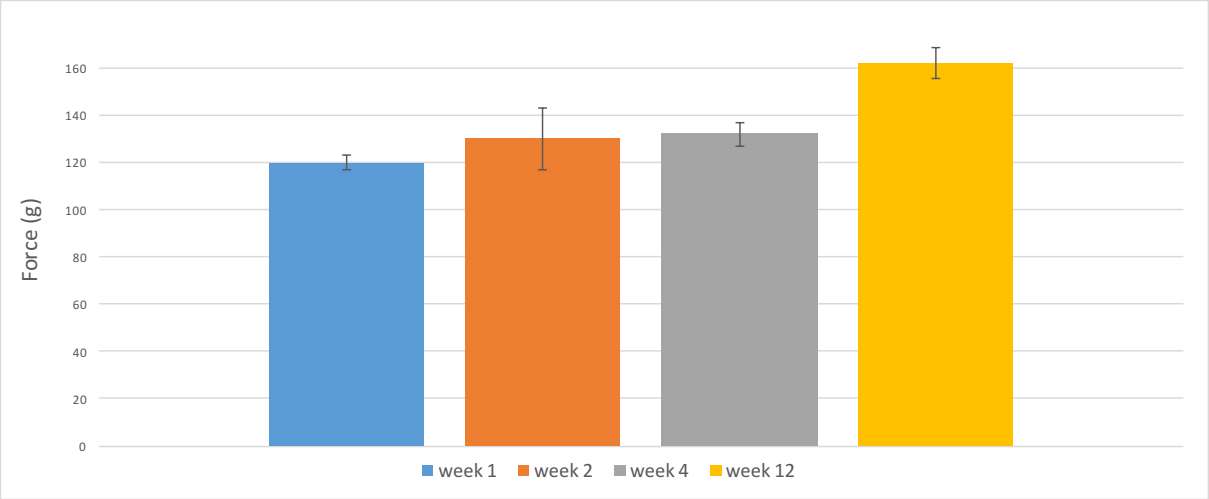

Appendix Figure 3*:* Hardness stability for empty liposomes in chitosan hydrogel for week 1, week 2, week 4 and week 12, (n=3).

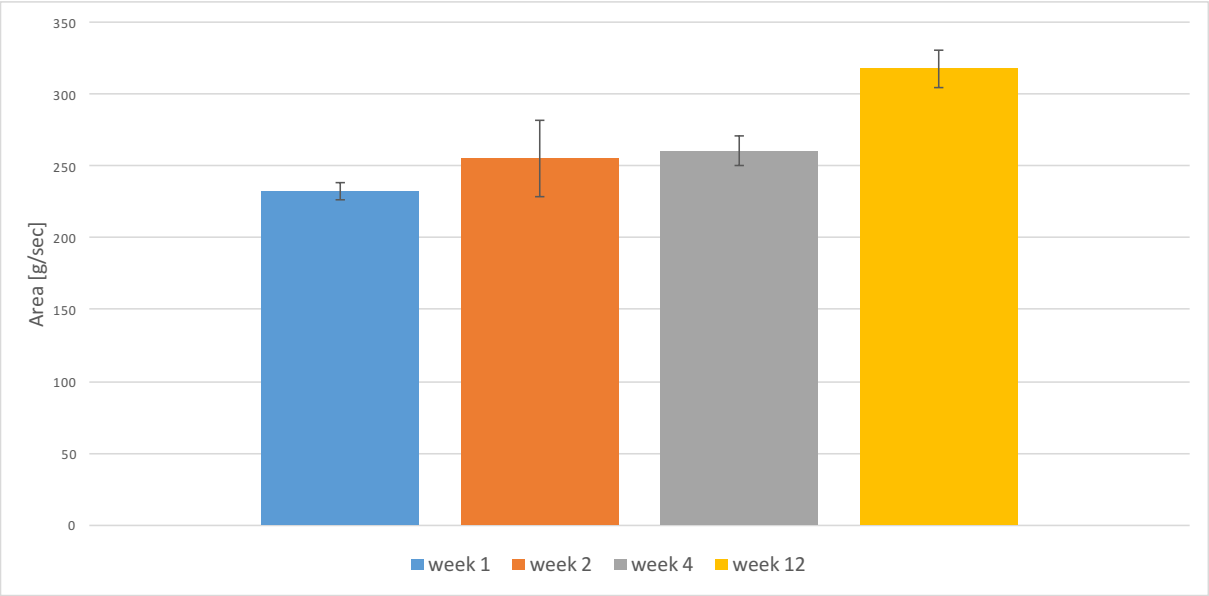

Appendix Figure 4: Cohesiveness stability for empty liposomes in chitosan hydrogel for week 1, week 2, week 4 and week 12, (n=3).

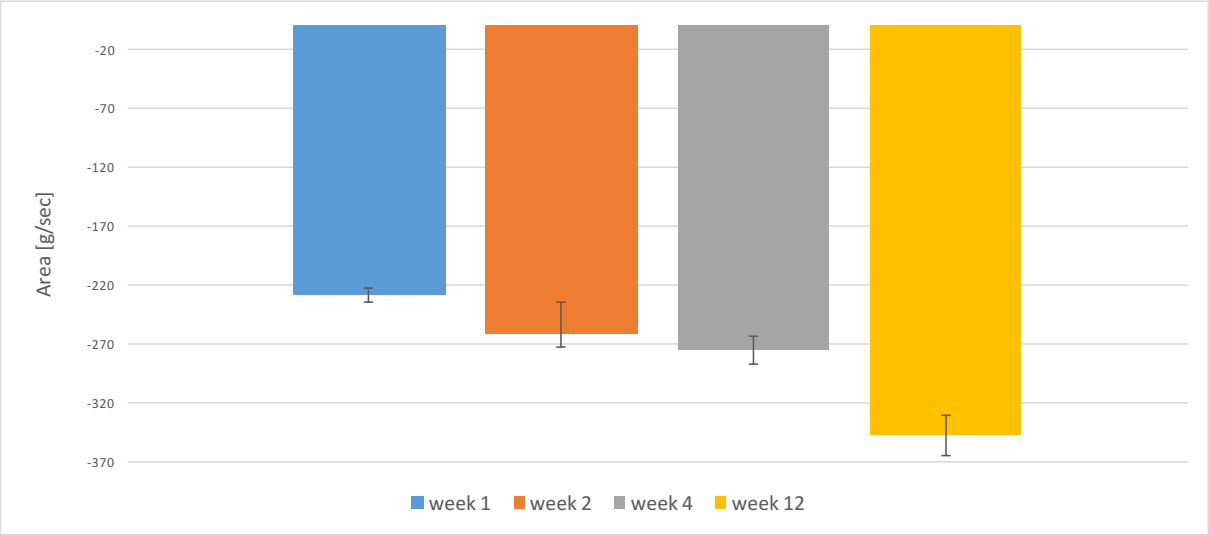

Appendix Figure 5: Adhesiveness stability for empty liposomes in chitosan hydrogel for week 1, week 2, week 4 and week 12, (n=3).

Current stability testing indicates an increase in textural properties for empty liposomes in chitosan hydrogel over time. The range amount hydrogel used for measuring empty liposomes in chitosan hydrogel was as follows: 62.1-63.2 g for week 2, 59.8-60.1 for week 4 and 51.1-

57.0 g for week 12. Because there are not equal conditions during each T.A. measurement, the results are not reliable. The same concern applies for CHX liposomes in hydrogel stability measurements, which are shown in Appendix Figure 6-8.

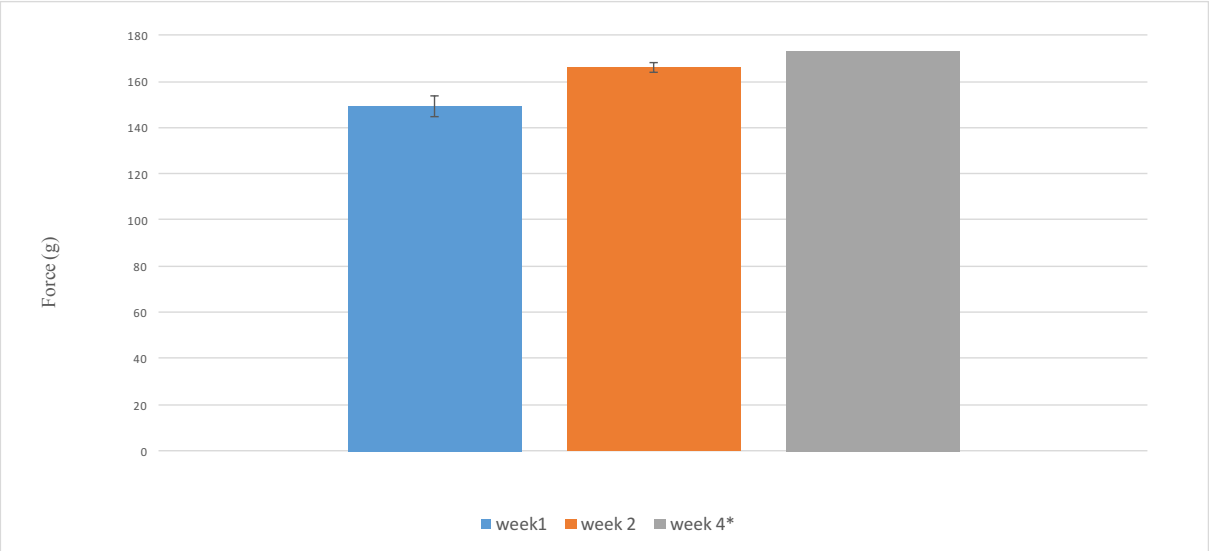

Appendix Figure 6: Hardness stability for CHX liposomes in chitosan hydrogel for week 1, week 2 and week 4, (n=3). *n=1

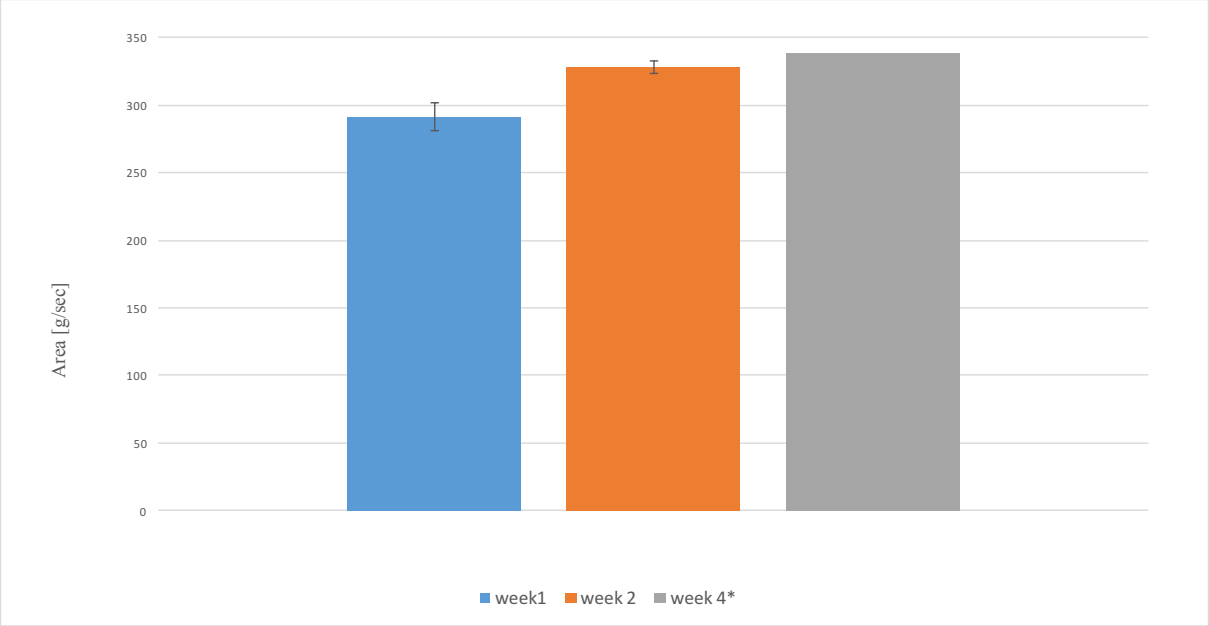

Appendix Figure 7*:* Cohesiveness stability for CHX liposomes in chitosan hydrogel for week 1, week 2 and week 4, (n=3). *n=1

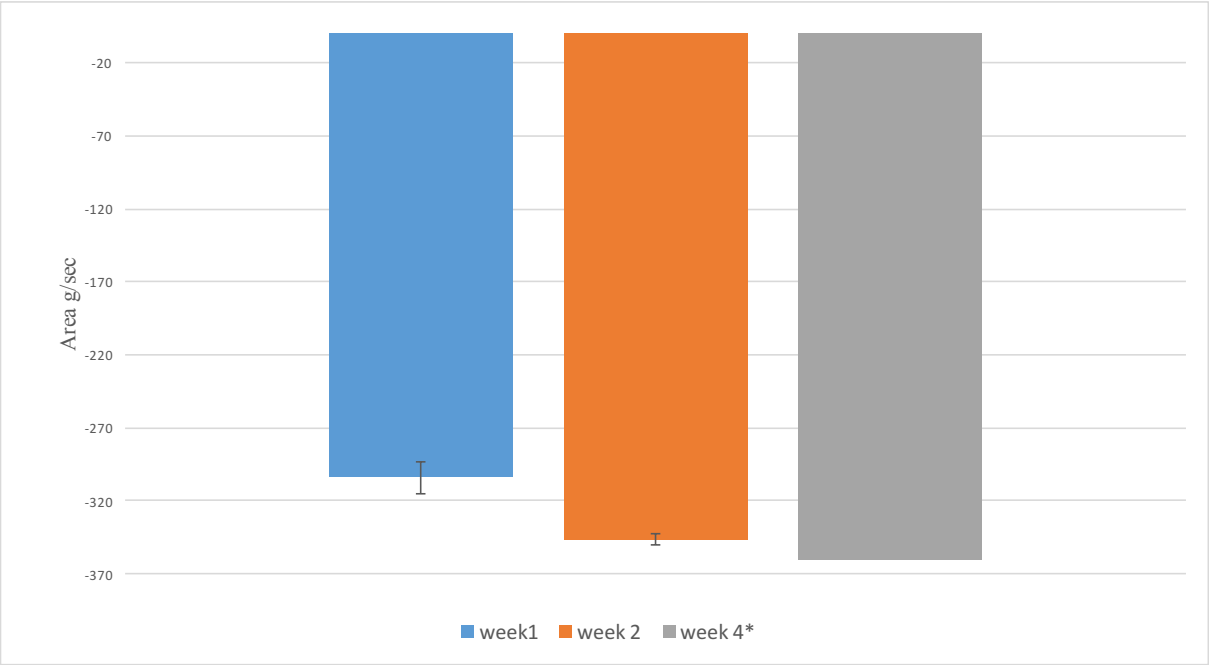

Appendix Figure 8: Adhesiveness stability for CHX liposomes in chitosan hydrogel for week 1, week 2 and week 4 (n=3). * n=1

Current stability measurement for CHX liposomes in chitosan hydrogel also indicates an increase in textural properties over time. The amount hydrogel used for stability measurement: 61.4-65.0 g for week 2 and 64.1 g for week 4. Event though, these stability measurements were not conducted under the same condition (different amount hydrogel in container), the standard deviations are low. Thus, these stability measurements give some indication of the stability to the hydrogels in terms of the hydrogels becoming mores stiff and acquire higher internal stickiness, but not having major changes in the textural properties over a period of 4 weeks. However, this needs to be further investigated and should also include changes in drug release from the hydrogel over time.

Appendix IV Absorbance scan

Different excipients can help enhance the solubility to CHX (Appendix Table 2). However, in an *in vitro* experiment it is important that the absorbance of the analyte is high but without interfering with other compounds on the chosen wavelength (λ_{max}), which was tested (Appendix Figure 9).

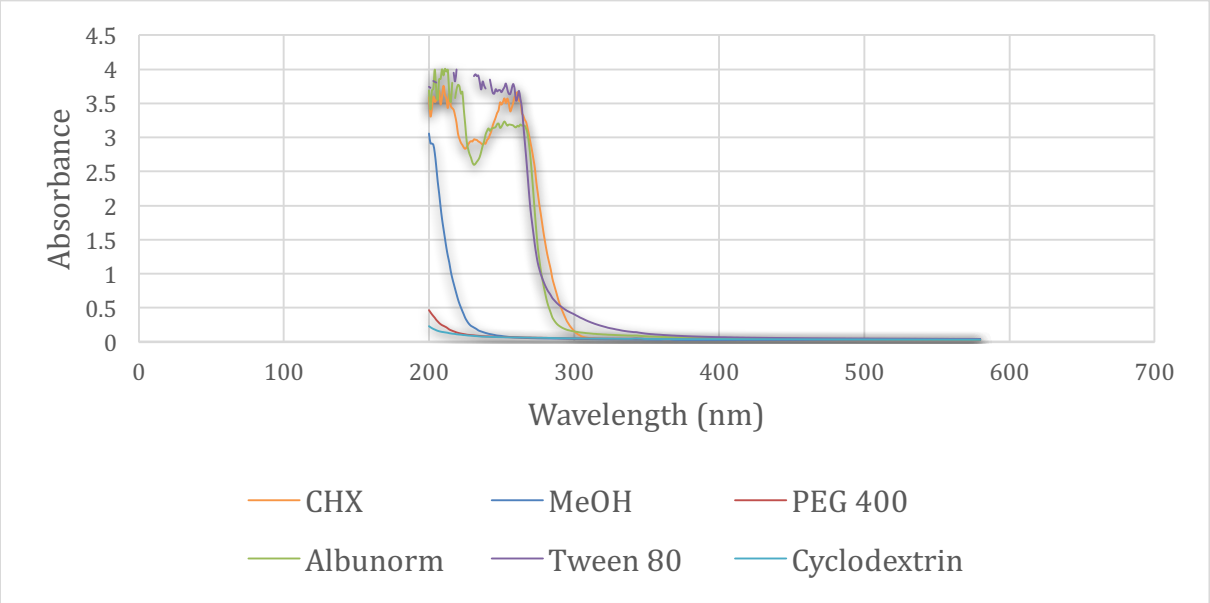

Appendix Figure 9: Absorbance scan of CHX in methanol (MeOH), MeOH, polyethyleneglycol (PEG) 400, Albunorm, Tween 80 and Cyclodextrin.

The absorbance scan showed that amongst all the excipients it was PEG 400 and cyclodextrin that did not interfere with CHX λ_{max}. We planned to conduct Franz diffusion experiments using PEG 400 as a solubilising agent in either concentration of 10 % (v/v) or 30 % (v/v) as acceptor medium. We chose to work with PEG 400 because this excipient was able to dissolve CHX and did not, as mentioned, interfere with λ_{max} to CHX. Another option was cyclodextrine, but CHX solubility in cyclodextrin was not tested. Standard curves with CHX in different concentration (1.25-40 µg/mL) dissolved in PEG 400 10 % (v/v) and 30 % (v/v) were prepared as one can see in Appendix Figure 10 and 11, respectively.

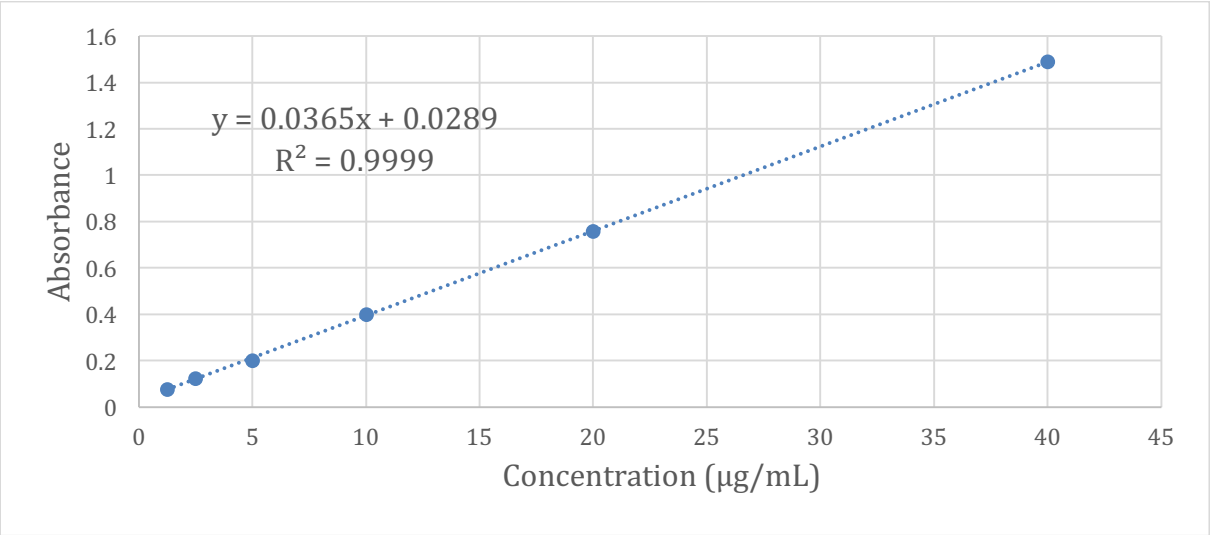

Appendix Figure 10: Standard curve of CHX in 10 % (v/v) PEG in water, at wavelength 261 nm on Tecan Spark M10 multimode plate reader in absorbance mode.

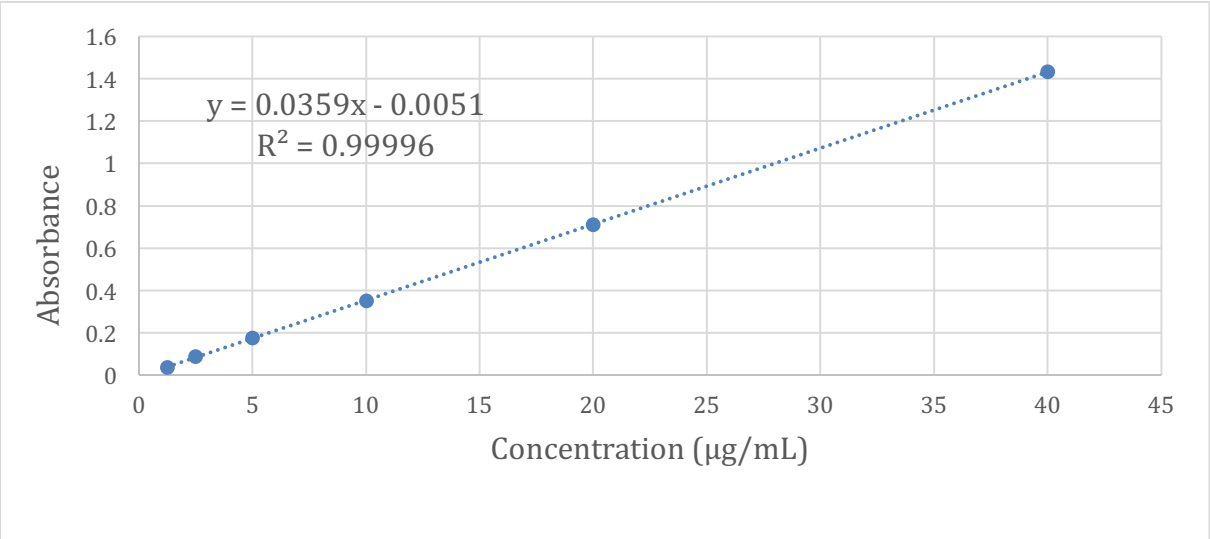

Appendix Figure 11: Standard curve of CHX in 30 % (v/v) PEG in water, at wavelength 261 nm on Tecan Spark M10 multimode plate reader in absorbance mode.

The standard curves prepared had god correlation. We were initially planning conducing Franz diffusion experiments with 10 % (v/v) PEG in water as medium and have 30 % (v/v) as a backup.

Appendix V CHX solubility testing

There are not a lot of published data on the solubility of CHX base, therefore we tested the solubility of CHX base in different aqueous medium, (Appendix Table 2), before selecting to work further PEG 400. We needed CHX base to have a certain degree of solubility in the medium used in release studies and CHX need to be dissolved to be detect with the aid of UV/VIS.

Organic compounds tend to dissolve well in solvents with similar properties to themselves, often referred to as the principle: “like dissolves like”. Since CHX base is an organic compound that is mainly nonpolar (Figure 4) it is expected that it dissolves in organic solvents, like methanol. It is not expected that CHX is dissolved in polar solvents and it is reported that the water solubility of CHX base is very low (Farkas et al., 2007). Since there is not a lot reported about the CHX base solubility, we tested it. We tried to dissolve CHX base in wound fluid with albumin to mimic the environment expected in wound. As we wanted to conduct a biorelevant release study. We also tried dissolving CHX in Albunorm since it has reported that album increase cutaneous permeation of lipophilic drugs, and have earlier been used in our group (Ternullo et al., 2019). However, we could not perform release experiment with Albunorm since it had high UV/Vis absorbance in same area as CHX (see Appendix Figure 9).

Since CHX was practically insoluble in water we wanted to use organic cosolvents with low toxicity, and cosolvents that are often selected are Tween 80, propylen glycol (PG) and PEG 400 (Kawakami et al., 2006). Even though Tween 80, PG and PEG are not present in the wound environment, the planned release studies were preliminary studies with a model compound, and considering that the desired AMP have better solubility properties than CHX, we considered using one of these cosolvents as acceptable in these preliminary studies. However, we could not use Tween 80 since it had high UV/Vis absorbance in the same are as CHX. Between PG and PEG 400, PEG 400 was able to dissolve CHX in various concentrations (Appendix Table 2). We further tried to dissolve CHX in PEG 400 in buffer (PBS), to control pH during release experiments, but we were not able to successfully dissolve all components in the PEG 400-buffer mixture.

Appendix Table 2: Overview of different approaches to dissolve CHX (n=1). (h=hours, min=minutes).

Concentration CHX	Solution	Comment	Dissolved/not dissolved
2 mg/mL	Methanol	Hand shaken	Not dissolved
1 mg/mL	Methanol	Hand shaken	Dissolved
0.5 mg/mL	PBS	Stirred with magnet	Dissolved
1 mg/mL	Wound fluid with albumin	Stirred with magnet 3 h on heat (55 °C)	Not dissolved
0.75 mg/mL	Wound fluid with albumin	Vortexed Bath sonicated Stirred with magnet 2 h on heat (55 °C)	Not dissolved
1 mg/mL	PG 2.5 %	Stirred on heat (55 °C) approx. 10 h, and total stirring with magnet approx. 24 h	Not dissolved
1 mg/mL	PG 5.0 %	Stirred on heat (55 °C) approx. 10 h, and total stirring with magnet approx. 24 h	Not dissolved
1 mg/mL	PG 10 %	Stirred on heat (55 °C) approx. 10 h, and total stirring	Not dissolved

		with magnet approx. 24 h	
1 mg/mL	PG 15 %	Stirred on heat (55 °C) approx. 10 h, and total stirring with magnet approx. 24 h	Not dissolved
1 mg/mL	PG 20. %	Stirred on heat (55 °C) approx. 10 h, and total stirring with magnet approx. 24 h	Not dissolved
1 mg/mL	PG 30 %	Stirred on heat (55 °C) approx. 10 h, and total stirring with magnet approx. 24 h	Not dissolved
0.33 mg/mL	PG 30 %	Stirred on heat (55 °C) approx. 10 h, and total stirring with magnet approx. 24 h	Not dissolved
0.1 mg/mL	5 % (v/v) Albunorm™ in PBS	Bath sonicated Stirred for a couple of minutes with magnet stirrer	Dissolved
0.5 mg/mL	5 % (v/v) Albunorm™ in PBS	Stirred with magnet for approx. 3 h	Dissolved

1 mg/mL	1 % (v/v) Tween 80 in water	Bath sonicated approx. 20 min Stirred with a magnet couple min	Dissolved
1 mg/mL	30 % (v/v) PEG 400 in water	Bath sonicated approx. 20 min Stirred with a magnet couple min	Dissolved
1 mg/mL	10 % (v/v) PEG 400 in water	Bath sonicated approx. 20 min Stirred with a magnet couple min Batch sonicated Stirred with magnet couple min	Dissolved
1 mg/mL	10 % (v/v) PEG 400 in PBS	Bath sonicated Stirred with magnet approx. 48 h	Not dissolved Unknown precipitate

Appendix VI Method Development

This section describes planned experiment in this master project, but due to unforeseen events, these specific experiments were not conducted.

Appendix VI.I EE – centrifugation

Repeat experiment in section 5.4.4.2 (Method) to attain more parallels (n=3) to strengthen the results.

Appendix VI.II Hydrogel characterisation

Conduct experiment at T.A. from section 5.7.2 (Method) at plain chitosan hydrogel (in concentration 4.5 % (w/w)) comprising 10 % (w/w) glycerol for comparison.

Appendix VI.III Phospholipid content measurement

The phospholipid content measurements were to be performed as described earlier in our group (Ternullo et al., 2019). In brief, 50 µL of liposomal dispersion were to be diluted to a final volume of 10 mL with distilled water and then add sulphuric acid (5 M) before incubation at 160 ºC for 3 hours. Then after 3 hours add hydrogen peroxide 30 % to the samples and incubate at 160 ºC for additional 1.5 hours. After the additional 1.5 hours add ammonium molybdate (0.22 % w/v) and Fiske-Subbarow reducer and incubate at 100 ºC for 7 minutes. Then analyse the samples spectrophotometrically and use a standard curve of phosphorous standard solution to calculate the amount.

Appendix VI.IV Viscosity measurements

The viscosity measurements were to be performed based on the rheological measurements method conducted by Ghica *et al.,* with some modification (Ghica et al., 2016). The experiment was to be conducted on a viscometer Rotavisc hi-vi II Complete with a thermometer attached to the measuring system to assure constant temperature during a test. The hydrogels were to be tested with different rotational speed, different time intervals and different temperatures. The set-up of the experiment included a beaker with 400 g hydrogel that was placed in a 3D printed holder that allowed tempered water to flow through it (Appendix Figure 12). Thereby, enabling temperature changes in the experiment.

Appendix Figure 12: Set-up for the beaker for the viscosity measurements. A 3D-printed holder with tempered water flowing through it makes it possible to heat up hydrogel loaded inside the beaker. This enables measuring viscosity over time in a range of temperatures. (Martin Skipperud Skarpeid, *with permission*).

Appendix VI.V *In vitro* drug release

Drug release of CHX from liposomes-in-hydrogel formulation and liposomes was to be explored with Franz cell manual diffusion system with the same method as in section 5.9.2. (Method). With exception using 10 % (v/v) polyethylene glycol (PEG) 400 in distilled water as medium. The experiment was based on result from solubility testing of CHX (Appendix IV and V).

Appendix VI.VI Stability testing of liposomal dispersion

Planned to complete stability testing measurement (see section 5.8 in Method) of liposomal dispersion week 4 and week 12.